SIMPLIFIED ANALYSIS OF PILED RAFT FOUNDATIONS SUBJECTED TO ACTIVE LOADING AND PASSIVE LOADING

Pastsakorn Kitiyodom
Research Associate, Kanazawa University

Tatsunori Matsumoto
Professor, Kanazawa University

SIMPLIFIED ANALYSIS OF PILED RAFT FOUNDATIONS SUBJECTED TO ACTIVE LOADING AND PASSIVE LOADING

REFERENCES

Kitiyodom, P. and Matsumoto, T. (2002): A simplified analysis method for piled raft and pile group foundations with batter piles, *Int. Journal for Numer. and Anal. Methods in Geomech*. 26: 1349-1369.

Kitiyodom, P. and Matsumoto, T. (2003): A simplified analysis method for piled raft foundations in non-homogeneous soils, *Int. Journal for Numer. and Anal. Methods in Geomech*. 27: 85-109.

Kitiyodom, P., Matsumoto, T. and Kawaguchi, K. (2005): A simplified analysis method for piled raft foundations subjected to ground movements induced by tunnelling, *Int. Journal for Numer. and Anal. Methods in Geomech*. 29: 1485-1507.

Kitiyodom, P., Matsumoto, T., Horikoshi, K. and Watanabe, T. (2005): Analyses of vertical and horizontal load tests on piled raft models in dry sand, *Proc. 16th Int. Conf. on Soil Mechanics and Geotechnical Engineering*. 2005-2008.

Yaegashi, K., Kitiyodom, P., Fujita, M., Matsumoto, T., Arai, T. and Hasei, H. (2006): Analyses of vertical and horizontal load tests of model piled rafts in sand using a hybrid model, *Proc. 6th Int. Conf. on Physical Modelling in Geotechnics*.1579-1585.

Simple raft foundation

Fully piled foundation

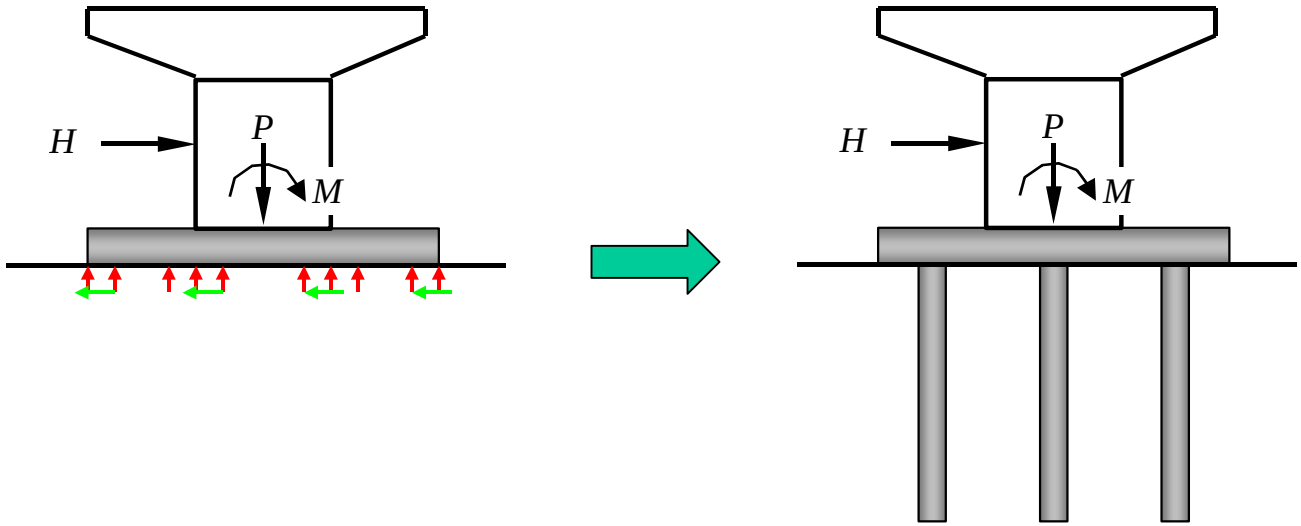

- In practice, from an economic viewpoint, a foundation designer is most likely to consider first the use of a simple raft foundation to support a superstructure.

- In the case where the use of a simple raft foundation is not sufficient, a fully piled foundation is employed.

- In most conventional design, the foundation has been designed ignoring any contribution from the raft.
- In the past few years, there has been an increasing recognition that the inclusion of the resistance of the raft in pile foundation design can lead to a considerable economy without compromising the safety or the performance of the foundation.

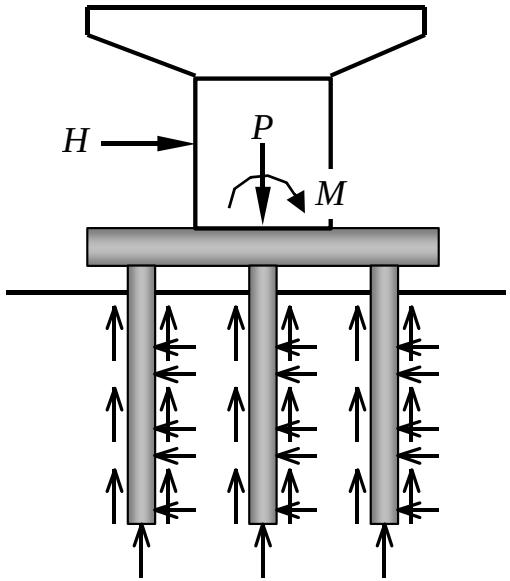

Conventional Design

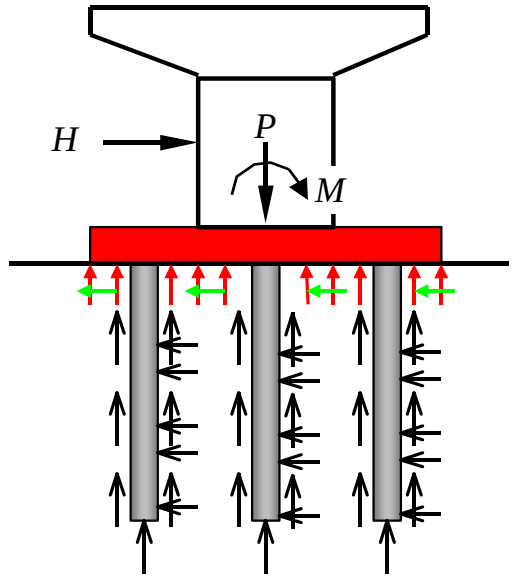

Design of Piled Raft

Design of Foundation

Allowable stress design ⇒ Limit state design,
Performance based design

- Considering current trends toward the limit state design or performance based design in the area of foundation engineering, precise estimation of deformation of a whole foundation and of stresses of its structural members is a vital issue in the frame work of this new design criterion.
- In the preliminary design stage, a number of alternative calculations are required.

"Hence a *feasible* but *reliable* deformation analysis method of piled raft foundations is sought for"

- In addition, in some cases, the existing foundations may be also subjected to ground movements induced by nearby excavation operations, settling embankments, pile driving operations, tunnelling operations, moving slopes, or landslides.

Objective

Development of a *feasible* but *reliable* simplified analytical method for deformation analysis of piled raft foundations subjected to active loading (vertical, lateral and moment loads) and passive loading (ground movement).

Contents of Today Presentation

Part I: Development of PRAB

Part II: Verified the validity of PRAB through comparison analysis with three-dimensional FEM

Part III: Verified the applicability of PRAB through analyses of the centrifuge model test results

Part IV: Application of PRAB

Part I: Development of PRAB

Plate-beam-spring Modelling of Piled Raft

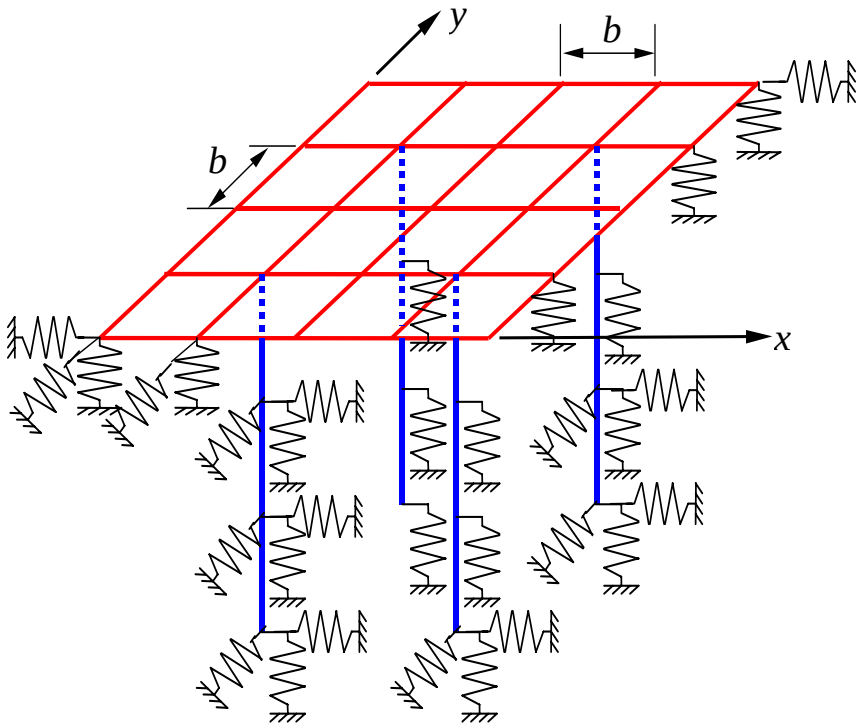

$$K_z^{\mathrm{R}} = \frac{4G_s a}{1-\nu_s}$$

$$K_x^{\mathrm{R}} = K_y^{\mathrm{R}} = \frac{32(1-\nu_s)G_s a}{7-8\nu_s}$$

$$K_z^{\mathrm{P}} = 2\pi G_s \Delta L / \ln(r_m / r_o)$$

$$K_x^{\mathrm{P}} = K_y^{\mathrm{P}} = \zeta E_s \Delta L$$

Soil : Springs at raft and pile nodes

Raft : Thin plate elements

Pile : Beam elements

G_s, ν_s Shear modulus, Poisson's ratio of soil

E_s Young's modulus of soil

$a = b/\sqrt{\pi}$ $\quad r_m = 2.5L(1-\nu_s)$

ΔL Pile element length $\quad r_o$ Pile radius

Plate-beam-spring Modelling of Piled Raft

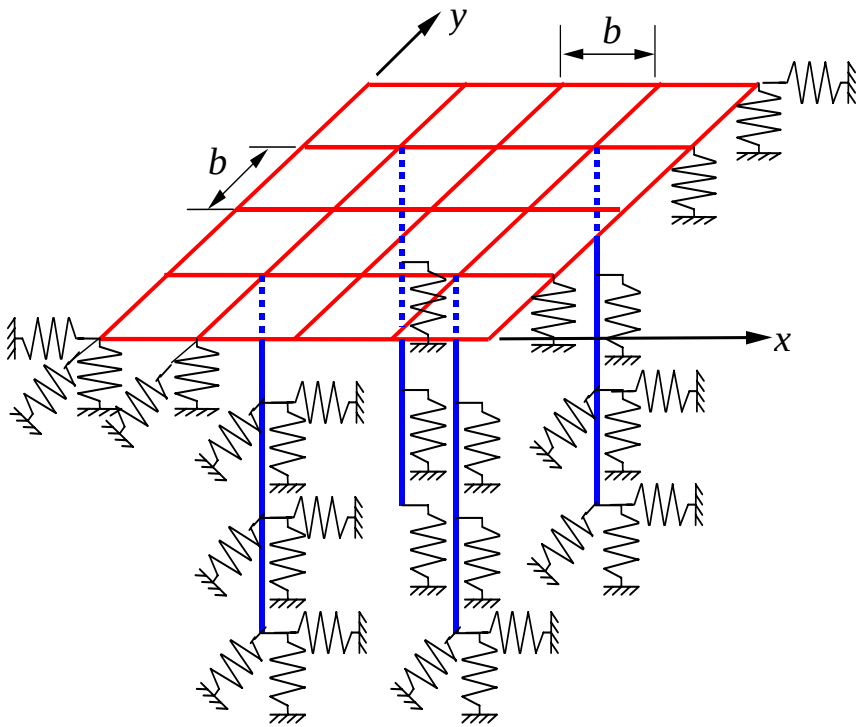

Raft Vertical soil springs

$$K_z^{\mathrm{R}} = \frac{4G_s a}{1-\nu_s}$$

Raft Lateral soil springs

$$K_x^{\mathrm{R}} = K_y^{\mathrm{R}} = \frac{32(1-\nu_s)G_s a}{7-8\nu_s}$$

Pile Vertical soil springs

$$K_z^{\mathrm{P}} = 2\pi G_s \Delta L / \ln(r_m / r_o)$$

Pile Lateral soil springs

$$K_x^{\mathrm{P}} = K_y^{\mathrm{P}} = \zeta E_s \Delta L$$

G_s, ν_s Shear modulus, Poisson's ratio of soil

E_s Young's modulus of soil

$a = b/\sqrt{\pi}$ $r_m = 2.5L(1-\nu_s)$

ΔL Pile element length r_o Pile radius

Incorporation of batter piles

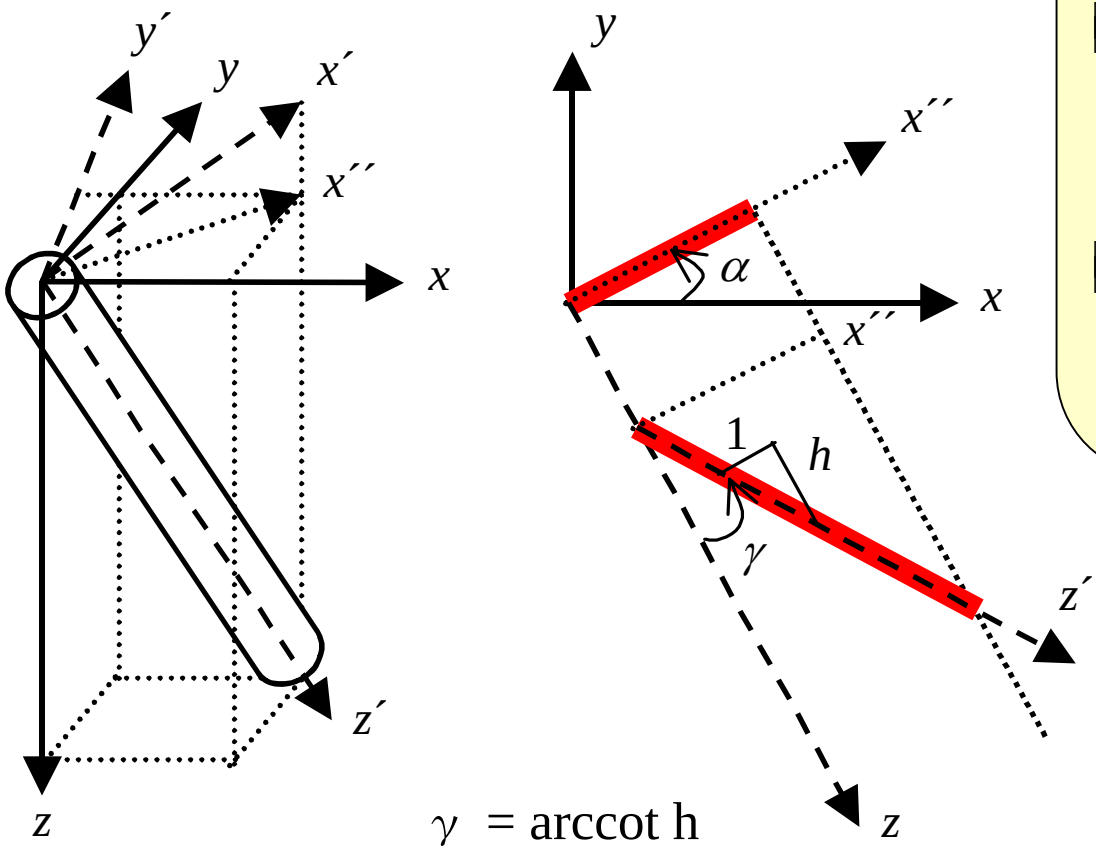

γ = arccot h

$$[T]=\begin{bmatrix}[R] & [0] & [0] & [0]\\ [0] & [R] & [0] & [0]\\ [0] & [0] & [R] & [0]\\ [0] & [0] & [0] & [R]\end{bmatrix}$$

$$[R]=\begin{bmatrix}\cos\gamma\cos\alpha & -\sin\alpha & \sin\gamma\cos\alpha\\ \cos\gamma\sin\alpha & \cos\alpha & \sin\gamma\sin\alpha\\ -\sin\gamma & 0 & \cos\gamma\end{bmatrix}$$

$0^\circ \le \alpha \le 360^\circ$ $\quad$ $0^\circ \le \gamma \le 90^\circ$

$$\{P\}=[T][K_p][T]^T\{w\}$$

$$\{P\}=[K_p^*]\{w\}$$

Poulos & Madhav (1971)

- Soil springs are independent of rake angle

$$[K_s^*]=[R][K_s][R]^T$$

Structure-soil-structure Interaction

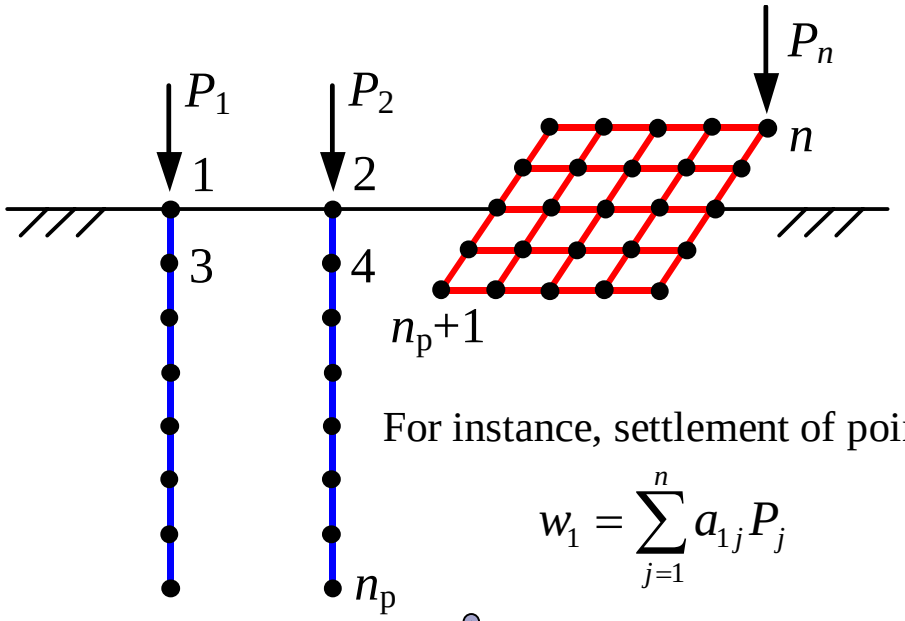

Diagonal coefficients of [*A*]

Inverse of $[K_s^*]$

Off-diagonal coefficients of [*A*]

Based on Mindlin's solutions

For instance, settlement of point 1

$$w_1 = \sum_{j=1}^{n} a_{1j} P_j$$

$$\{w\} = [A]\{P\}, \quad [C]\{w\} = \{P\}$$

Raft Element

$$[K_r]\{w\} = \{F\} - \{P\}$$

Total Stiffness Matrix of Piled Raft

$$[C + K_r + K_p^*]\{w\} = [K]\{w\} = \{F\}$$

$$[C + K_r + K_p]\{w\} = [K]\{w\} = [C]\{w_0\}$$

Multi-layer soil

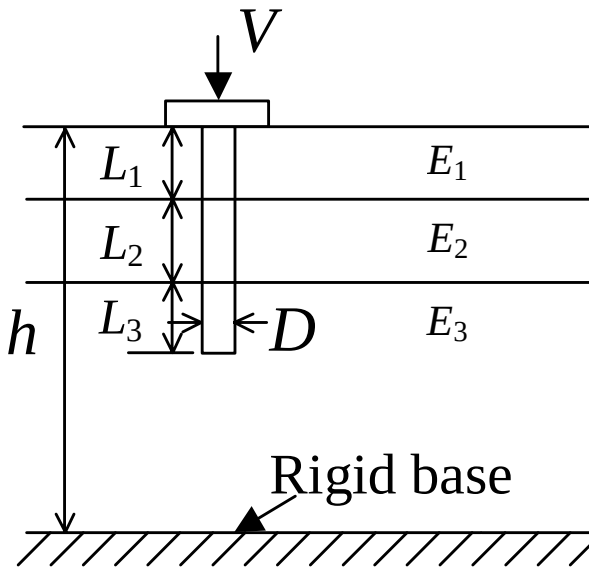

$\bar{G}$ Equivalent soil shear modulus
G_m Maximum soil shear modulus
G_i Soil shear modulus at element i
G_b Soil shear modulus at pile base
G_r Soil shear modulus at raft base
L_i Length of element i
ΔL Pile element length
r_o Pile radius

Raft Vertical soil springs

$$K_z^R = \frac{4\bar{G}a}{1-\nu_s}\left(1-\exp\left(-h/2a\right)\right)$$

Pile Vertical soil springs

$$K_z^{Pb} = \frac{4G_b r_o}{1-\nu_s}\left(1-\exp\left(-h^*/D\right)\right)$$

$$K_z^P = 2\pi G_s \Delta L / \ln(r_m / r_o)$$

$$r_m = 2.5\left[\frac{(1-\nu_s)}{G_m L}\sum_{i=1}^{n} G_i L_i \left(1-\exp(-h/L)\right)\sqrt{\frac{G_m}{G_b}}\right]L$$

Raft lateral soil springs

$$K_x^R = K_y^R = \frac{32(1-\nu_s)G_r a}{7-8\nu_s}$$

Pile lateral soil springs

$$K_x^{Pb} = K_y^{Pb} = \frac{32(1-\nu_s)G_b r_o}{7-8\nu_s}$$

$$K_x^P = K_y^P = \zeta E_s \Delta L$$

Equivalent shear modulus, $\bar{G}$

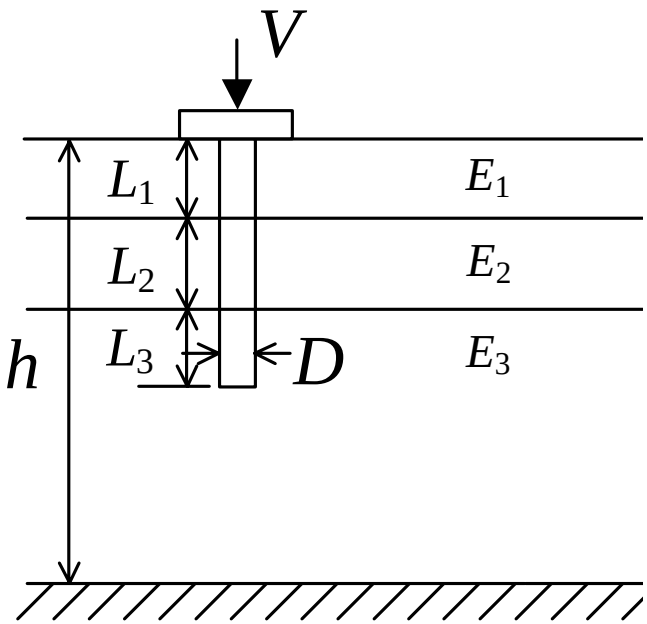

$$\frac{1}{\bar{E}_s} = \sum_{i=1}^{n} \frac{1}{E_i} \Delta I_i / \Delta I_{\text{total}}$$

$$\Delta I_i = I\left(z_i^{\text{top}}\right) - I\left(z_i^{\text{bottom}}\right)$$

$$\Delta I_{\text{total}} = I(0) - I(h)$$

$$\bar{G} = \frac{\bar{E}_s}{2(1+\nu_s)}$$

I is the vertical settlement influence factor which is given by Harr(1966).

Average soil modulus

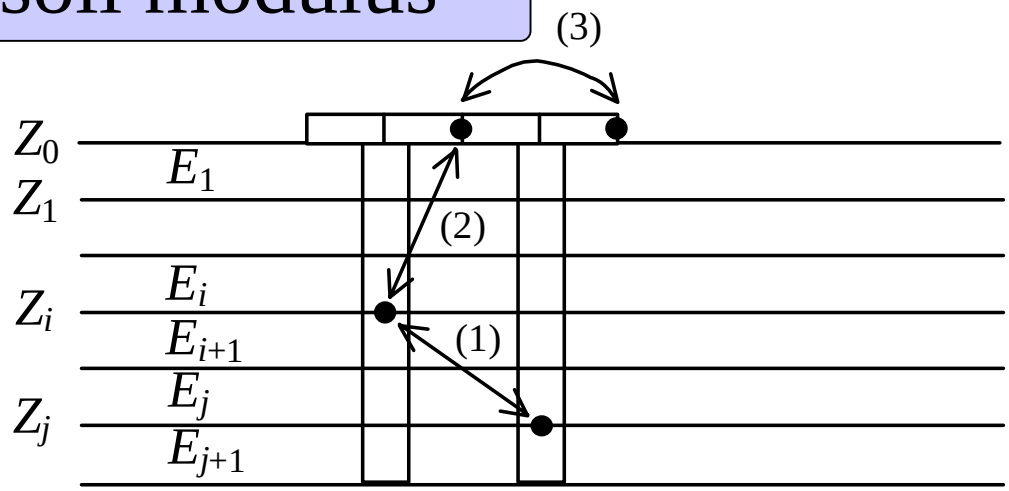

(1) pile-soil-pile interaction

(2) pile-soil-raft interaction

(3) raft-soil-raft interaction

$$E_{s(ij)} = \frac{\left(E_{s(i)} + E_{s(i+1)}\right) + \left(E_{s(j)} + E_{s(j+1)}\right)}{4}$$

Average soil modulus is employed in the analysis to approximate for the interactions.

Part II: Verified the validity of PRAB through comparison analysis with three-dimensional FEM

Comparison Analysis

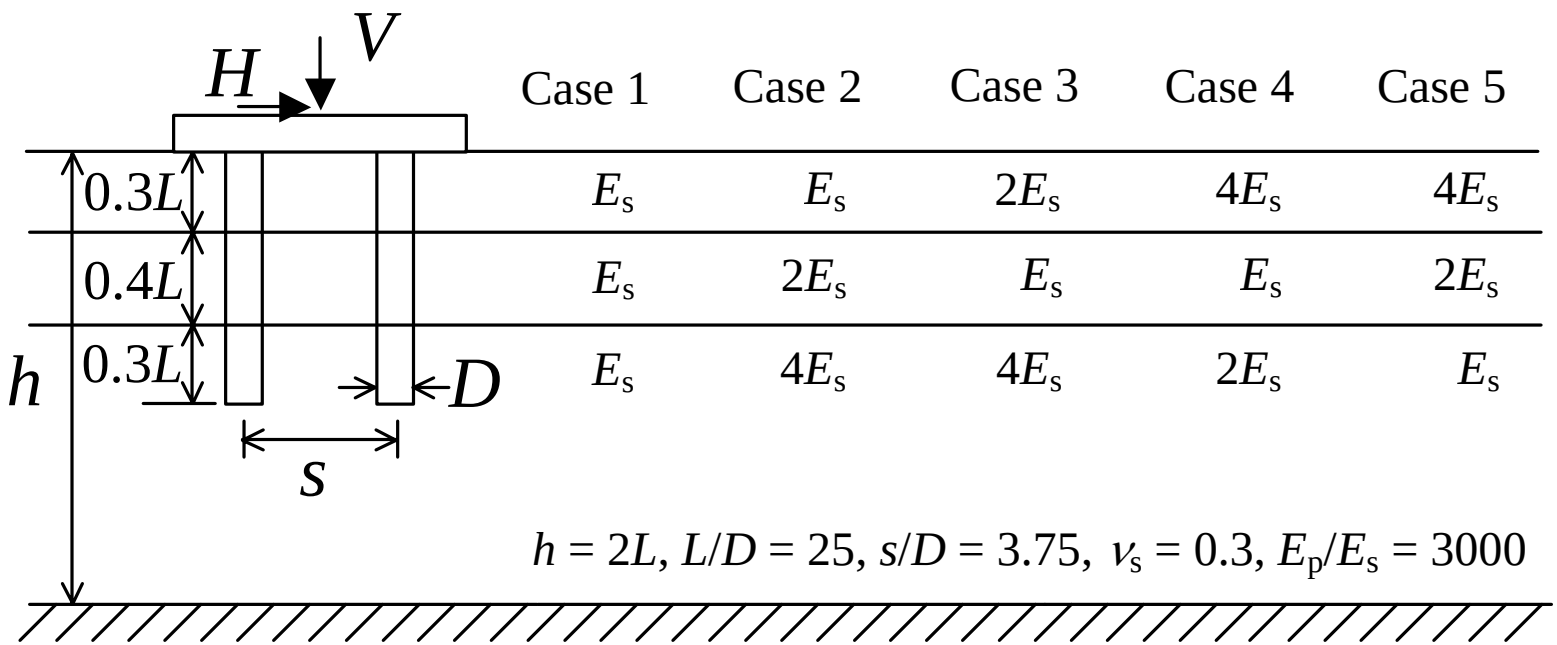

	Case 1	Case 2	Case 3	Case 4	Case 5
	E_s	E_s	$2E_s$	$4E_s$	$4E_s$
	E_s	$2E_s$	E_s	E_s	$2E_s$
	E_s	$4E_s$	$4E_s$	$2E_s$	E_s

$h = 2L$, $L/D = 25$, $s/D = 3.75$, $\nu_s = 0.3$, $E_p/E_s = 3000$

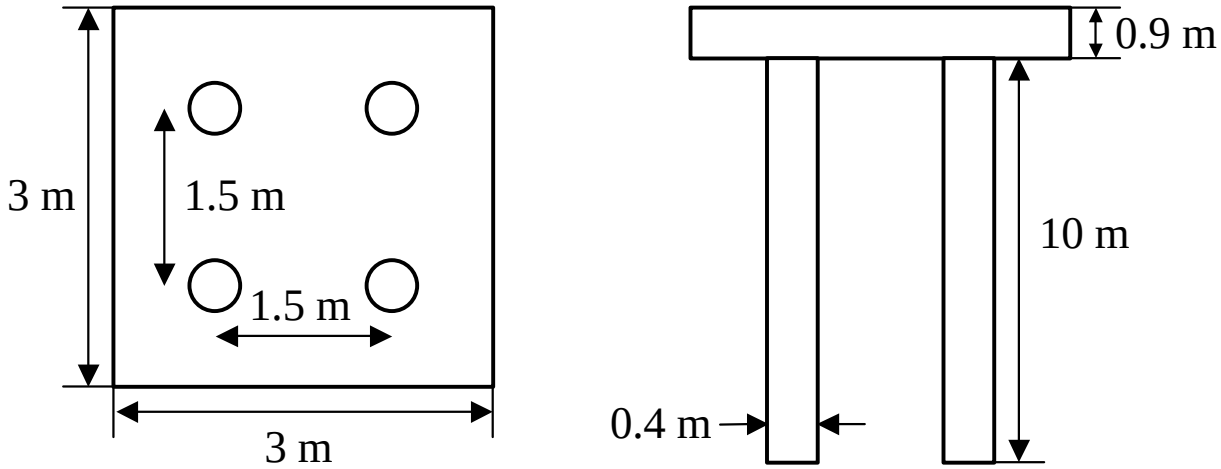

Three-dimensional FEM

$E_p = E_r = E_c = 30$ GN/m^2

$\nu_p = \nu_r = \nu_c = 0.16$

$E_s = 30$ MPa

$\nu_s = 0.3$

$D = 1$ m

$K_{rs} = 10$

$V, H = 100$ kN/m^2 (900 kN)

(a) Whole mesh

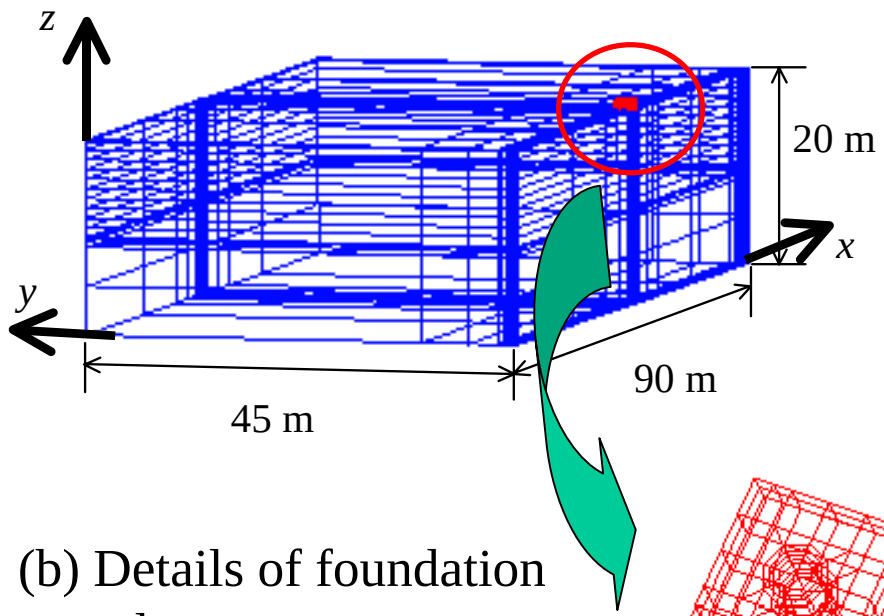

(b) Details of foundation elements

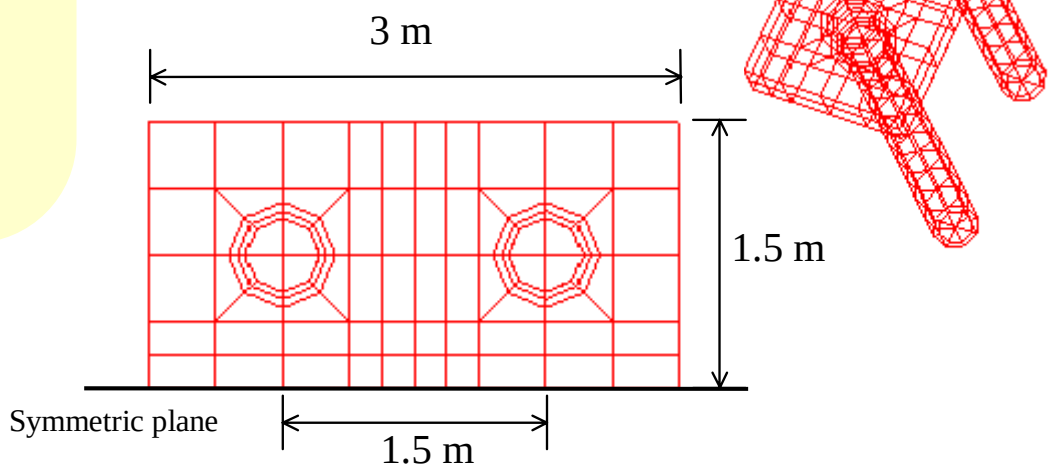

Comparison Analysis

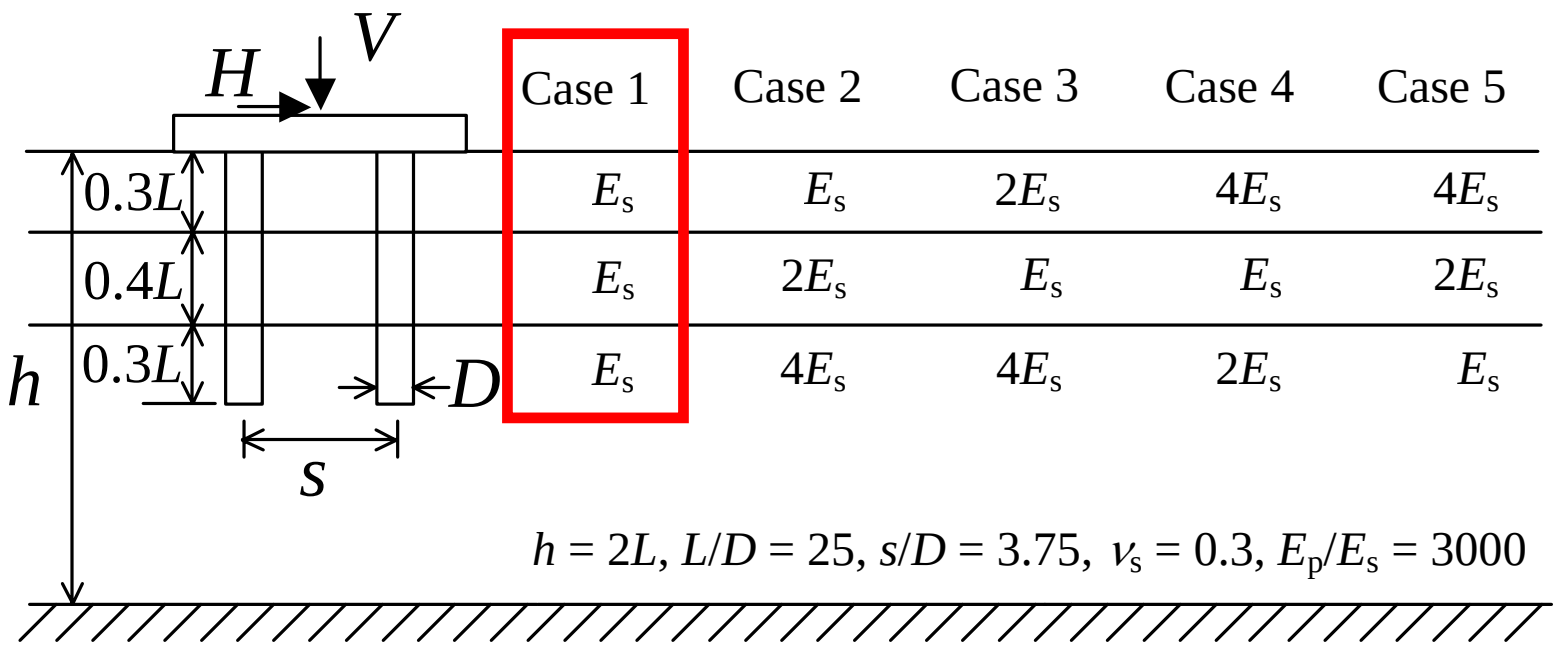

	Case 1	Case 2	Case 3	Case 4	Case 5
0.3L	E_s	E_s	$2E_s$	$4E_s$	$4E_s$
0.4L	E_s	$2E_s$	E_s	E_s	$2E_s$
0.3L	E_s	$4E_s$	$4E_s$	$2E_s$	E_s

$h = 2L$, $L/D = 25$, $s/D = 3.75$, $\nu_s = 0.3$, $E_p/E_s = 3000$

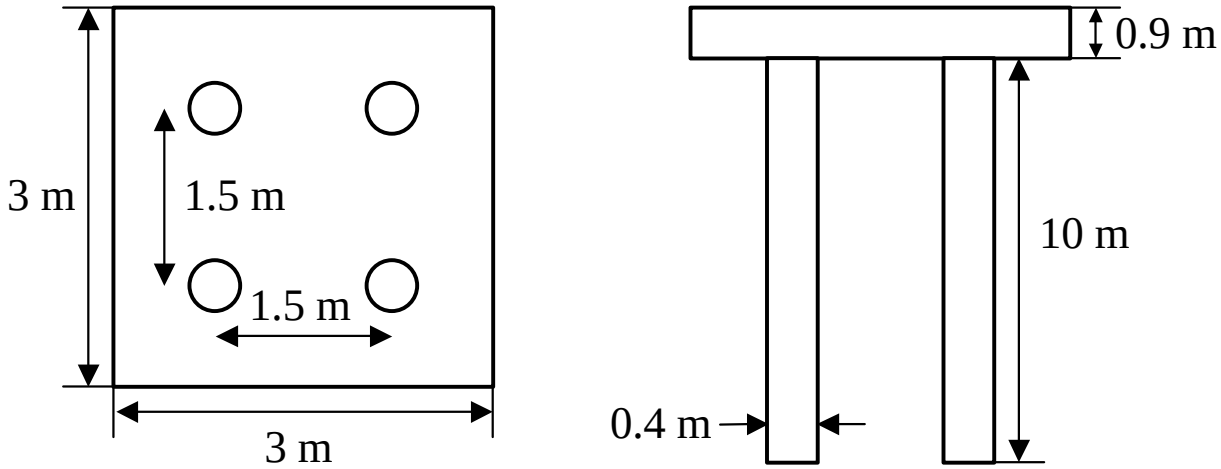

Settlement of the pile

$$I_{wV} = \frac{wE_s D}{V}$$

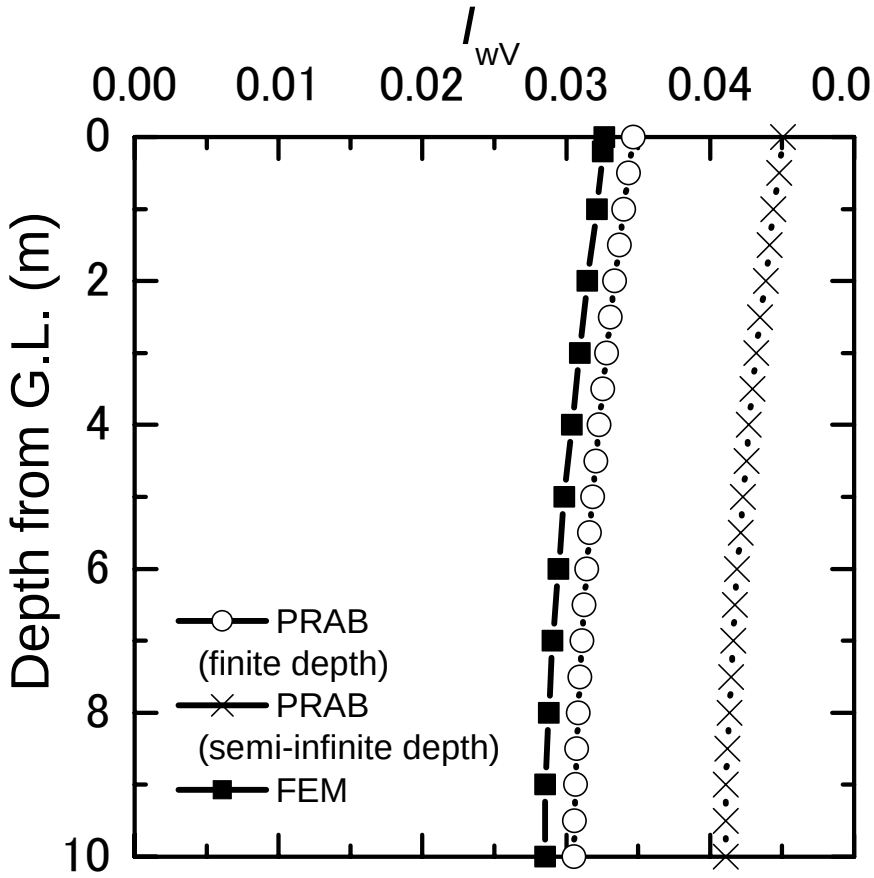

Piled raft

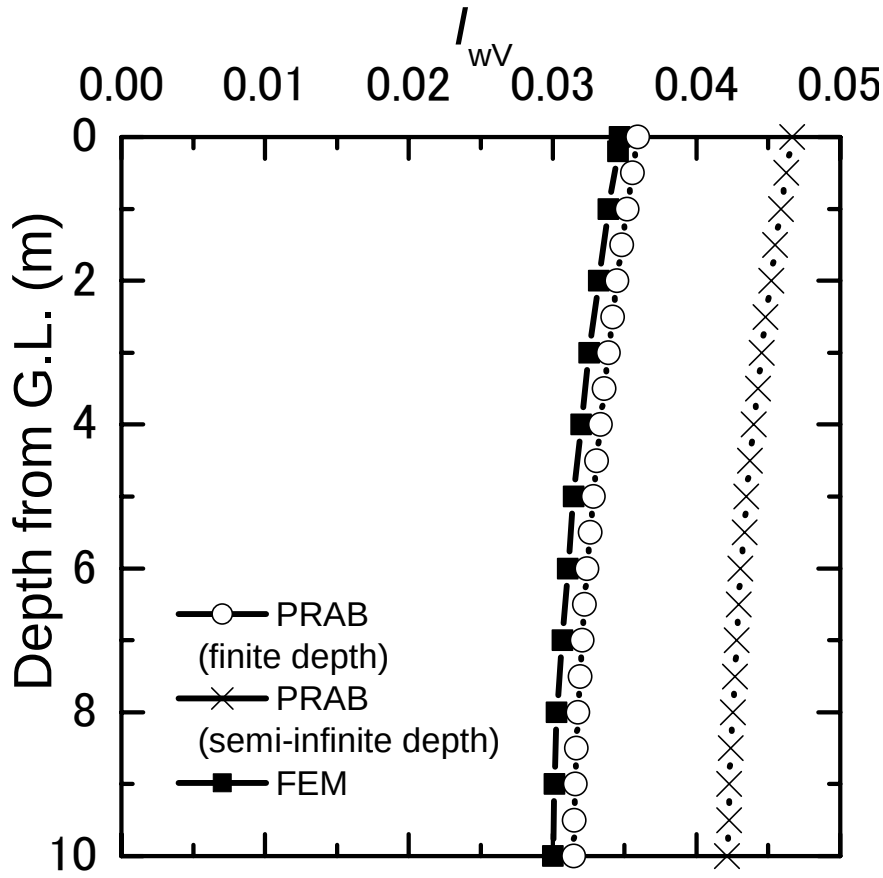

Pile group

Axial forces along pile

$$C_{aV} = \frac{A}{V}$$

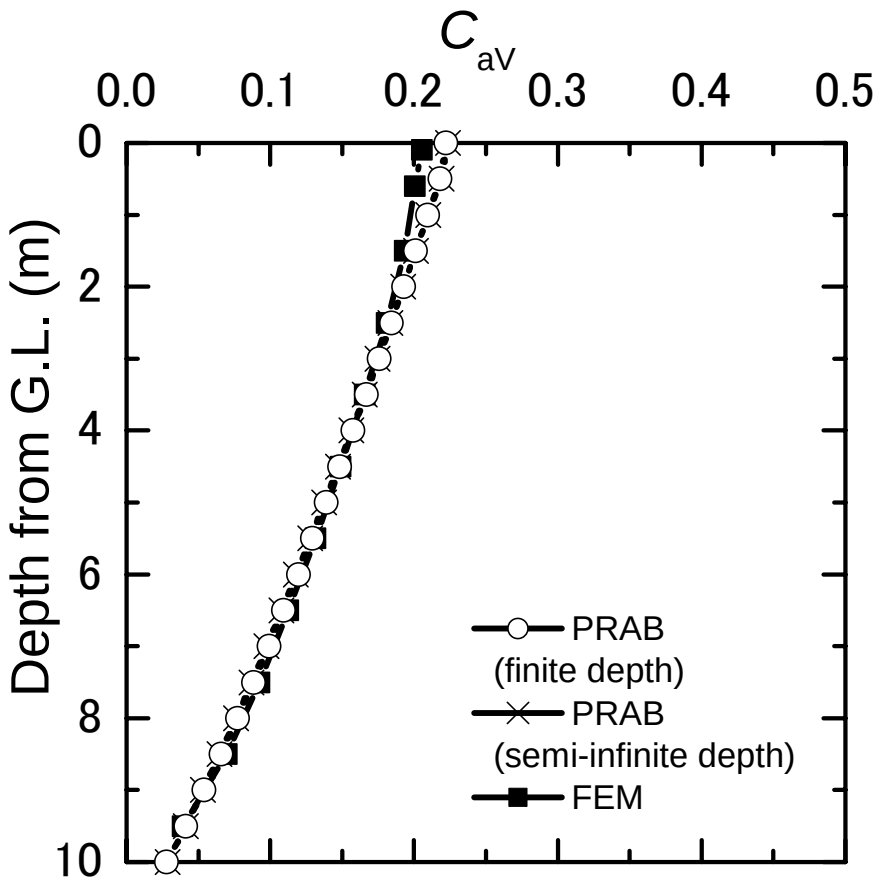

Piled raft

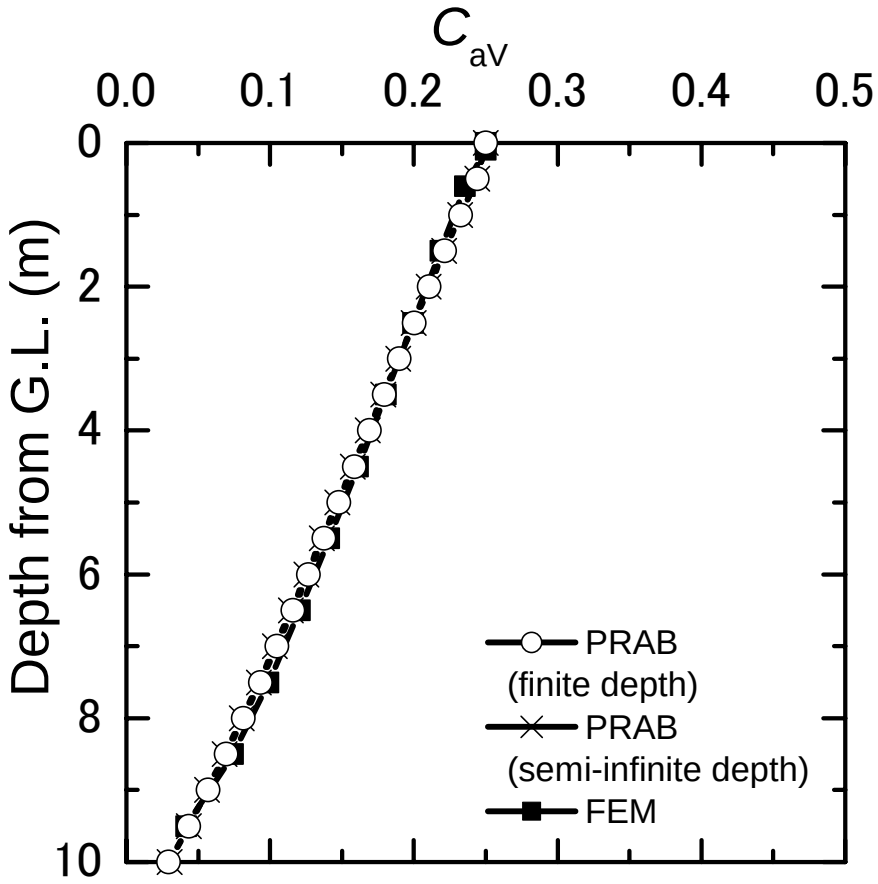

Pile group

Lateral displacement of the pile

$$I_{uH} = \frac{uE_s D}{H}$$

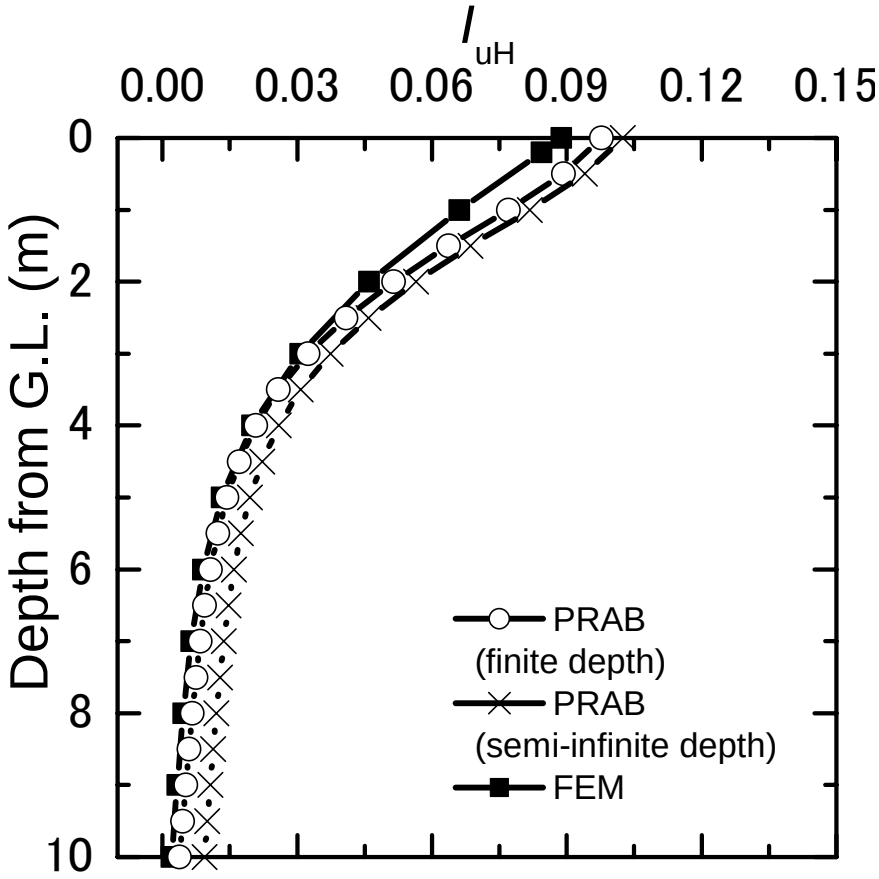

Piled raft

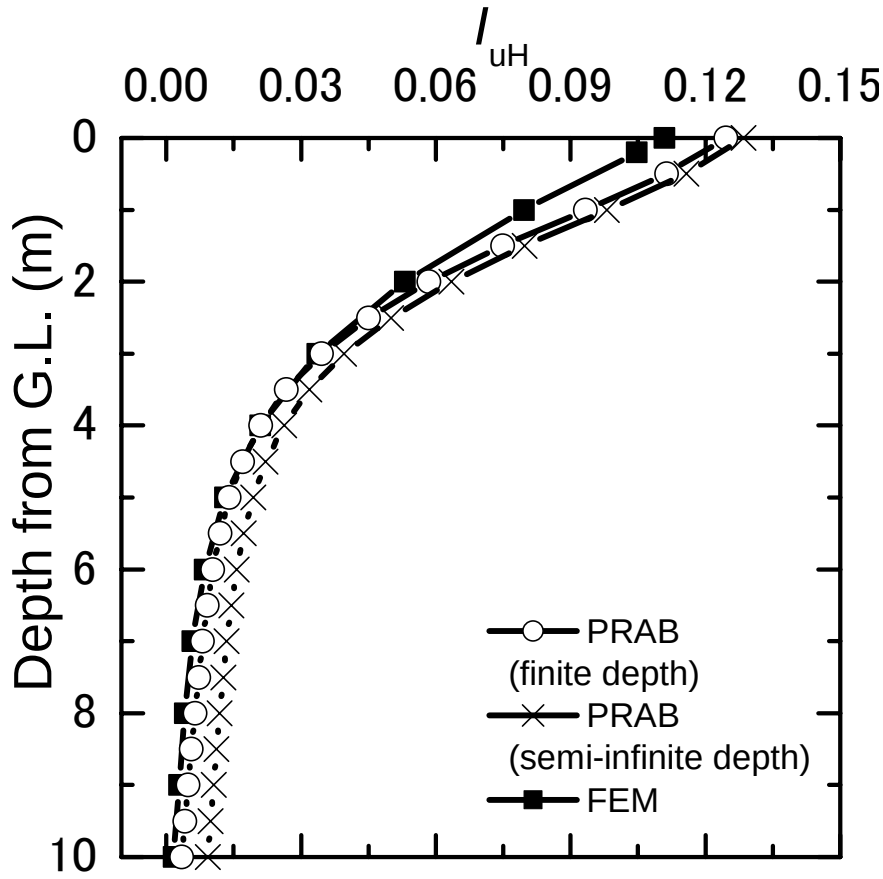

Pile group

Shear forces along piles

$$C_{sH} = \frac{S}{H}$$

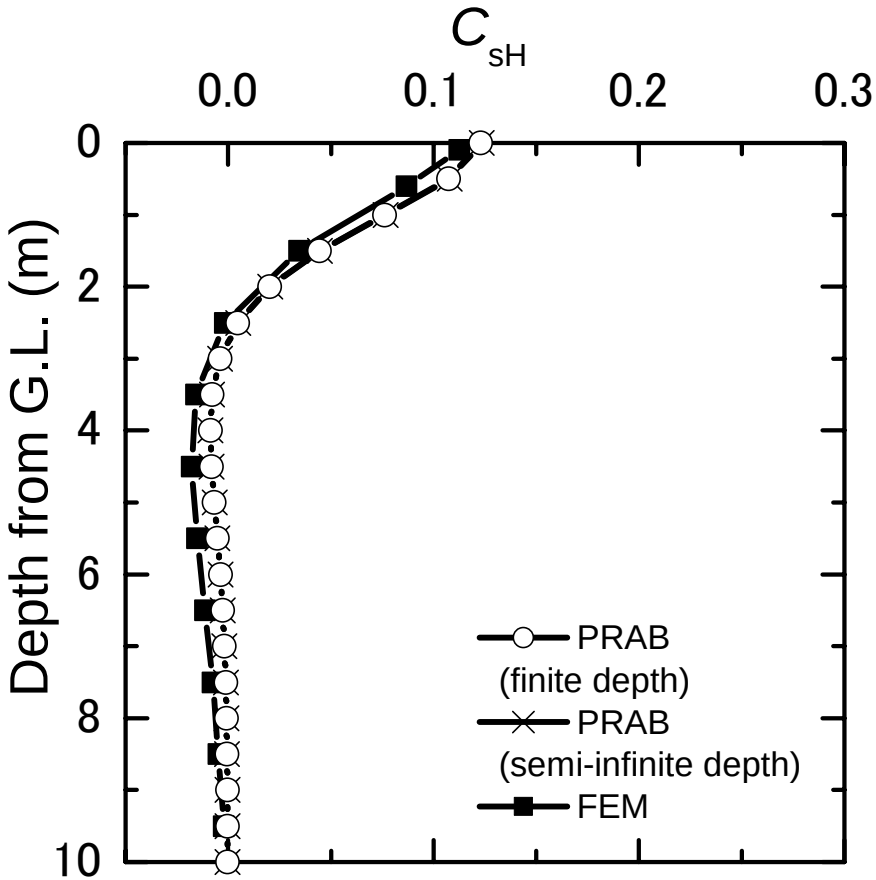

Piled raft

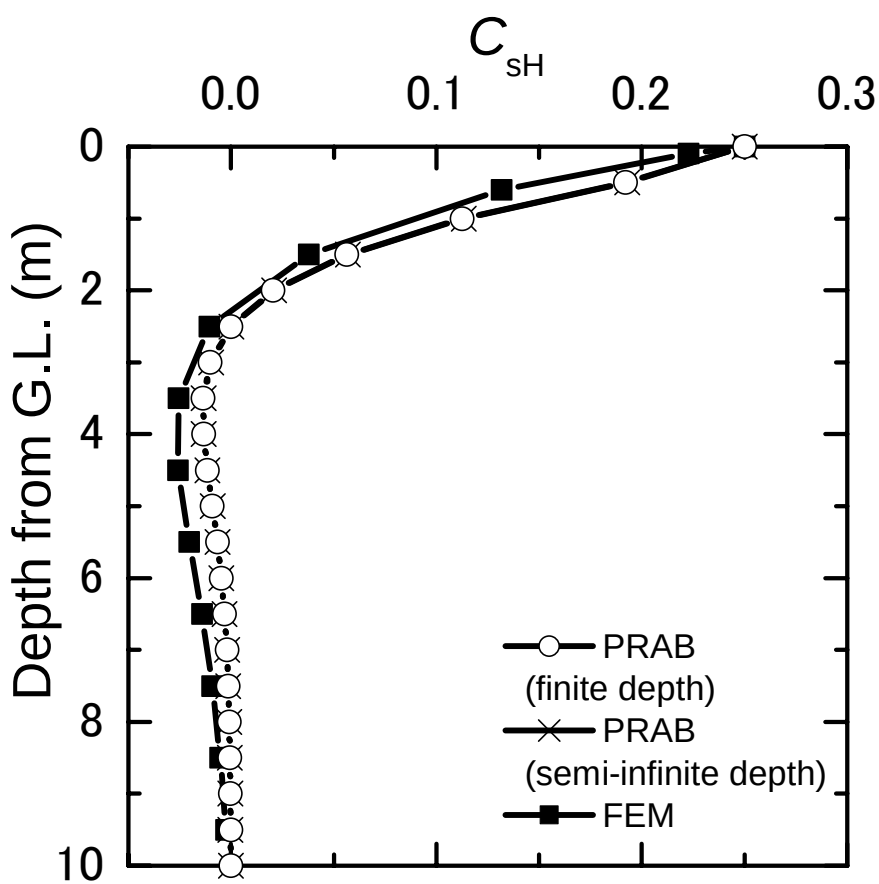

Pile group

Bending moments along piles

$$C_{bH} = \frac{B}{HD}$$

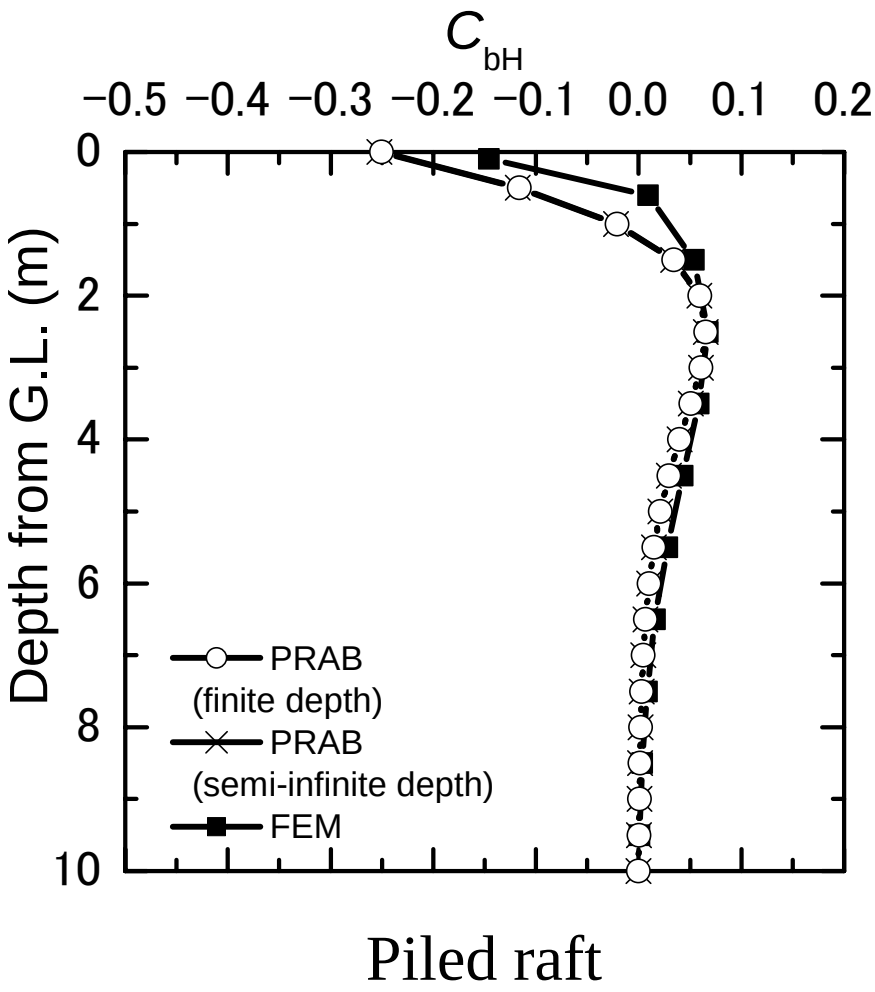

Piled raft

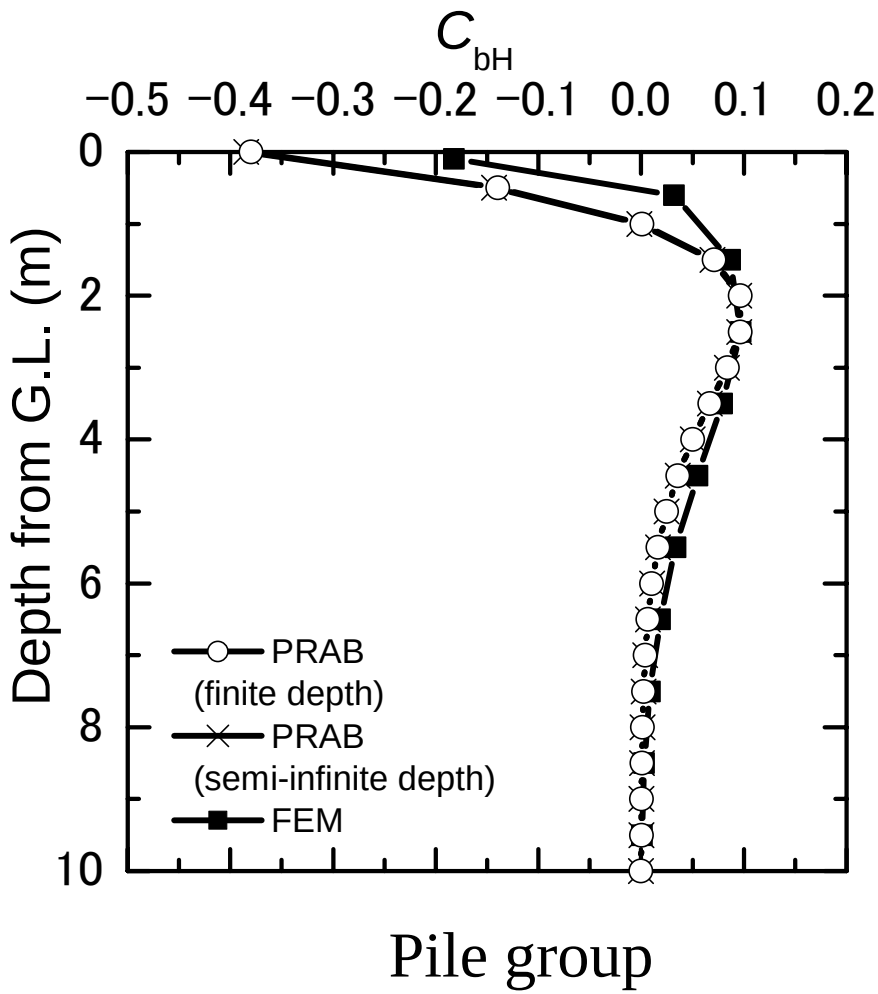

Pile group

Comparison Analysis

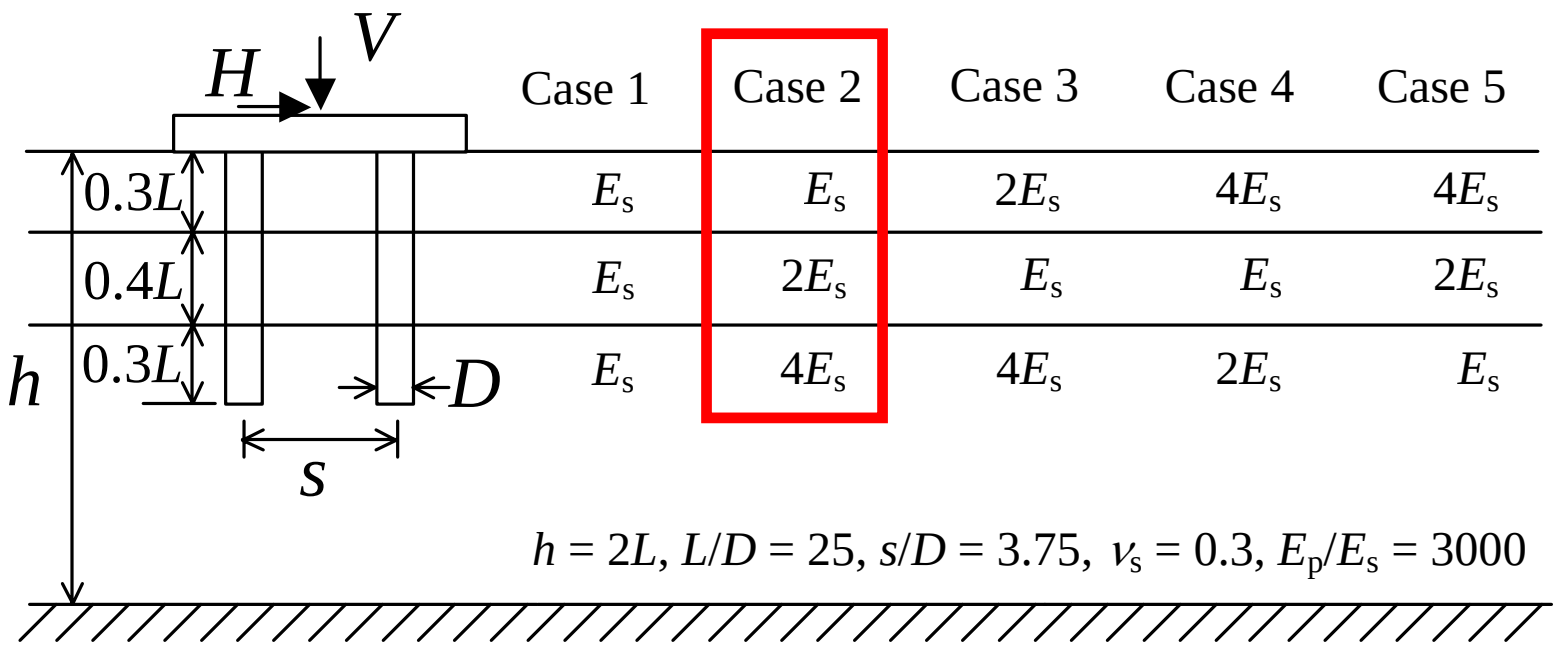

	Case 1	Case 2	Case 3	Case 4	Case 5
0.3L	E_s	E_s	$2E_s$	$4E_s$	$4E_s$
0.4L	E_s	$2E_s$	E_s	E_s	$2E_s$
0.3L	E_s	$4E_s$	$4E_s$	$2E_s$	E_s

$h = 2L$, $L/D = 25$, $s/D = 3.75$, $\nu_s = 0.3$, $E_p/E_s = 3000$

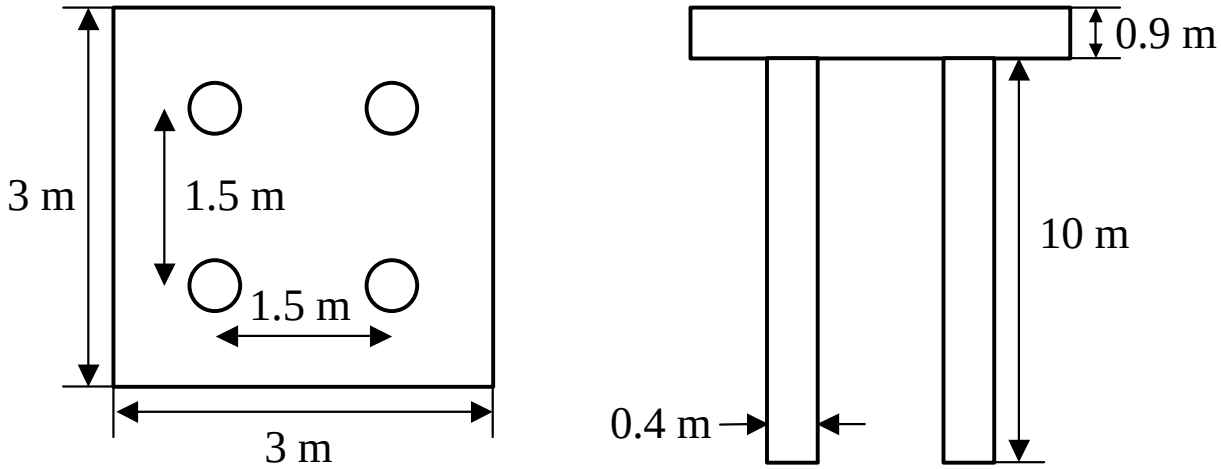

Comparison of calculated results

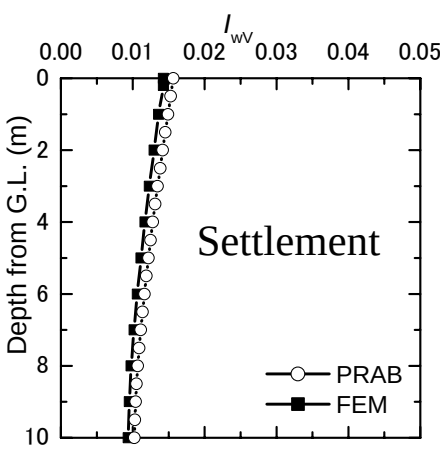

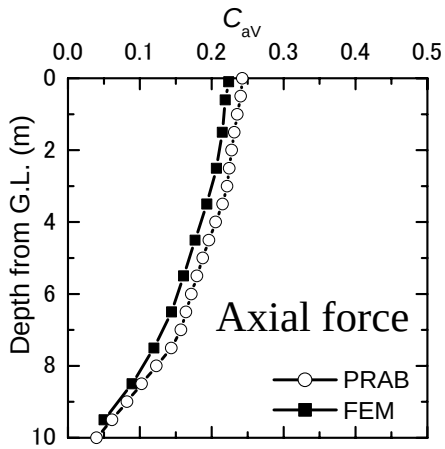

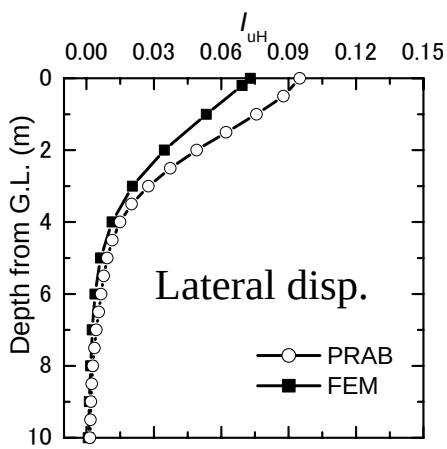

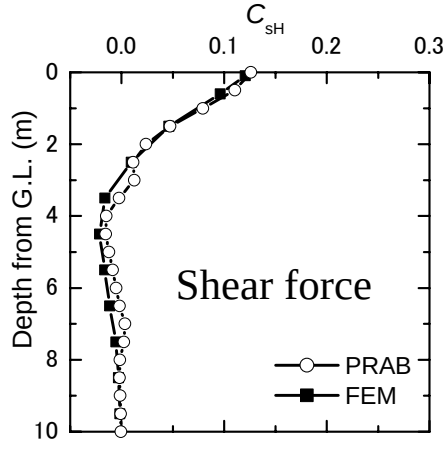

Piled raft

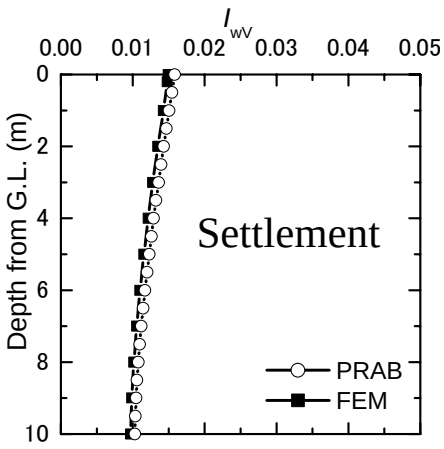

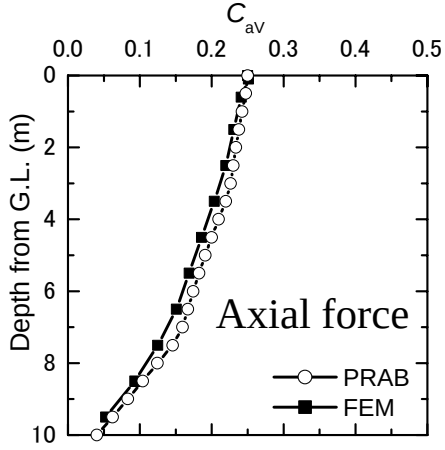

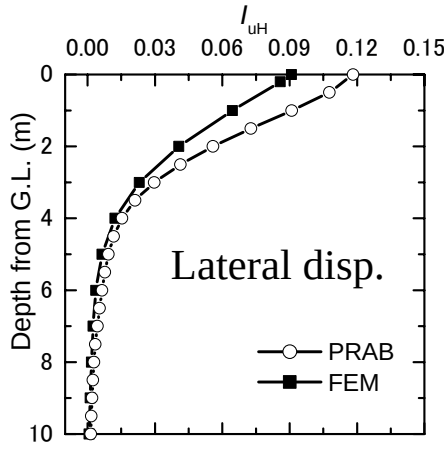

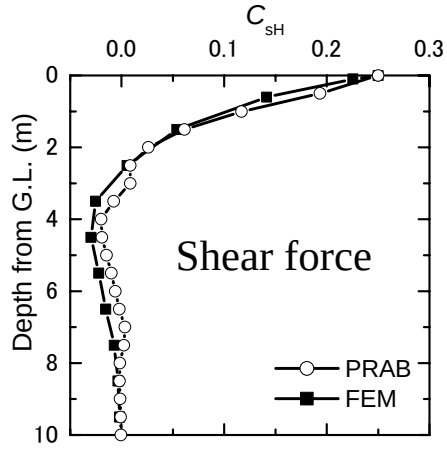

Pile group

Comparison Analysis

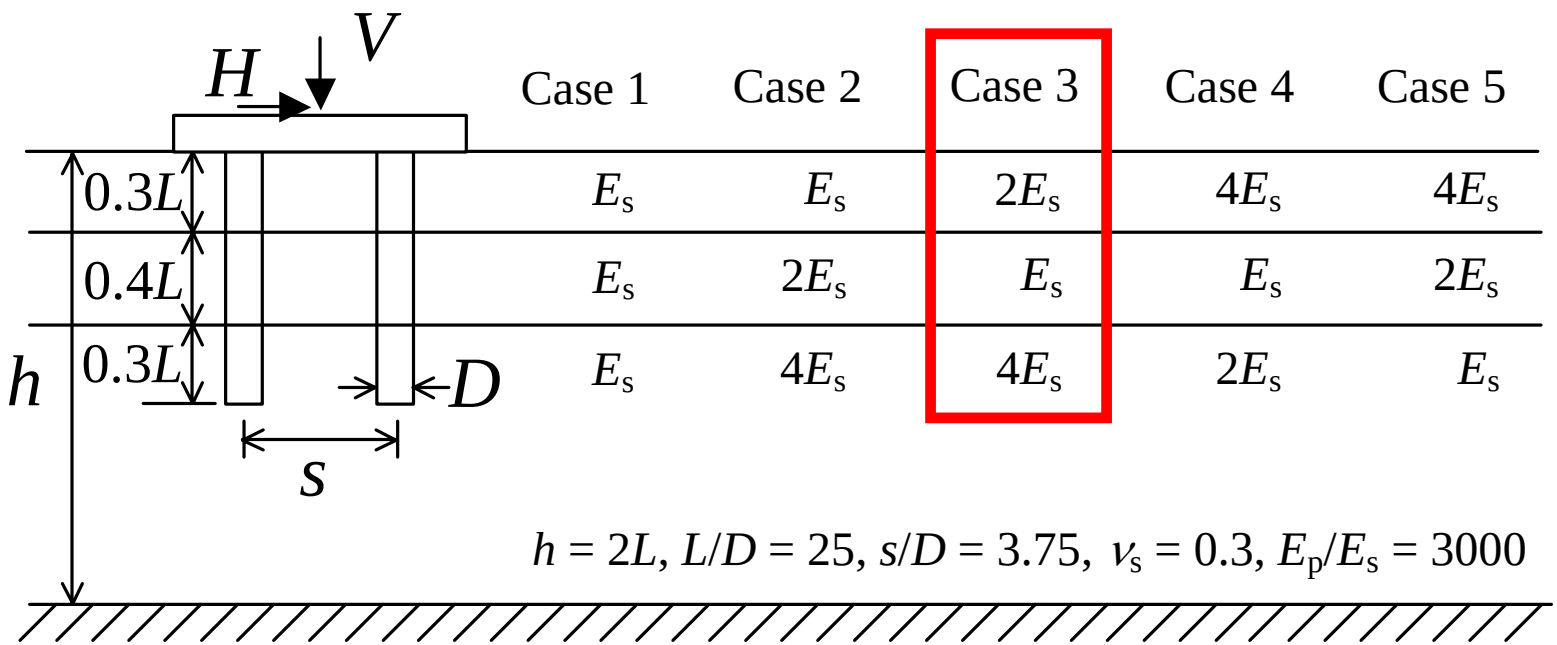

	Case 1	Case 2	Case 3	Case 4	Case 5
0.3L	E_s	E_s	$2E_s$	$4E_s$	$4E_s$
0.4L	E_s	$2E_s$	E_s	E_s	$2E_s$
0.3L	E_s	$4E_s$	$4E_s$	$2E_s$	E_s

$h = 2L$, $L/D = 25$, $s/D = 3.75$, $\nu_s = 0.3$, $E_p/E_s = 3000$

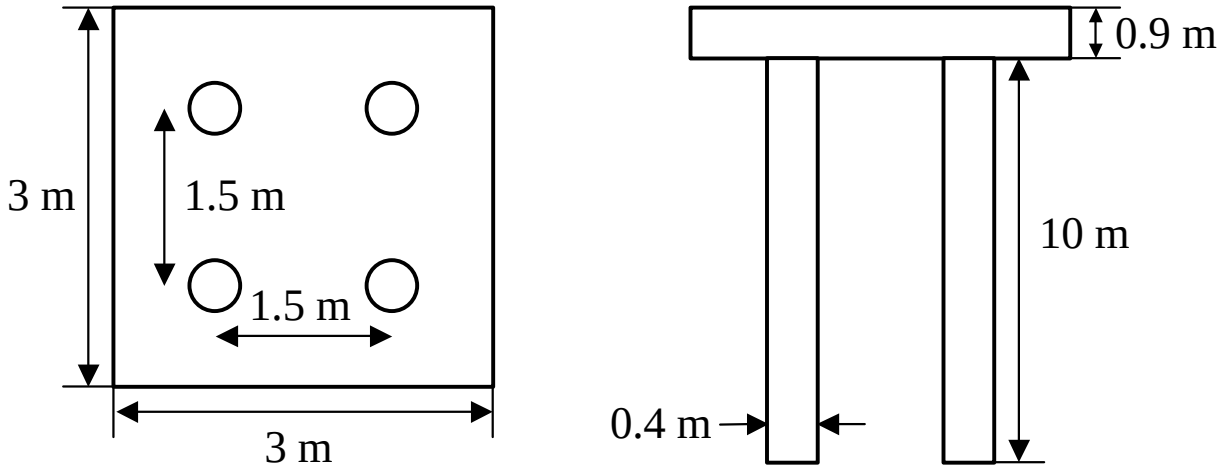

Comparison of calculated results

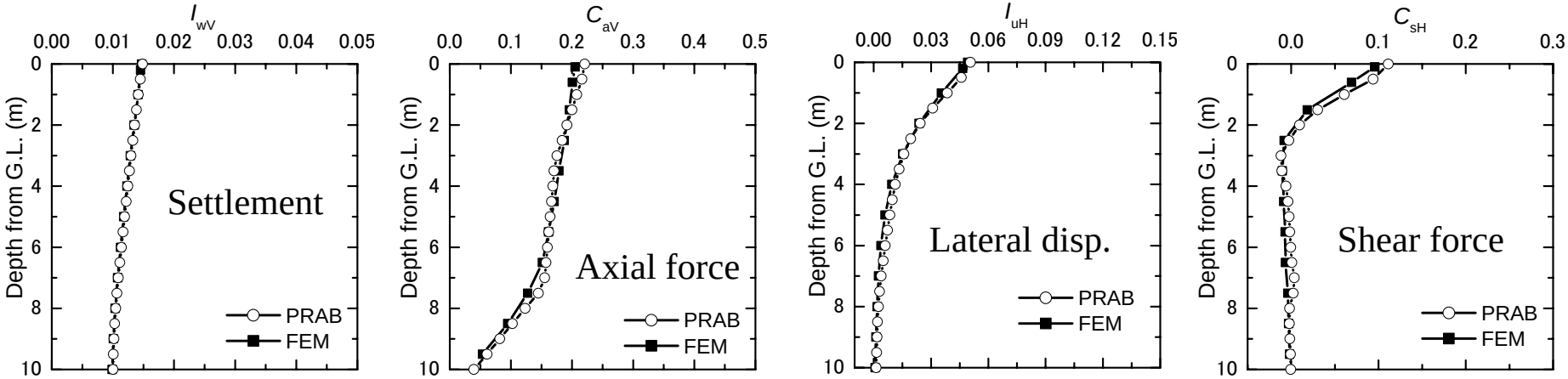

Piled raft

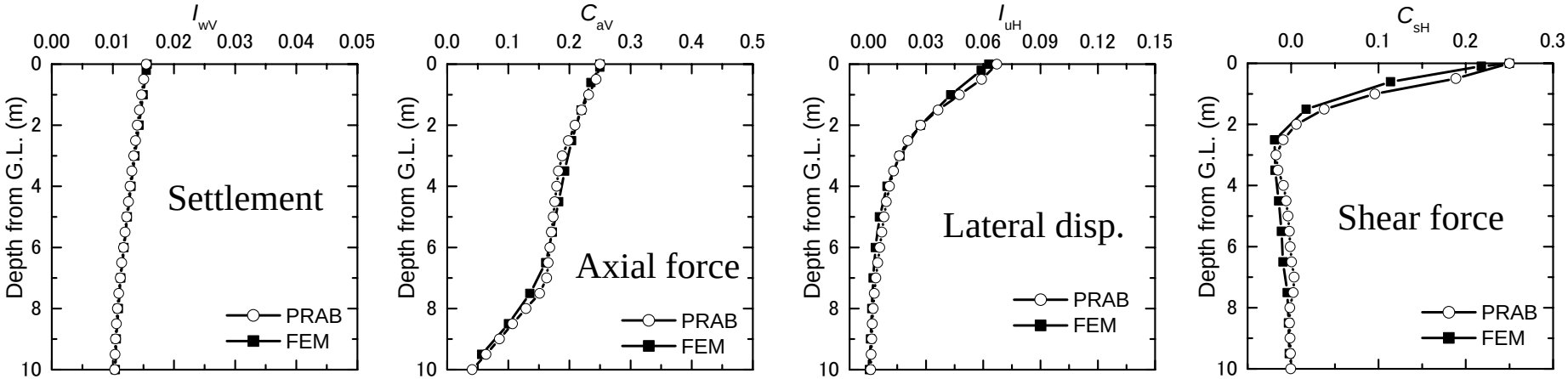

Pile group

Comparison Analysis

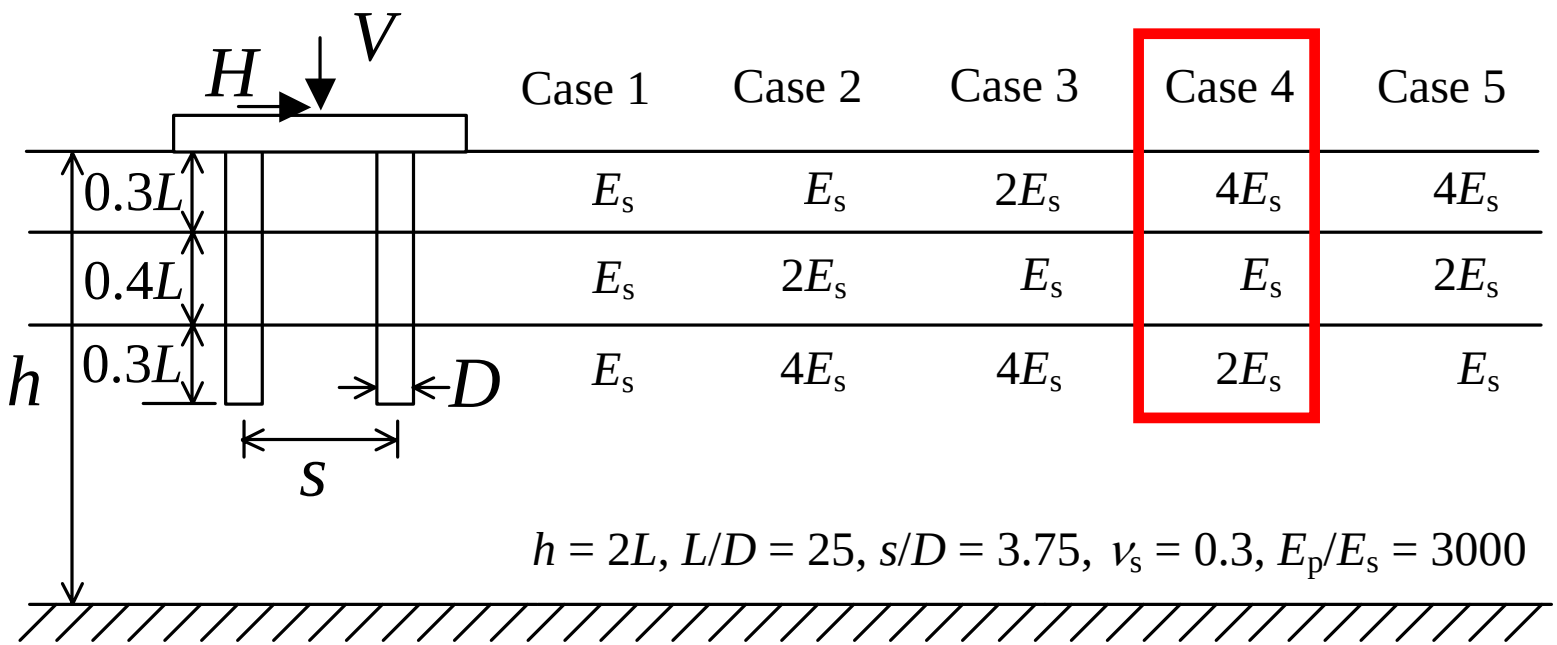

	Case 1	Case 2	Case 3	Case 4	Case 5
0.3L	E_s	E_s	$2E_s$	$4E_s$	$4E_s$
0.4L	E_s	$2E_s$	E_s	E_s	$2E_s$
0.3L	E_s	$4E_s$	$4E_s$	$2E_s$	E_s

$h = 2L$, $L/D = 25$, $s/D = 3.75$, $\nu_s = 0.3$, $E_p/E_s = 3000$

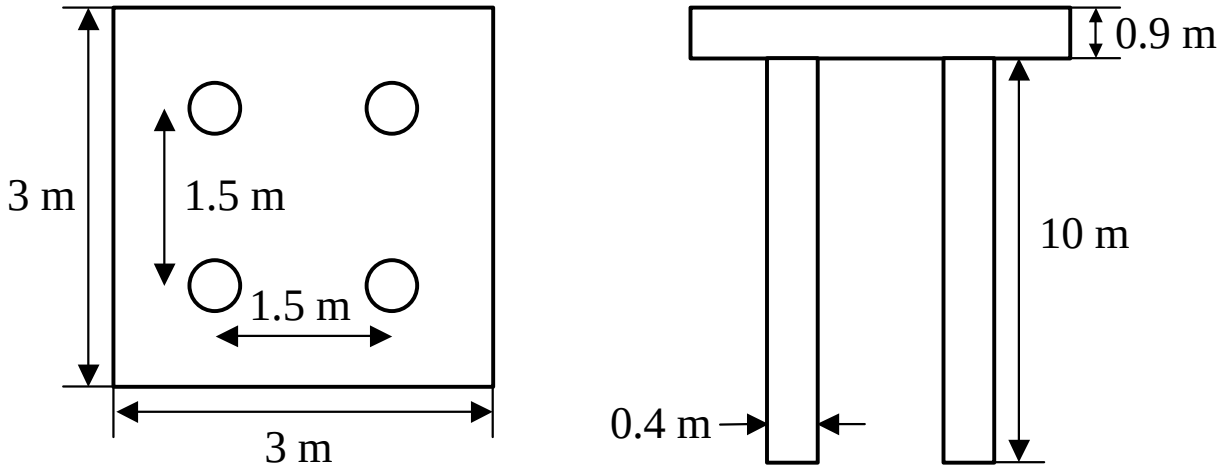

Comparison of calculated results

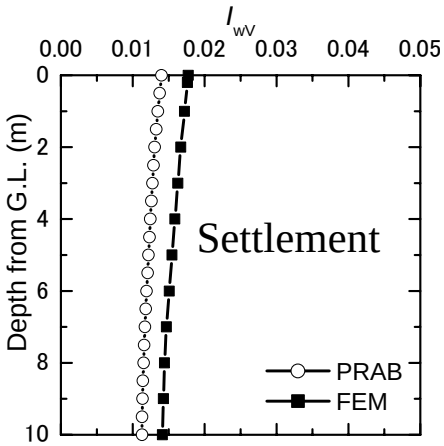

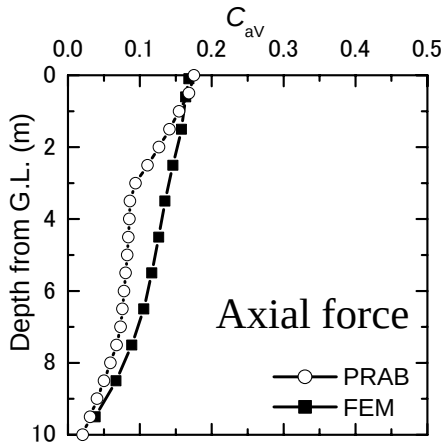

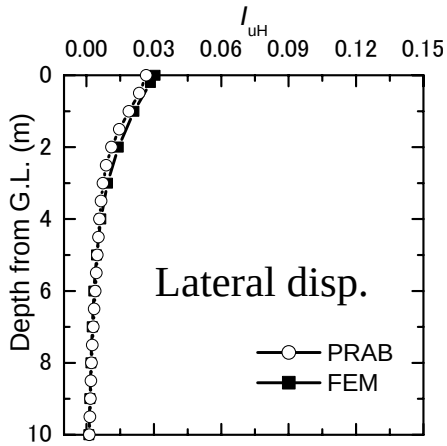

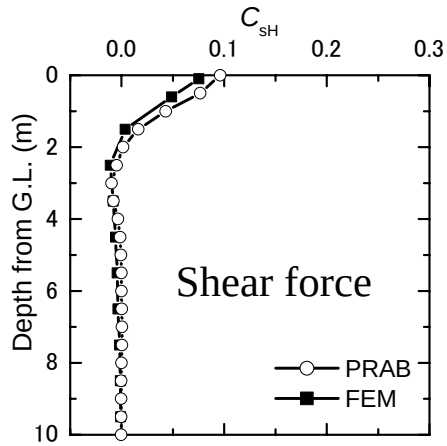

Piled raft

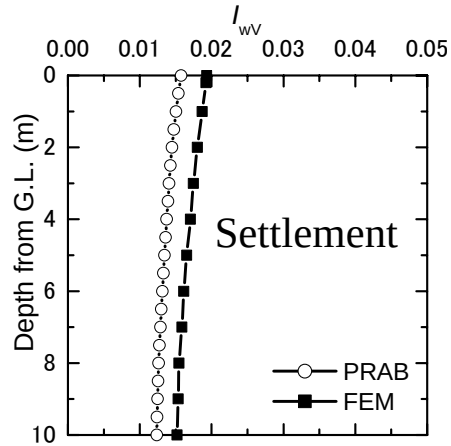

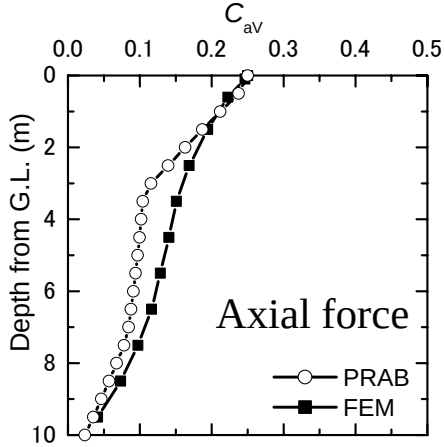

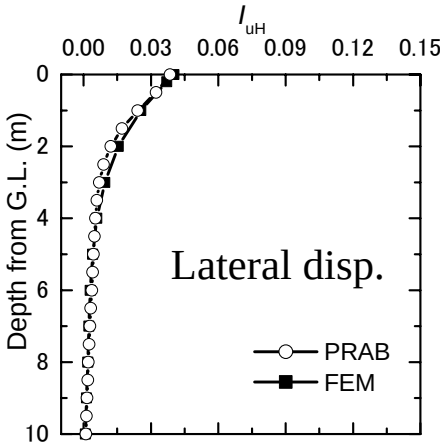

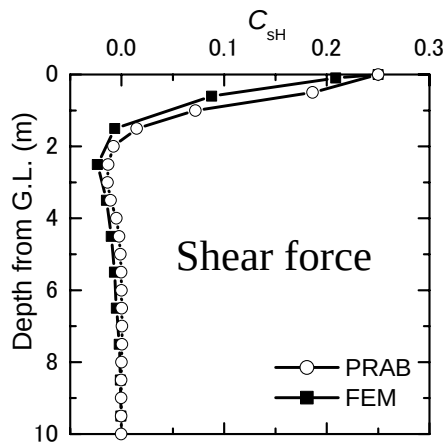

Pile group

Comparison Analysis

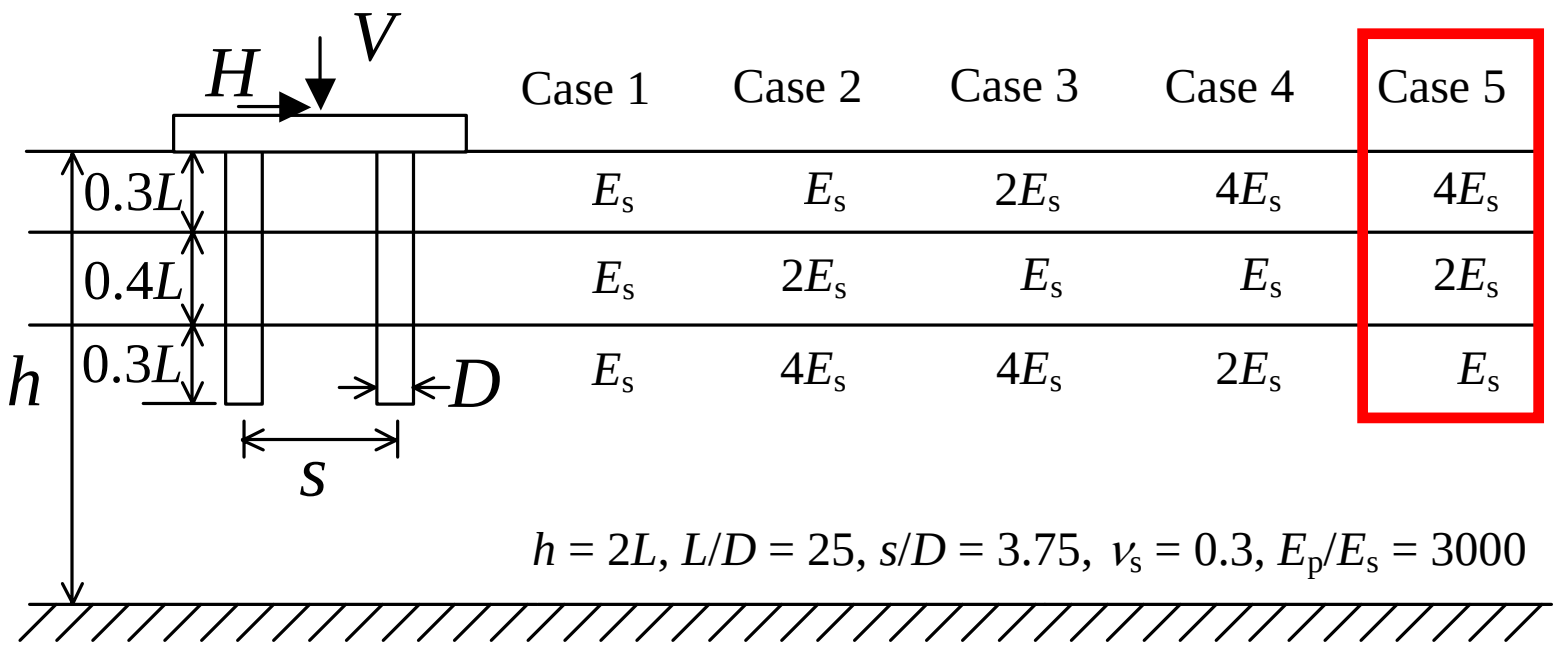

	Case 1	Case 2	Case 3	Case 4	Case 5
	E_s	E_s	$2E_s$	$4E_s$	$4E_s$
	E_s	$2E_s$	E_s	E_s	$2E_s$
	E_s	$4E_s$	$4E_s$	$2E_s$	E_s

$h = 2L$, $L/D = 25$, $s/D = 3.75$, $\nu_s = 0.3$, $E_p/E_s = 3000$

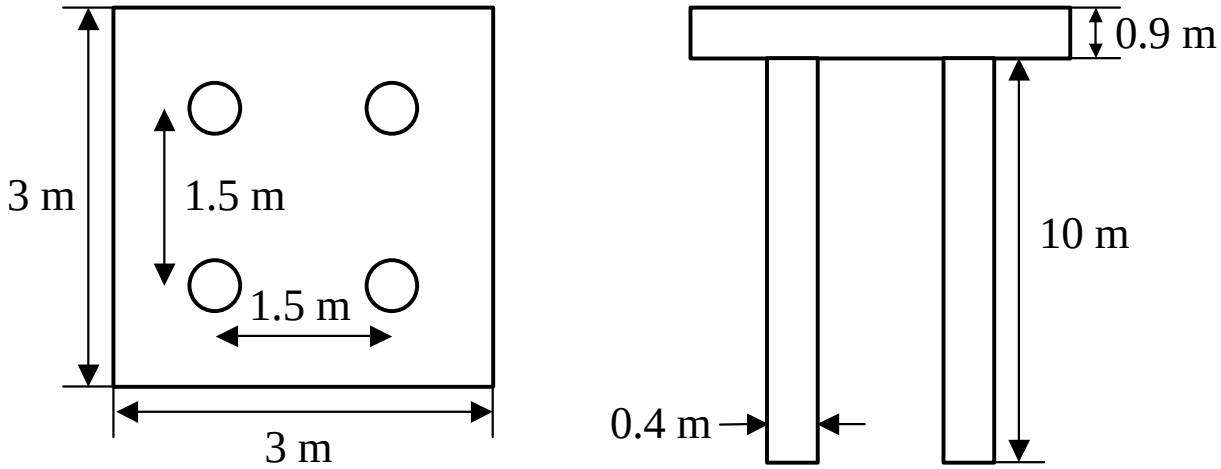

Comparison of calculated results

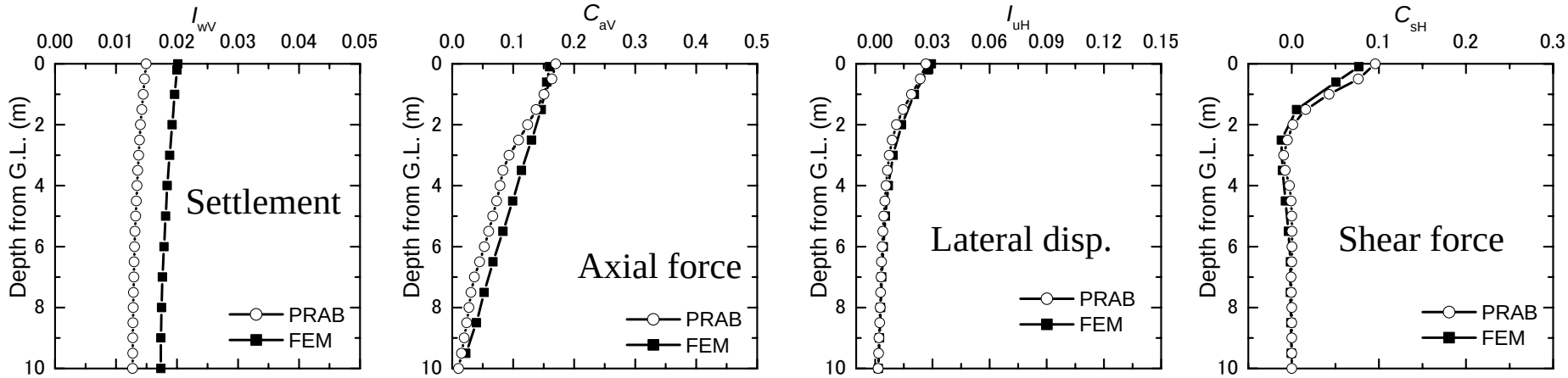

Piled raft

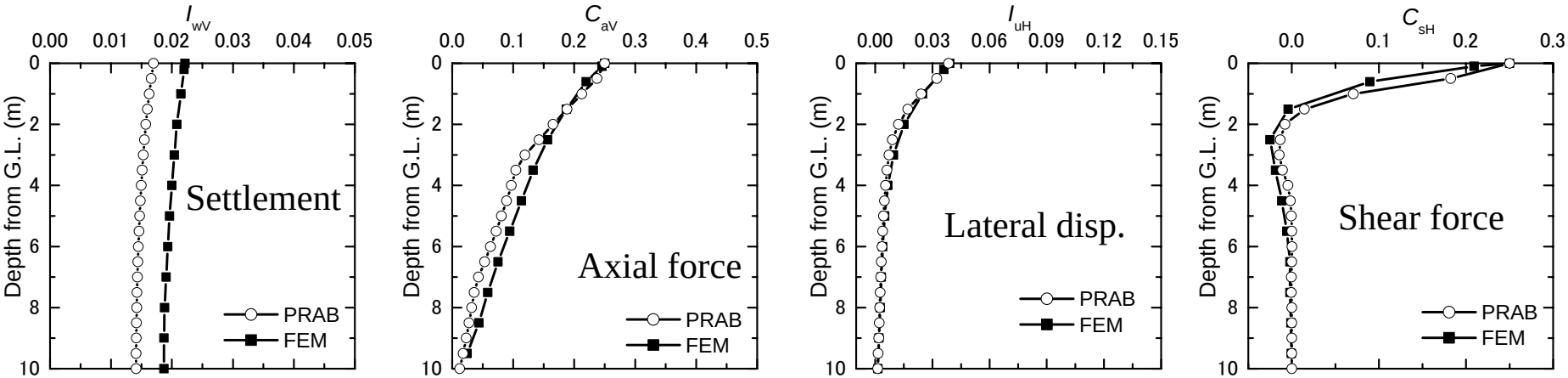

"A simplified analysis method for piled raft foundation has been developed. The validity of the proposed method was verified"

Part III: Verified the applicability of PRAB through analyses of the centrifuge model test results

Centrifuge test to be analyzed

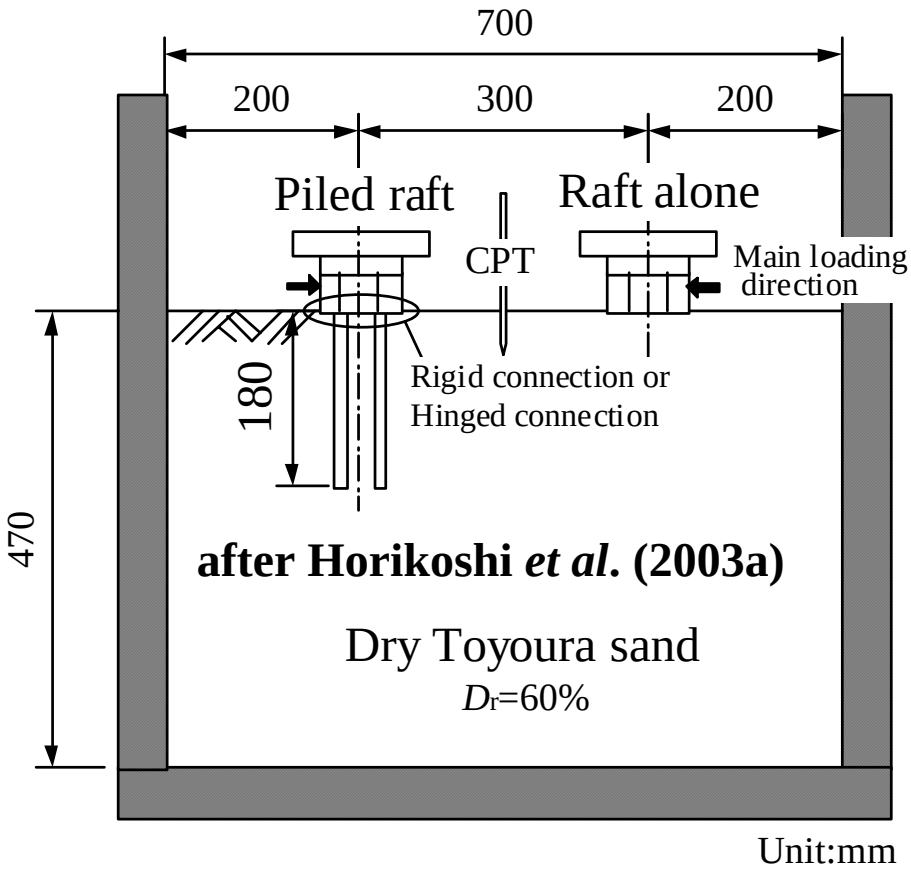

- Horikoshi *et al*. (2003a) has conducted a series of static vertical loading tests and lateral loading tests on piled raft models.
- Much focus was placed on the load-displacement relationship and the load sharing between the piles and the raft.
- Effects of the rigidity at pile head connection on the piled raft behaviour were also examined in their work.

In order to investigate applicability of PRAB, analysis of these centrifuge model test results were carried out.

Rigid pile head connection

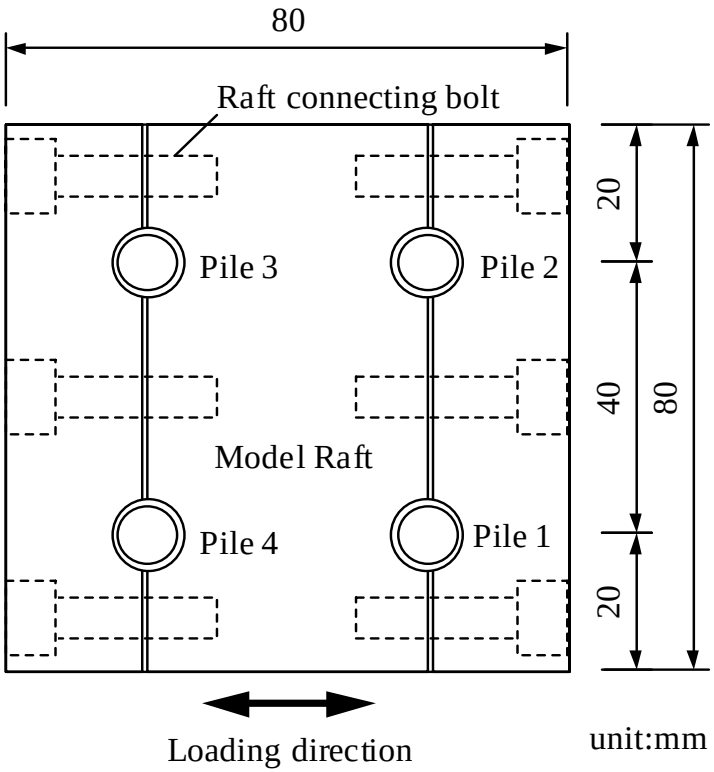

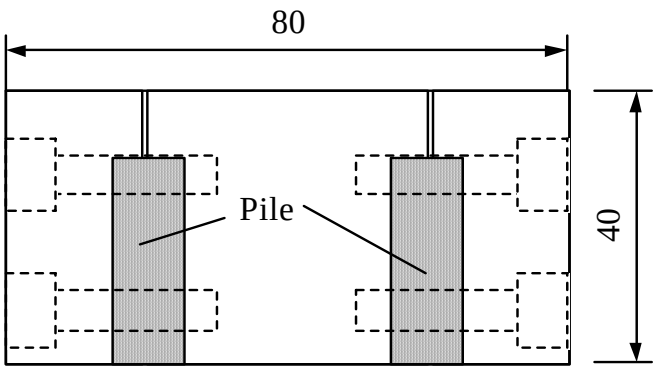

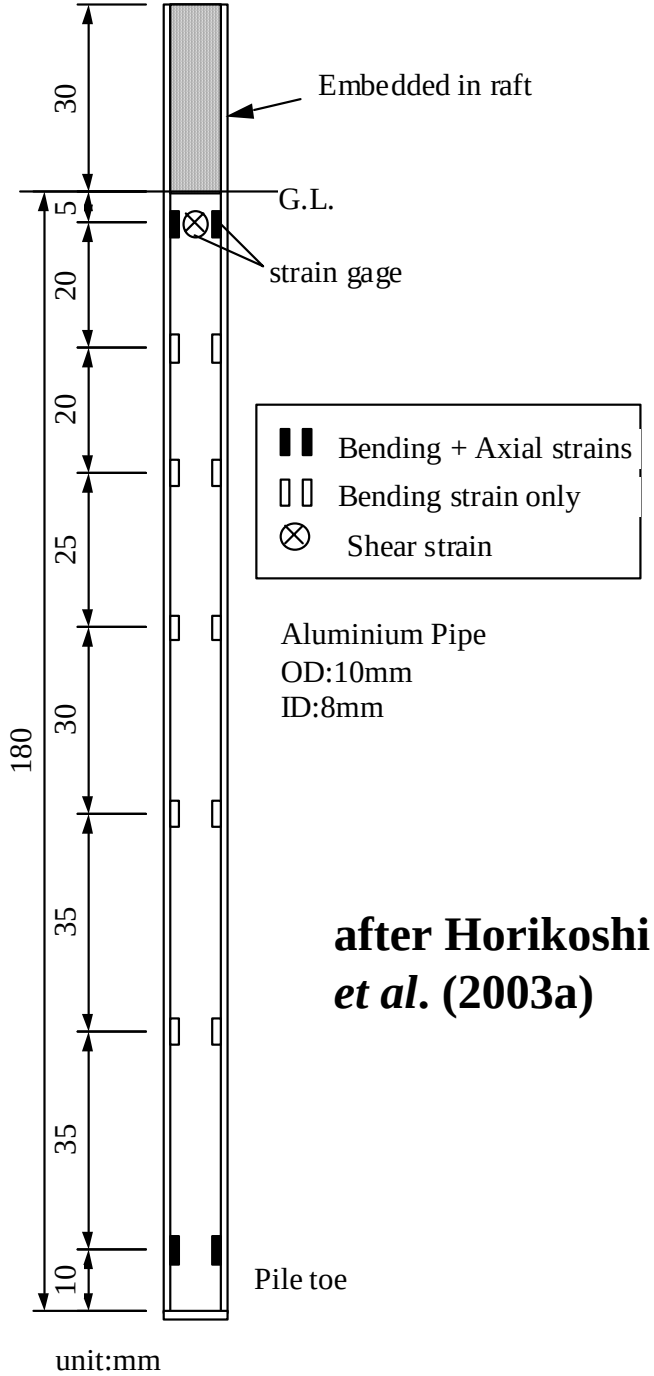

after Horikoshi *et al*. (2003a)

Hinged pile head connection

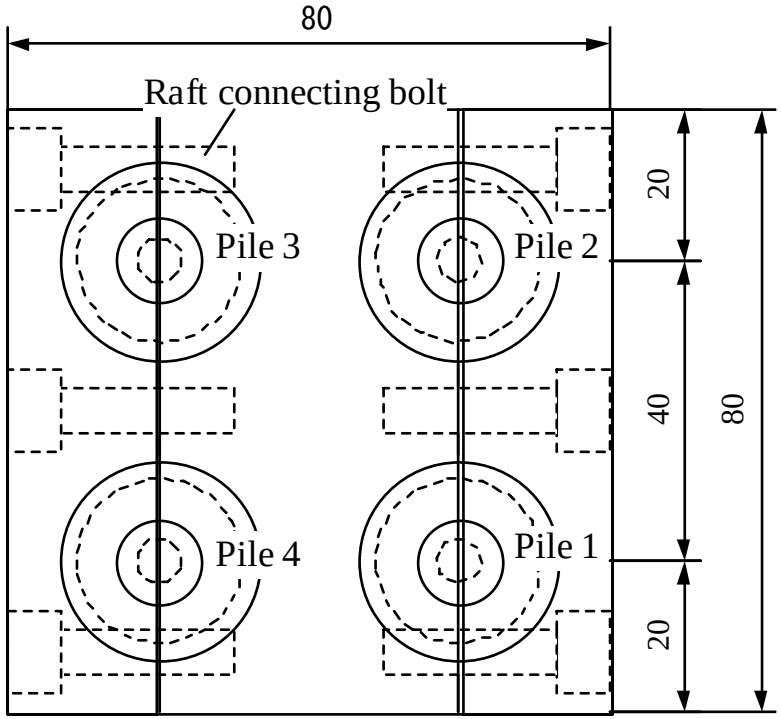

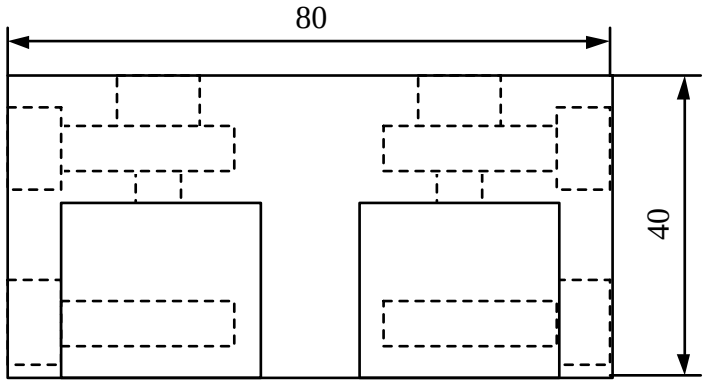

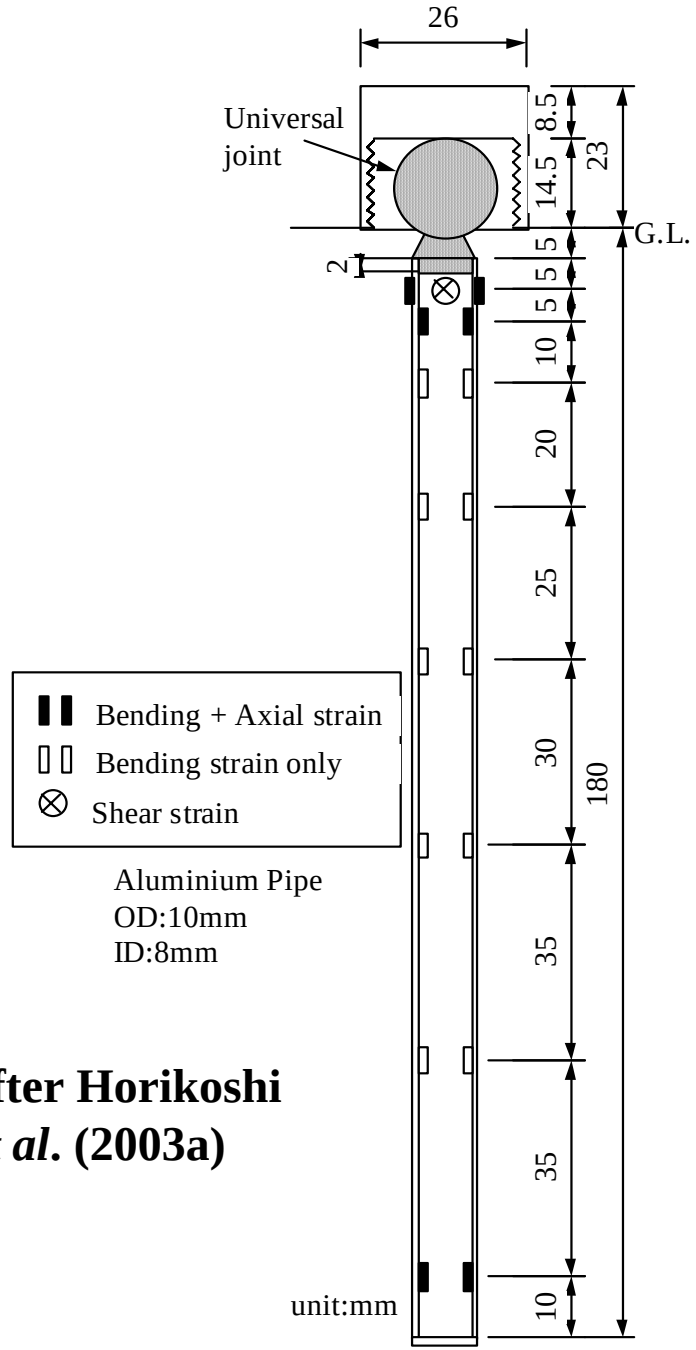

after Horikoshi *et al.* (2003a)

Analysis conditions

	Loading direction	
	Vertical loading	Lateral loading
Pile	Pile length = 170 mm	Pile length = 180 mm
	Outer diameter = 10 mm, Inner diameter = 8 mm Young's modulus = 70.6 GN/m^2 Poisson's ratio = 0.16	
Raft	Mass = 0.90 kg	Mass = 4.69 kg
	Width = 80 mm, Breadth = 80 mm Thickness = 25 mm (substantially rigid) Young's modulus = 70.6 GN/m^2 Poisson's ratio = 0.16	
Soil	Layer depth = 470 mm	Layer depth = 480 mm
	Density = 1.52 t/m^3, Internal friction angle = 35˚ Void ratio = 0.76, Poisson's ratio = 0.3 Finite homogeneous layer	

Analysis conditions (Vertical direction)

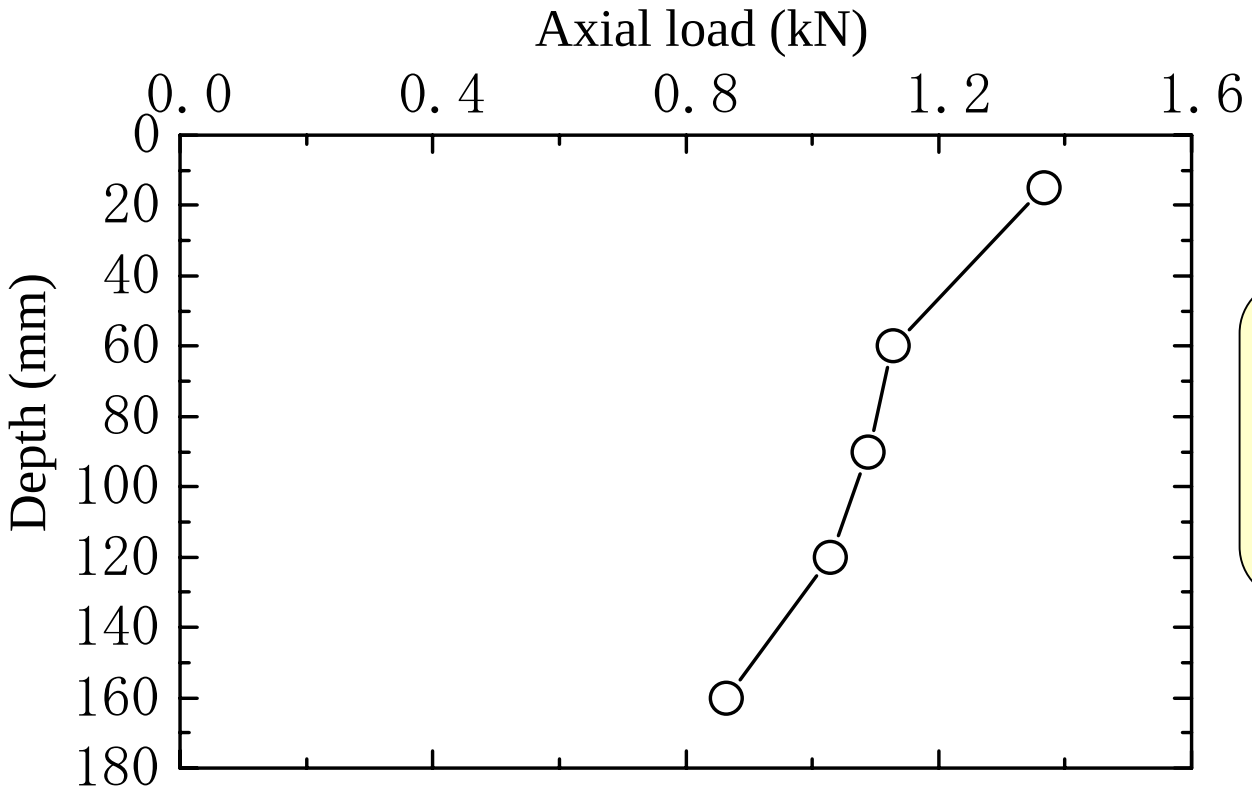

τ_s = 100 kN/m^2
q = 10000 kN/m^2

- In order to take into account the non-linear response, the value of the uniform pile shaft resistance and the pile base bearing capacity were set as 100 kN/m^2 and 10000 kN/m^2, respectively.
- No failure occurred at the raft base.

Load-settlement relationship

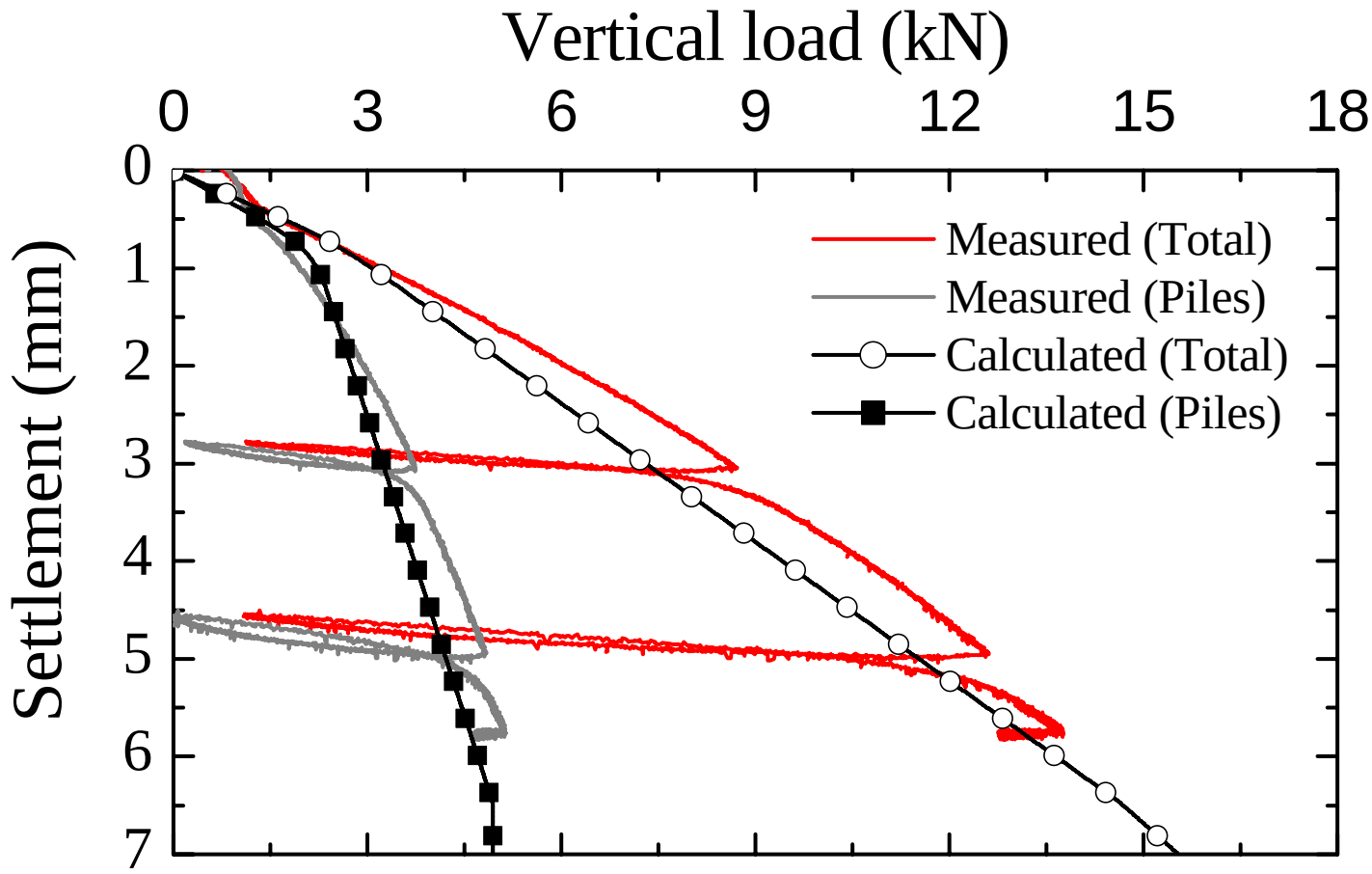

Proportions of vertical loads carried by raft and piles

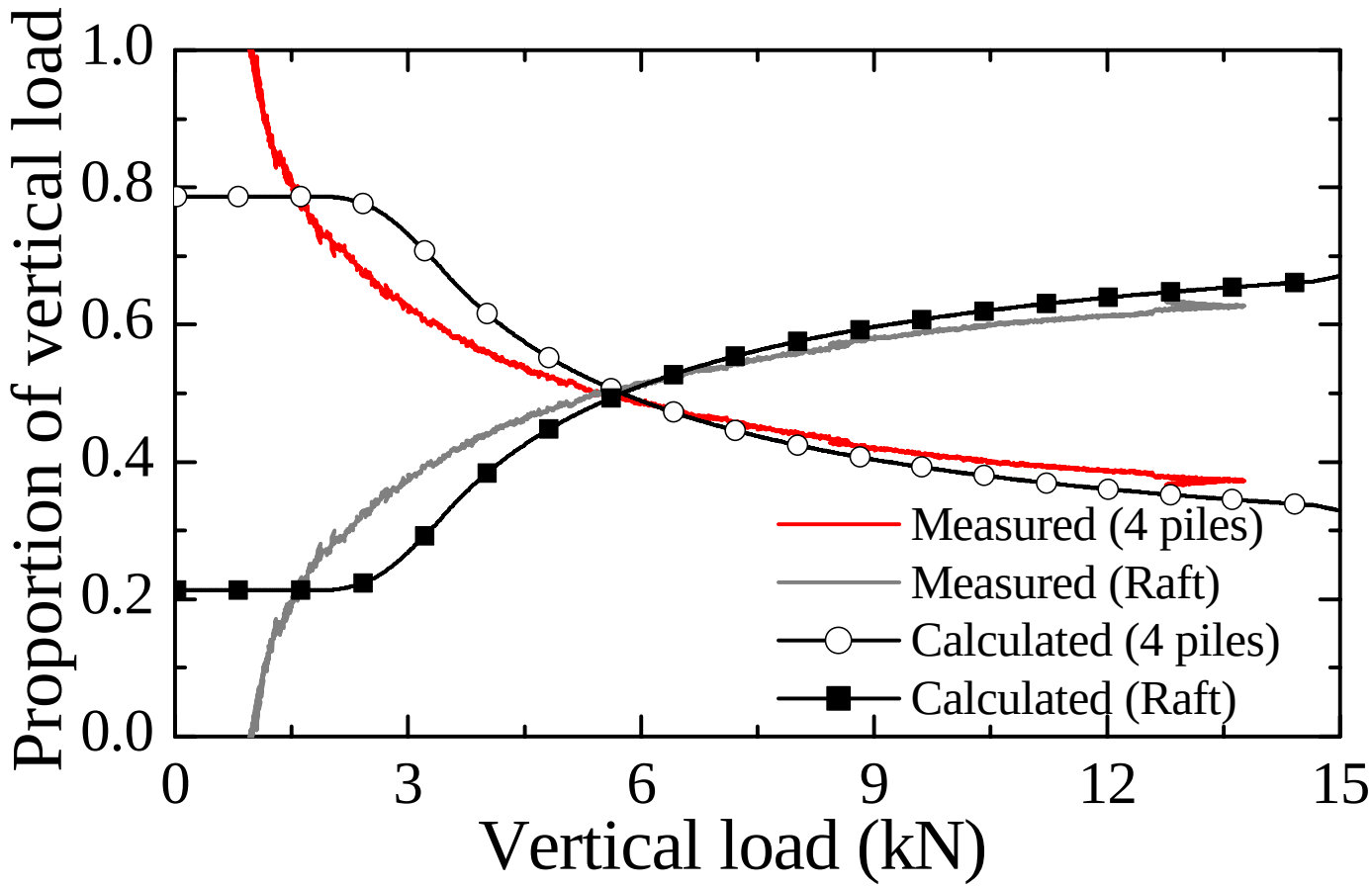

Analysis conditions (Lateral direction)

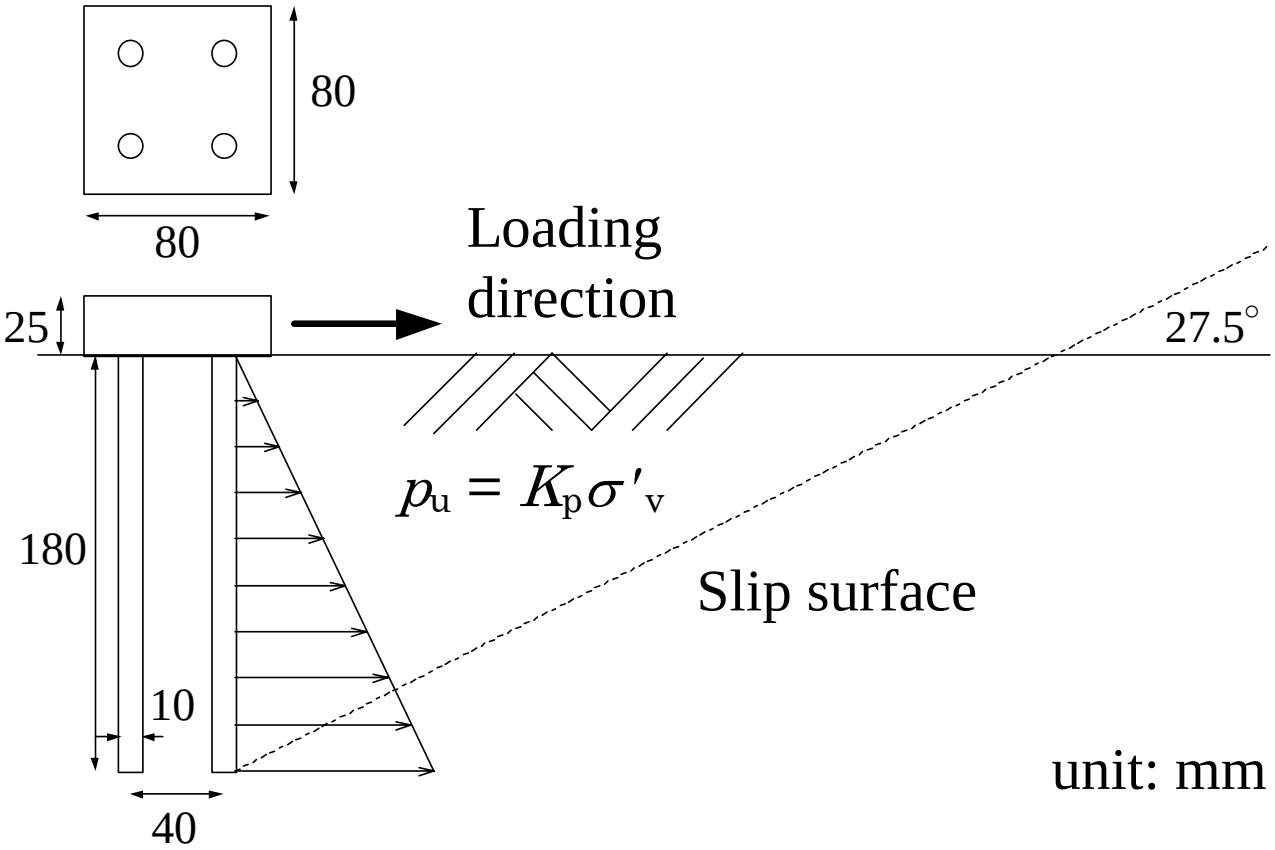

- The analysis is conducted for only lateral loading stage. The vertical load carried by the raft before the lateral loading is taken into account as the initial condition and is assumed to distribute uniformly over the raft base.

- In the estimation of the limit lateral pressure of the piles located just beneath the raft in cohesionless soils, the effect of the increase in the vertical stress of the soil due to the vertical load transferred through the raft should be taken into account.

Limit lateral pressure of the piles

Limit lateral pressure of pile $p_u = K_p \sigma'_v$

Effective stress $\sigma'_v = \sigma'_{v0} + \Delta\sigma'_{v0}, \quad \sigma'_{v0} = \gamma_t H$

Increase of stress due to overburden pressure $$\Delta\sigma'_{v0} = \frac{q_0 \times B \times L}{(B+z)(L+z)}$$

Rankine passive earth pressure coefficient $$K_p = \frac{1+\sin\phi}{1-\sin\phi}$$

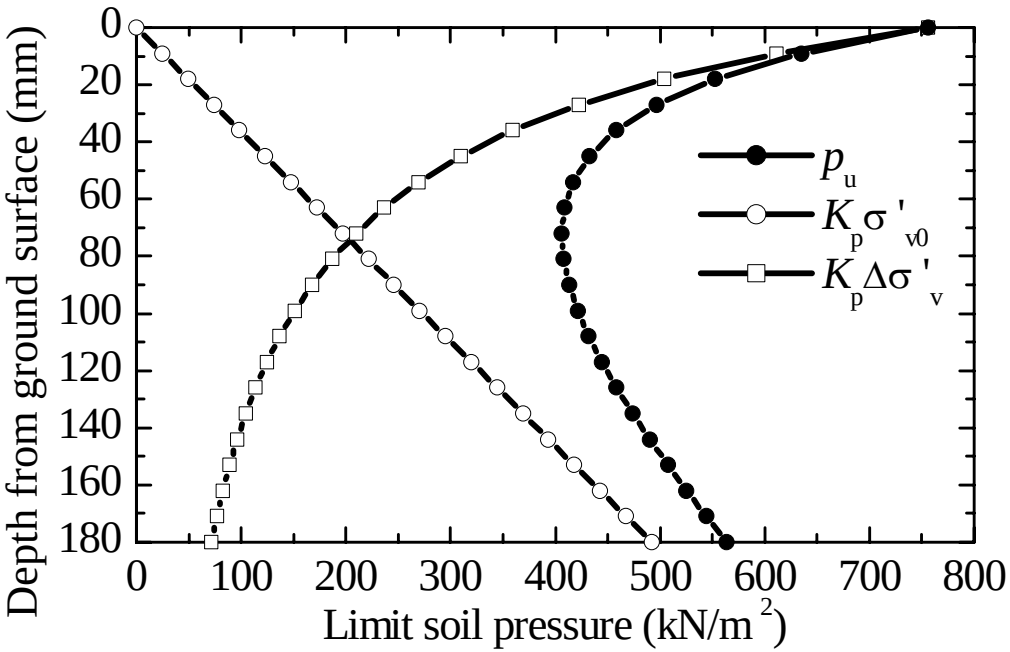

Finite Homogeneous soil

(bi-linear spring model)

$\phi = 35^\circ$

$\gamma_t = 14.9\ \text{kN/m}^3$

$\mu = 0.42$

Load-displacement relationship

Rigid pile head connection

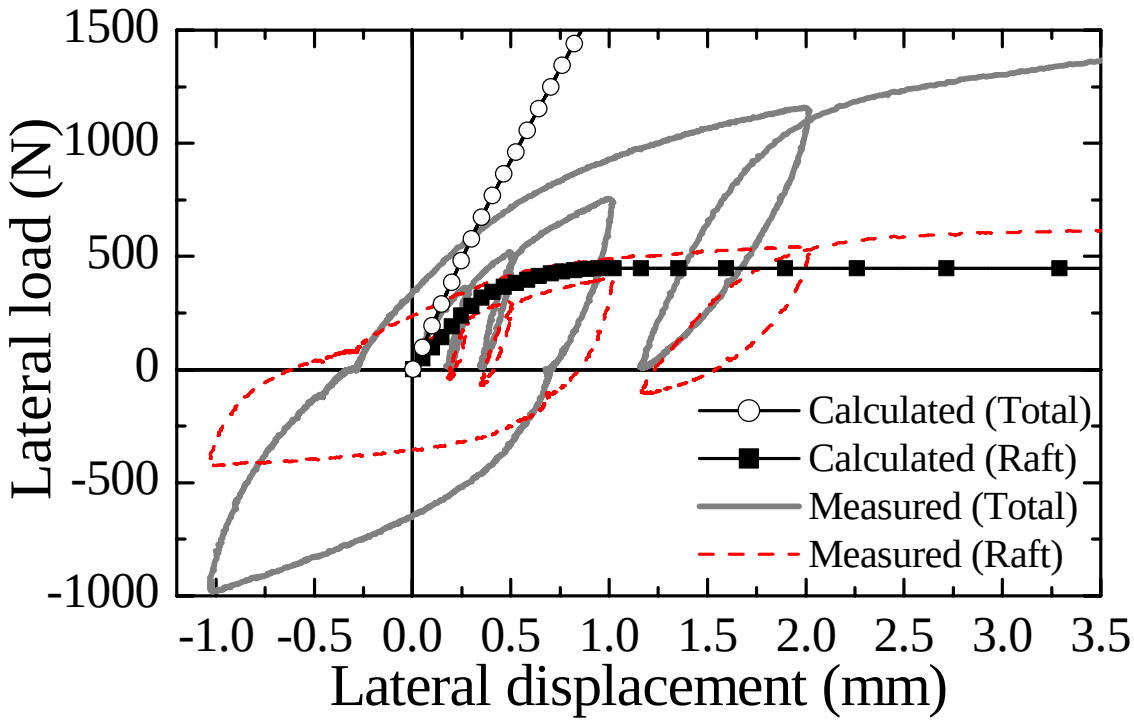

- The calculated results that consider the effect of the increase in the soil stress beneath the raft overestimate the measured total lateral resistance, because of the overestimate of the lateral pile resistance.

Configuration of the model piled raft

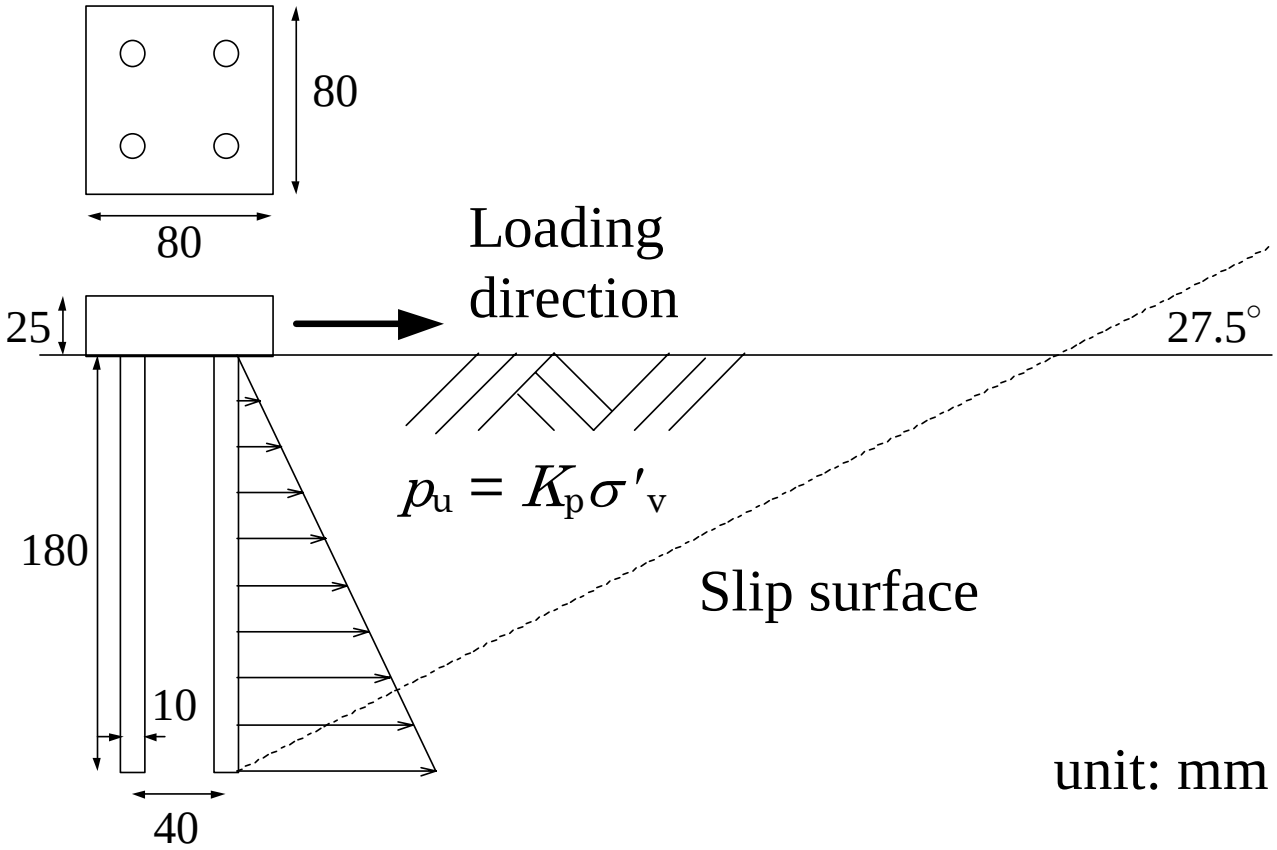

- The raft breadth is relatively narrow compared to the pile length.
- Hence the effect of the increase in the soil stress beneath the raft on the value of the limit lateral pressure of the pile is small.

Load-displacement relationship

Rigid pile head connection

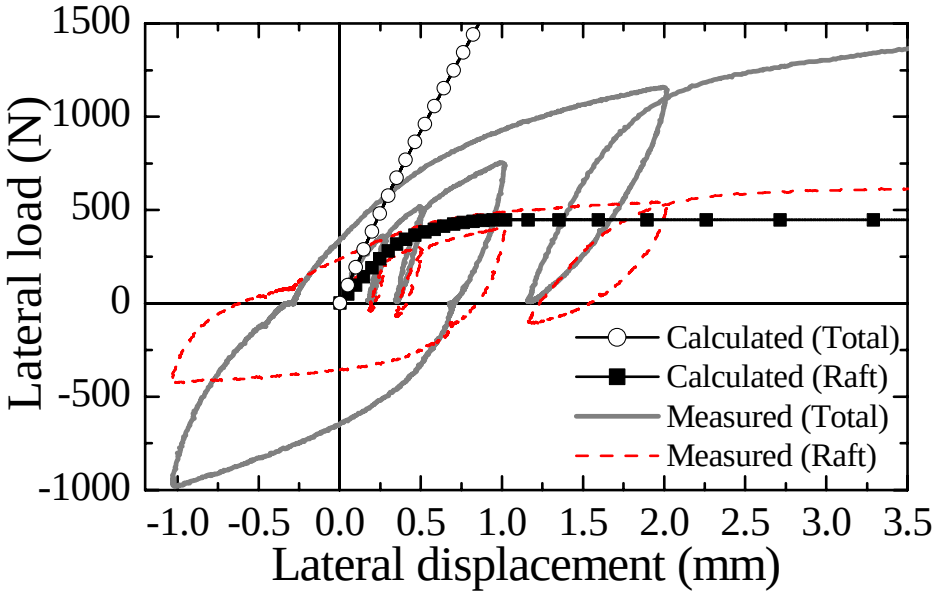

a) Consider increase in the soil stress beneath the raft0

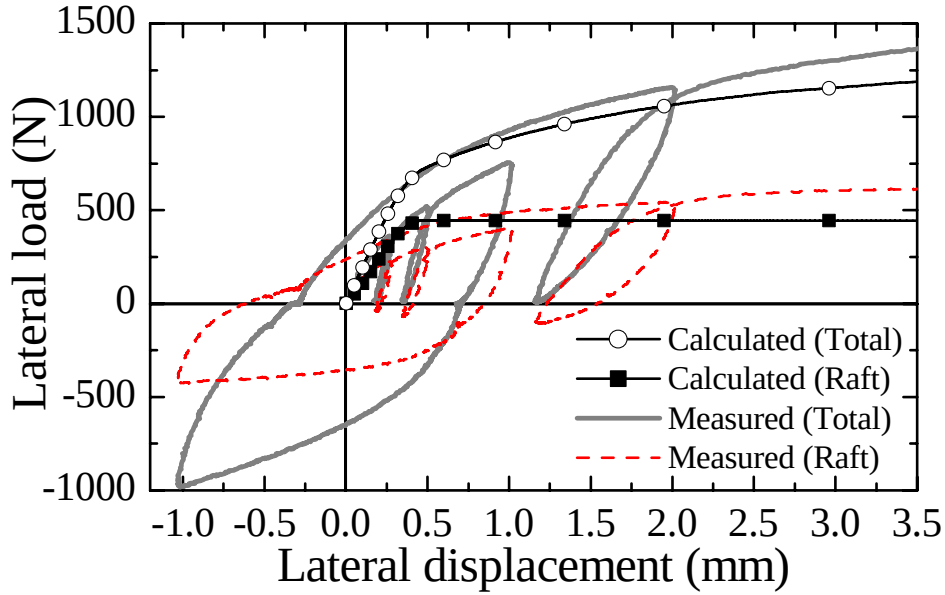

b) No increase in the soil stress beneath the raft

- Consequently, the calculated results which neglected the effect of the increase in the soil stress beneath the raft are closer to the measured values.
- The analysis results hereafter were calculated using the limit soil pressure value without the effect of the increase in the soil stress beneath the raft.

Load-displacement relationship

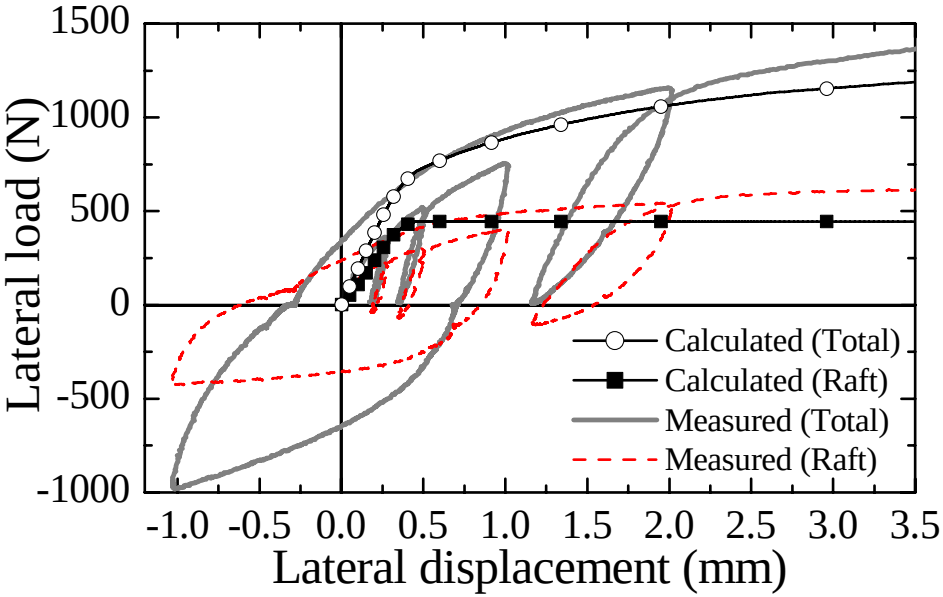

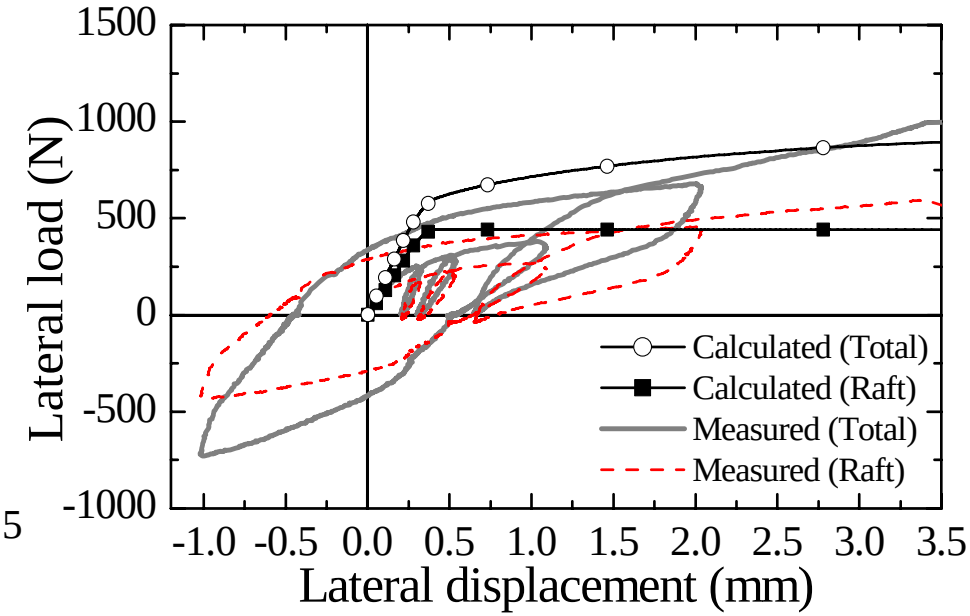

Rigid pile head connection **Hinged pile head connection**

- The piles in the piled raft with the hinged pile head connection carry smaller amount of the lateral load than those in the piled raft with the rigid pile head connection, while the amount of the lateral load carried by the raft is almost the same.

Proportion of lateral load carried by piles

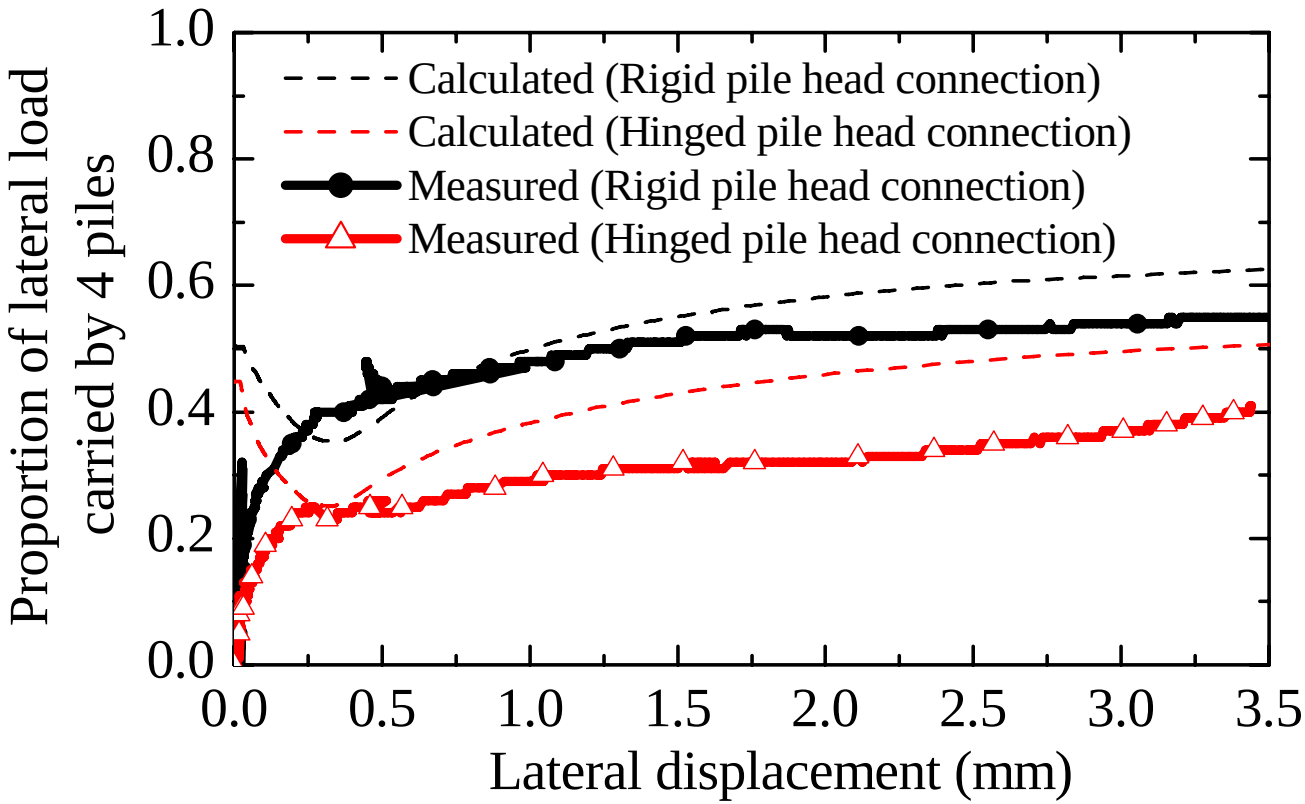

"Even though the proposed method is *simple*, the method can be used with a *confidence* as a design tool for piled raft foundations"

Horizontal load test to be analyzed

- Analyses of the static vertical and horizontal load test results of model pile group and model piled raft foundations with different pile head connection rigidities are carried out using a computer program PRAB (Piled Raft Analysis with Batter piles).
- Good agreements between the calculated results and the experimental results will be demonstrated.

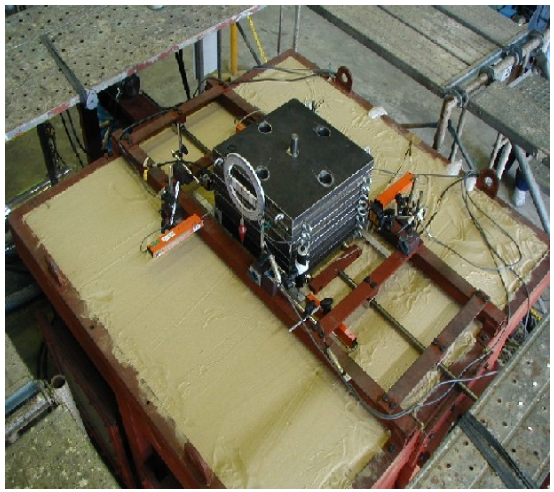

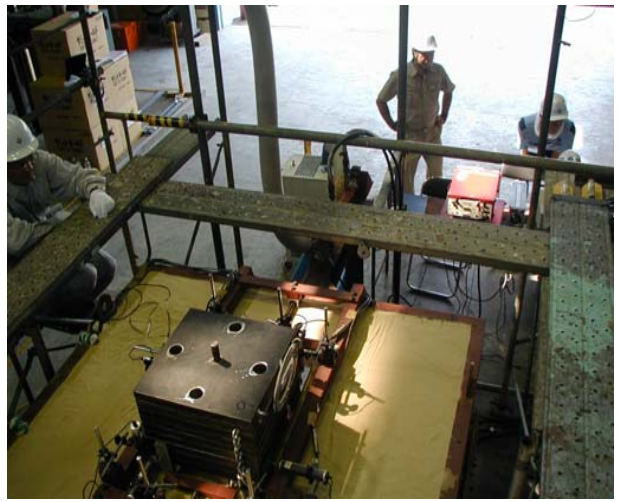

Horizontal load tests of pile group and piled raft models after Nemoto et al. (2006)

Test set-up

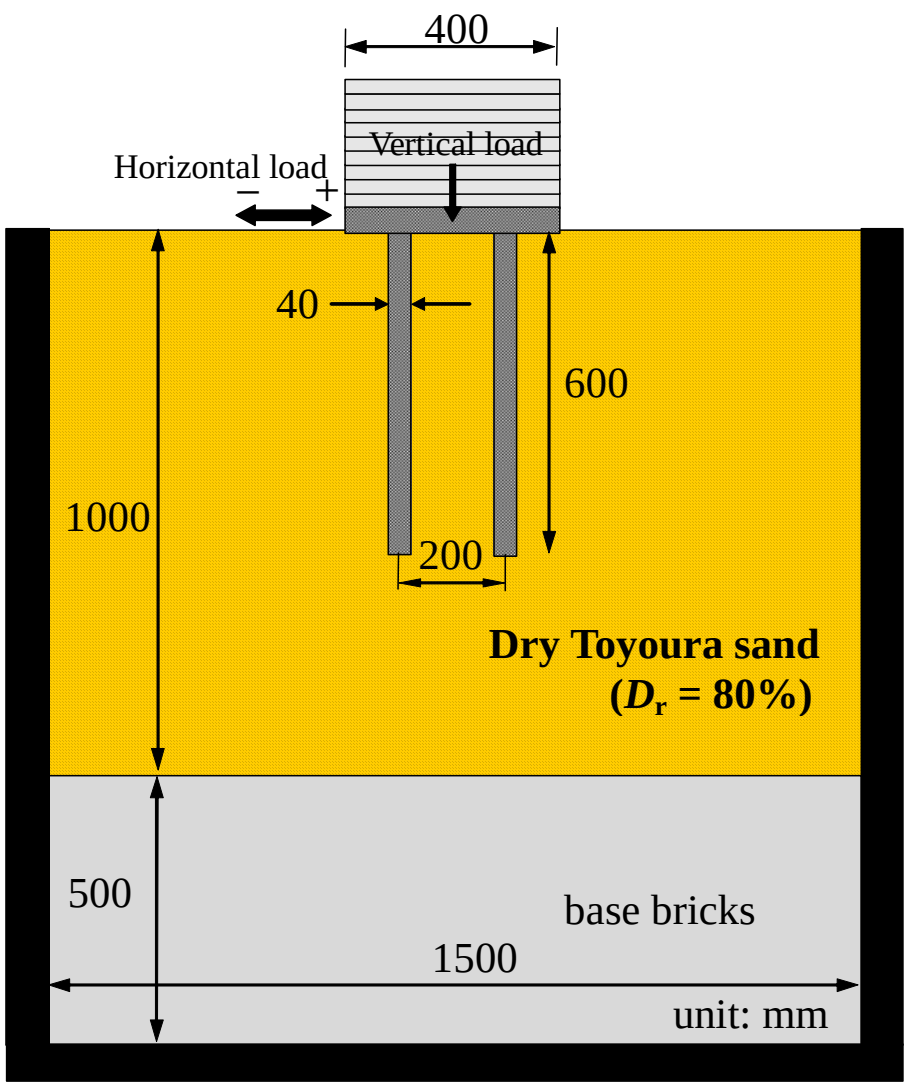

Analysis conditions

	Property	Value
Pile	Pile length	600mm
	Outer diameter	40mm
	Inner diameter	36mm
	Young's modulus	7×10^4kPa
	Poisson's ratio	0.3
Raft	Width	400mm
	Breadth	400mm
	Thickness	40mm
	Young's modulus	1.93×10^5 kPa
	Poisson's ratio	0.3
Soil	Layer depth	1000mm
	Poisson's ratio	0.3

Model foundations

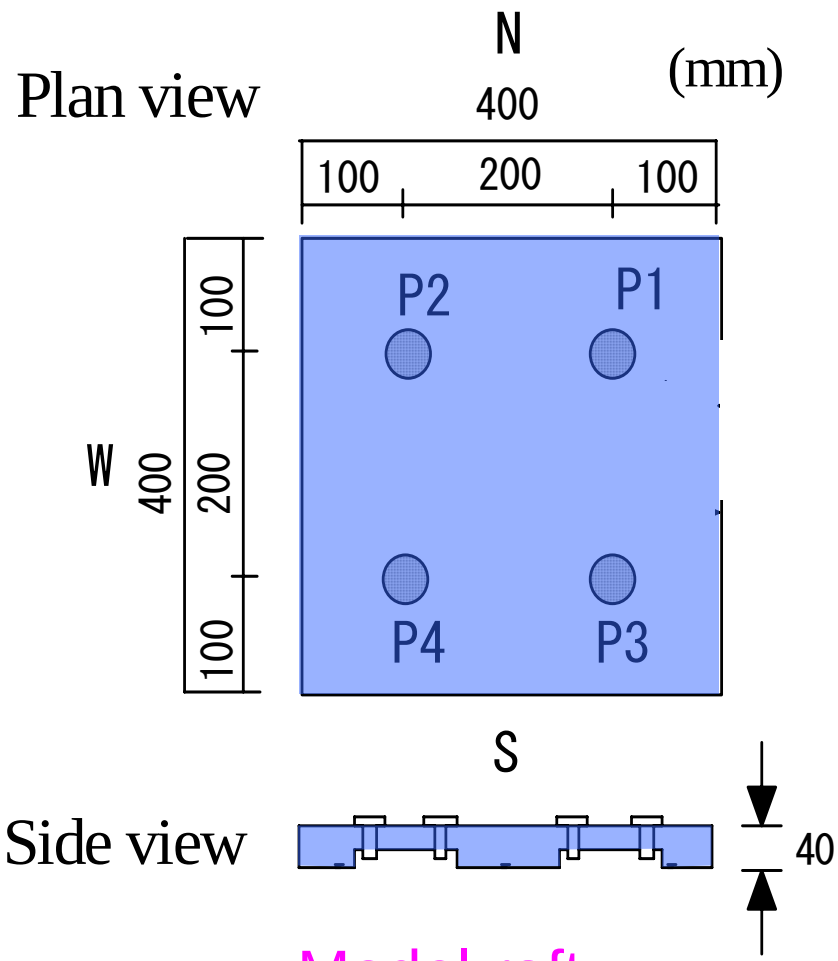

Model raft

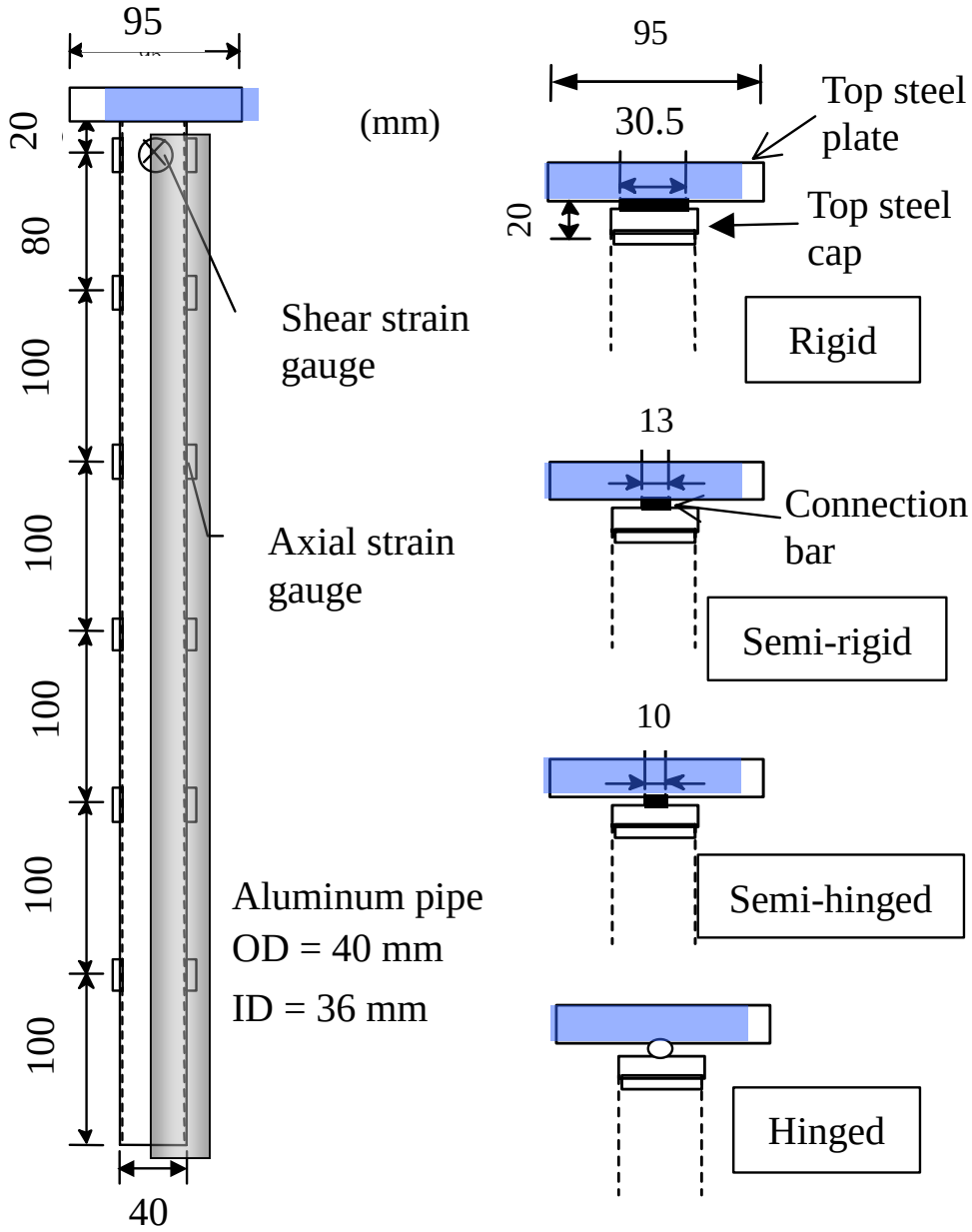

Model piles with different pile head connection conditions

Hybrid analytical model

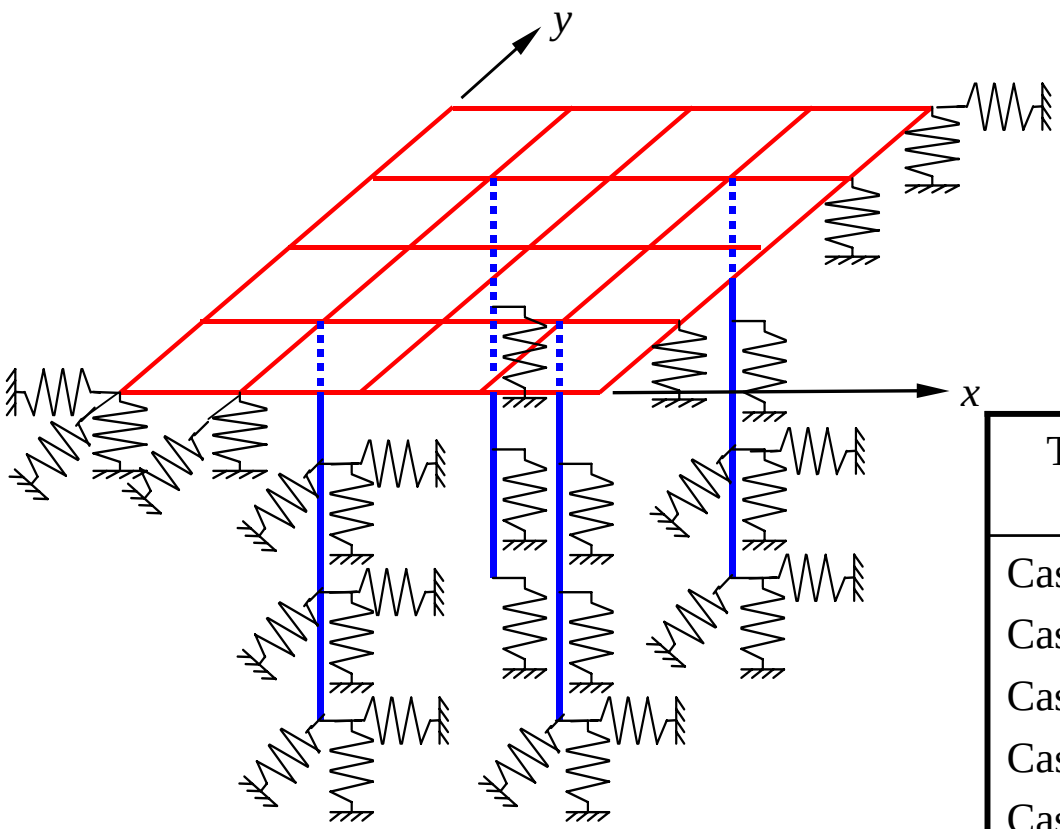

Plate-beam-spring modelling of a piled raft

Raft: thin plates

Piles: elastic beams

Soil: interactive springs

Model load test cases

Test name	Type of foundation	Pile head condition
Case1:Raft	Raft alone	–
Case2:PG-R	Pile group	Rigid
Case3:PG-H	Pile group	Hinged
Case4:PR-R	Piled raft	Rigid
Case5:PR-SR	Piled raft	Semi-rigid
Case6:PR-SH	Piled raft	Semi-hinged
Case7:PR-H	Piled raft	Hinged

Soil properties

Physical properties of Toyoura sand

D_r = 80 %

Property	Value
Maximum dry density, ρ_{dmax}	1.621t/m^3
Minimum dry density, ρ_{dmin}	1.328t/m^3
Density of soil particle, ρ_s	2.637t/m^3
Mean grain size,D_{50}	0.17 mm
Internal friction angle, ϕ'	40 degrees

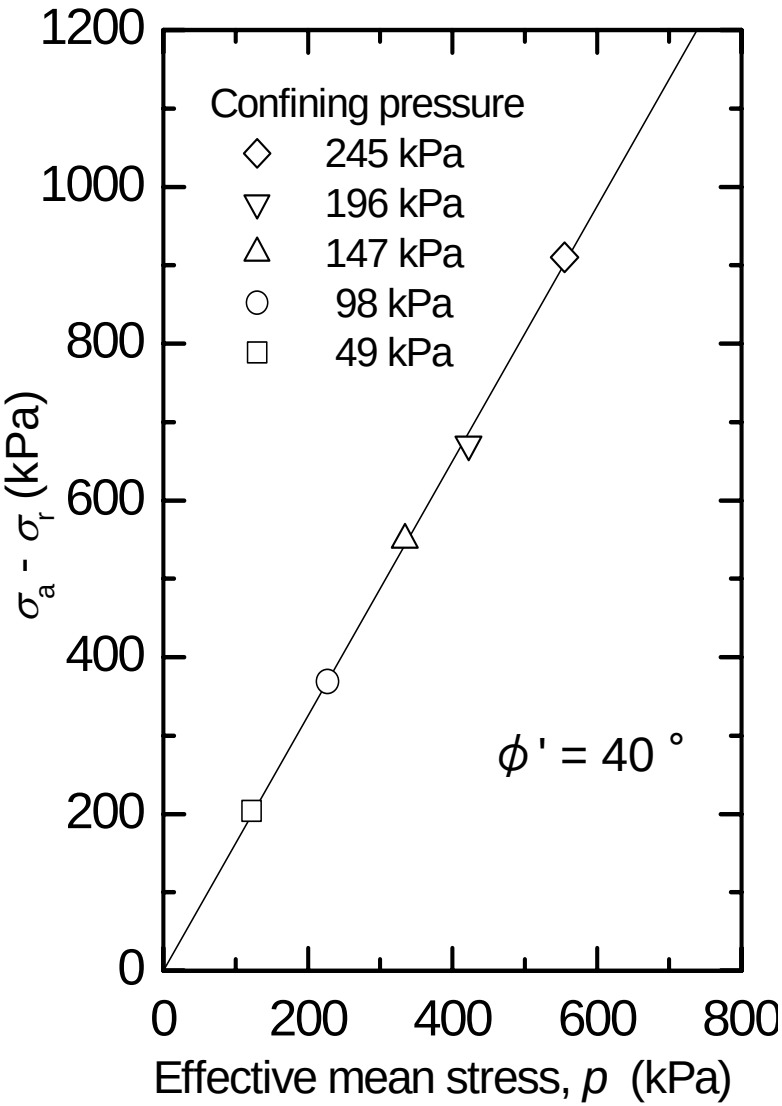

Deviator stress versus effective mean stress

Soil properties

Physical properties of Toyoura sand

D_r = 80 %

Property	Value
Maximum dry density, ρ_{dmax}	1.621t/m^3
Minimum dry density, ρ_{dmin}	1.328t/m^3
Density of soil particle, ρ_s	2.637t/m^3
Mean grain size,D_{50}	0.17 mm
Internal friction angle, ϕ'	40 degrees

$$G = G_{ref}\left(\frac{p}{p_{ref}}\right)^{0.5} \qquad (1)$$

$$p = (1+2K_0)\cdot\sigma'_v/3 \qquad (2)$$

$$K_0 = 1-\sin\phi' \qquad (3)$$

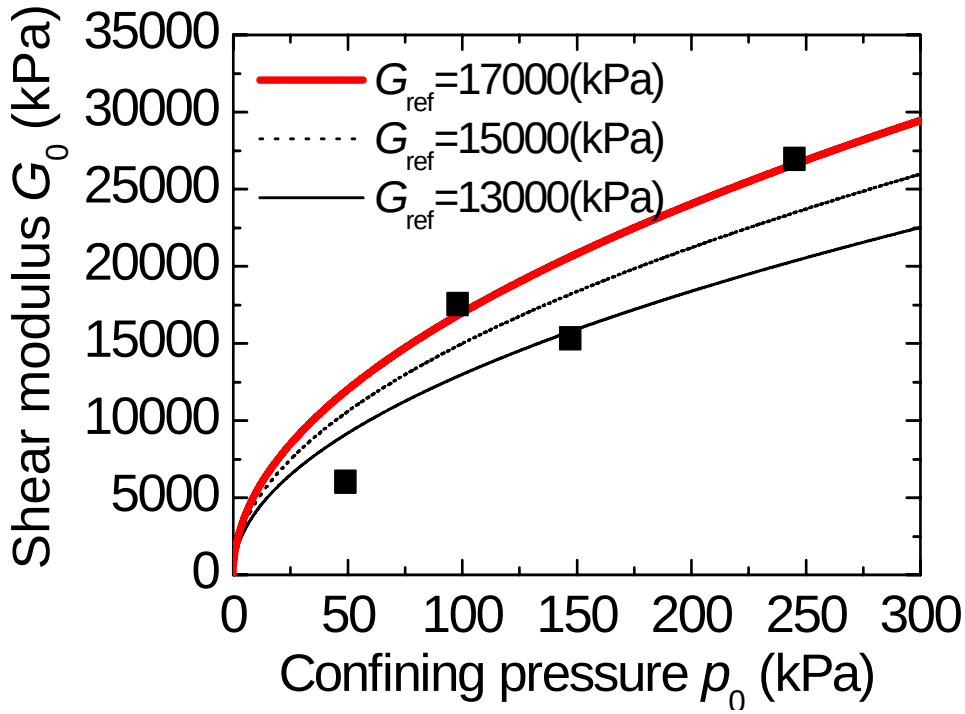

Shear modulus versus confining pressure

Resistance properties

Horizontal raft base resistance

$$q_h = c + \mu_b \sigma'_{vb} \quad (c = 0, \mu_b = \tan\phi' = 0.84) \qquad (4)$$

Vertical raft base resistance

$$q_u = \alpha \cdot c \cdot N_c + \beta \cdot \gamma_1 \cdot B \cdot \eta \cdot N_\gamma + \gamma_2 \cdot D_f \cdot N_q$$

$$(\alpha = 1.2, \beta = 0.3, N_c = 75.3, N_\gamma = 93.7 \text{ for } \phi' = 40^\circ) \qquad (5)$$

Maximum shaft resistance of pile

$$f_{max} = \mu \cdot \gamma \cdot z \cdot K_0 \quad (\mu = 0.84) \qquad (6)$$

Maximum horizontal resistance of pile

$$p_{max} = \alpha_p \cdot \gamma \cdot z \cdot K_p \quad (\alpha_p = 3.0) \qquad (7)$$

$$K_p = (1+\sin\phi')/(1-\sin\phi') \qquad (8)$$

End-bearing capacity of pile

$$R_p = q_c \cdot A_p \quad (q_c = 5000 \text{ kPa from CPT results}) \qquad (9)$$

Physical vs numerical

Load–settlement relationship

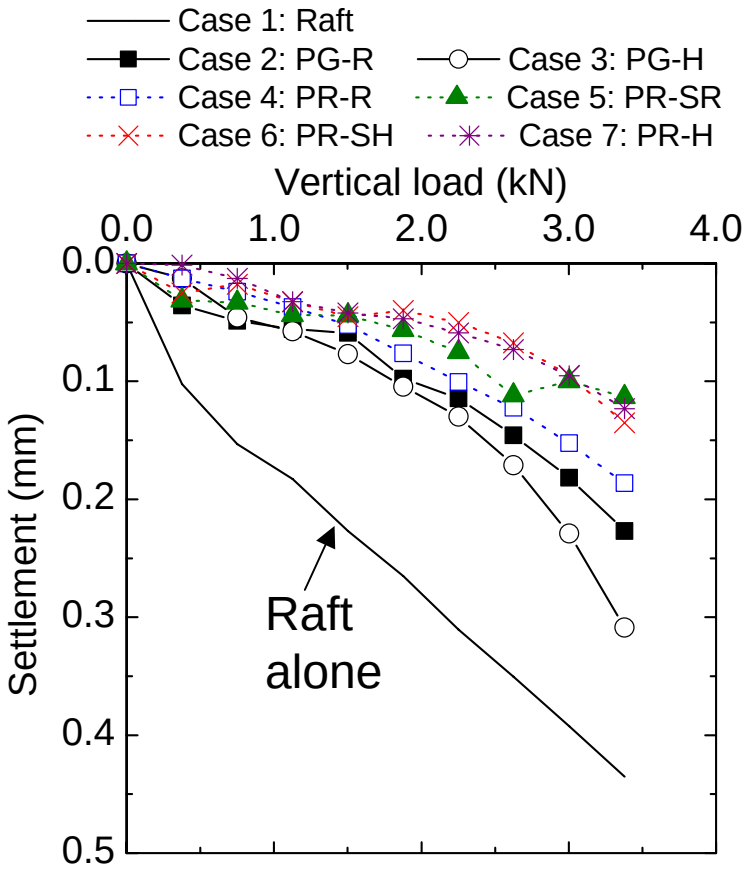

Experimental results

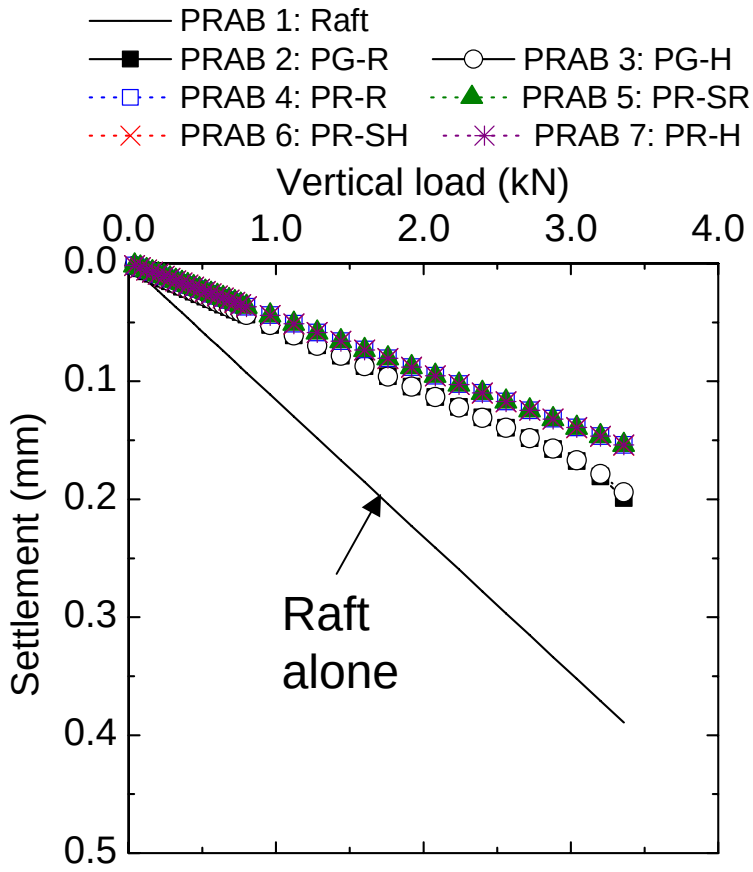

Analysis results

- At the same vertical load, pile groups settle more than piled rafts.
- The load - settlement curves are almost identical for the same type of foundation regardless of pile head connection rigidities.

Physical vs numerical

Load–settlement relationship

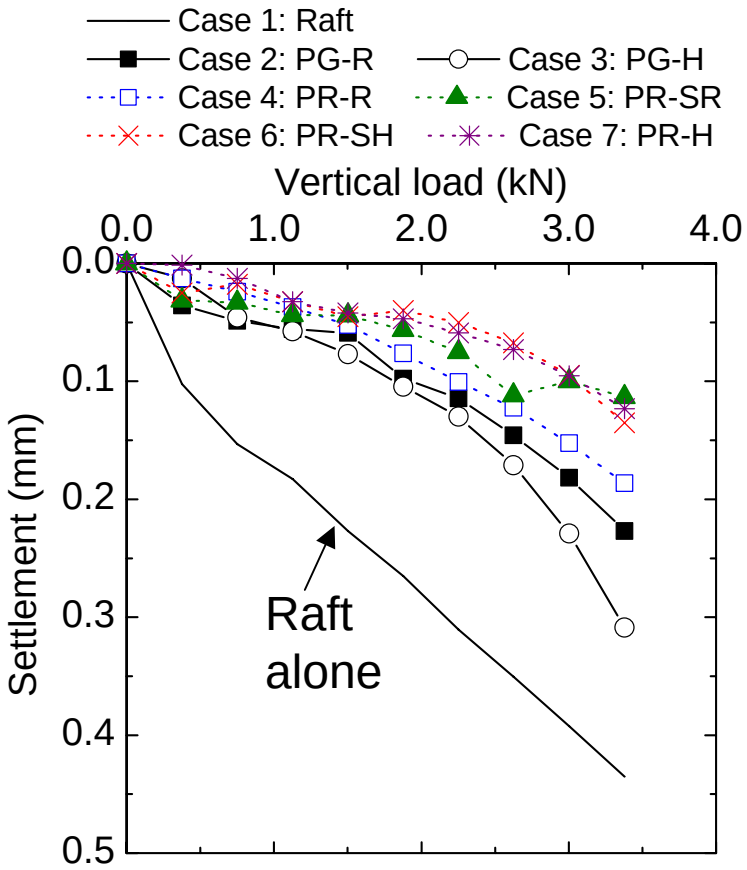

Experimental results

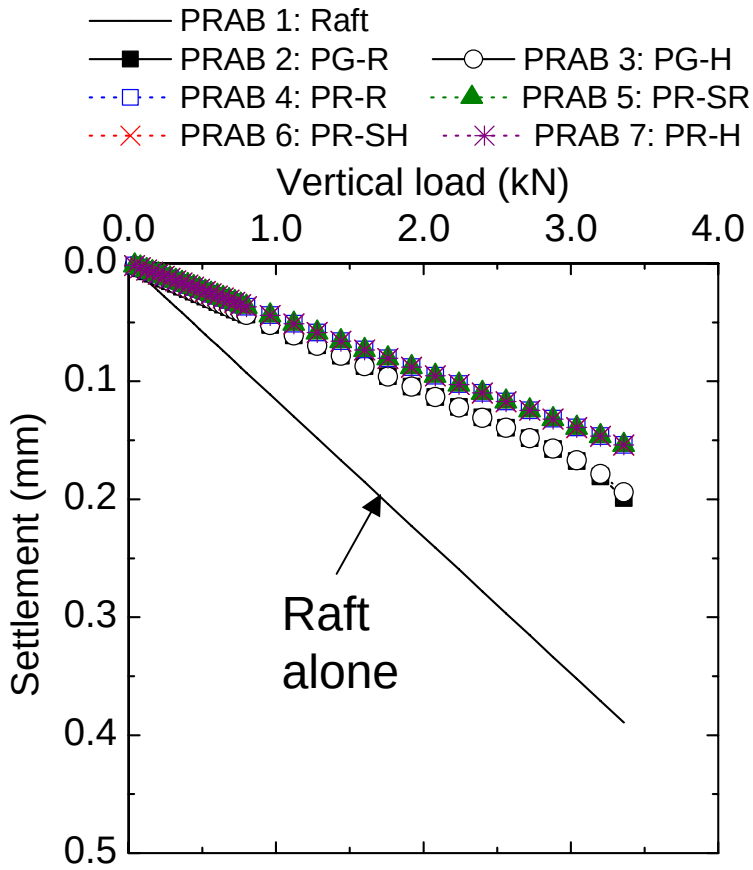

Analysis results

- Analysis results simulate the experimental results well.

Physical vs numerical

Proportion of vertical load carried by raft

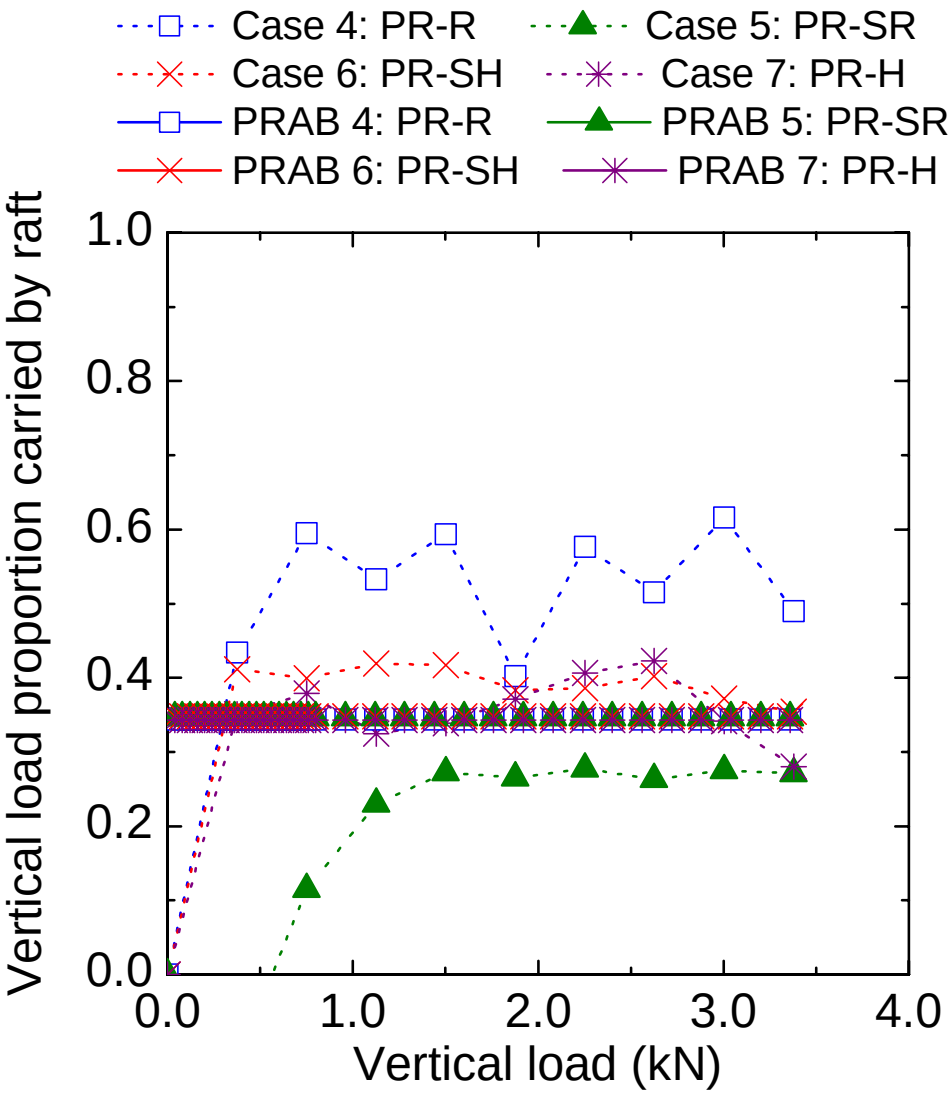

At the initial stage of the vertical loading, only small vertical load is carried by the raft in the experimental results, due to the small stress level in the sand near the surface.

The proportions of the vertical load carried by the raft is about 0.35 for all types of pile head connection condition from the calculated results.

From the analyses, the rigidity of the pile head connection has little influence on the behavior of the pile foundation subjected to vertical load.

Physical vs numerical

Horizontal load–displacement curves

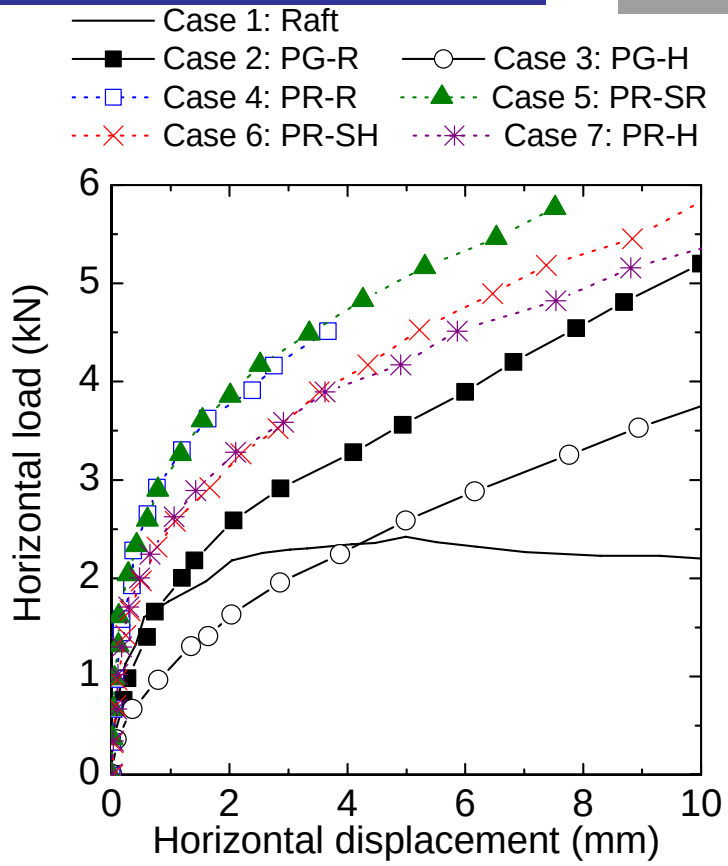

Experimental results

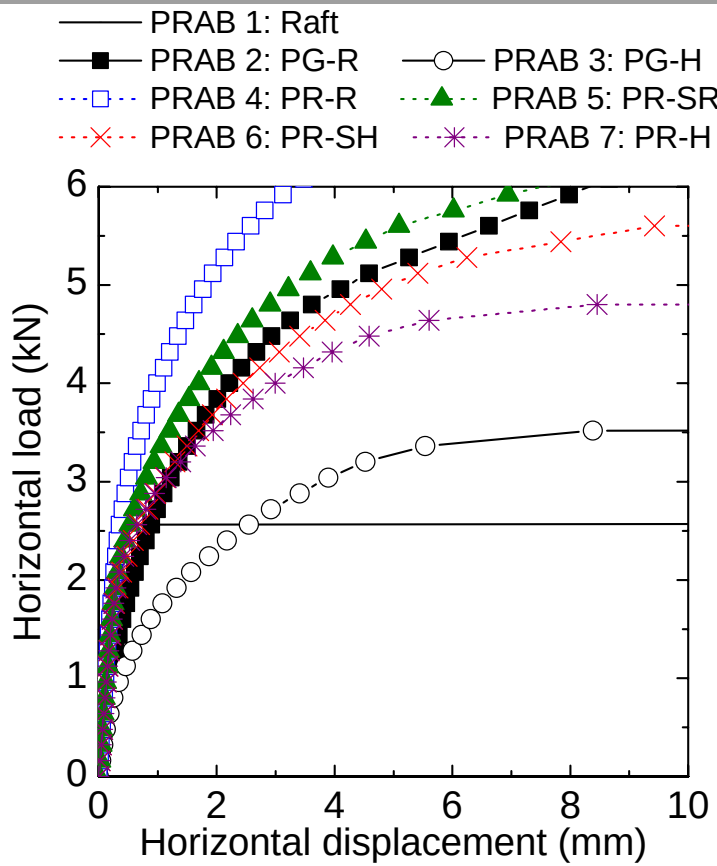

Analysis results

- The initial horizontal stiffness is higher in the case of piled raft than that of corresponding pile group from both experimental and analysis results.
- For the same type of foundation, the higher horizontal stiffness and horizontal resistance can be found in the foundation that has higher rigidity of pile head connection in both experimental and analysis results.

Physical vs numerical

Proportion of horizontal load carried by raft

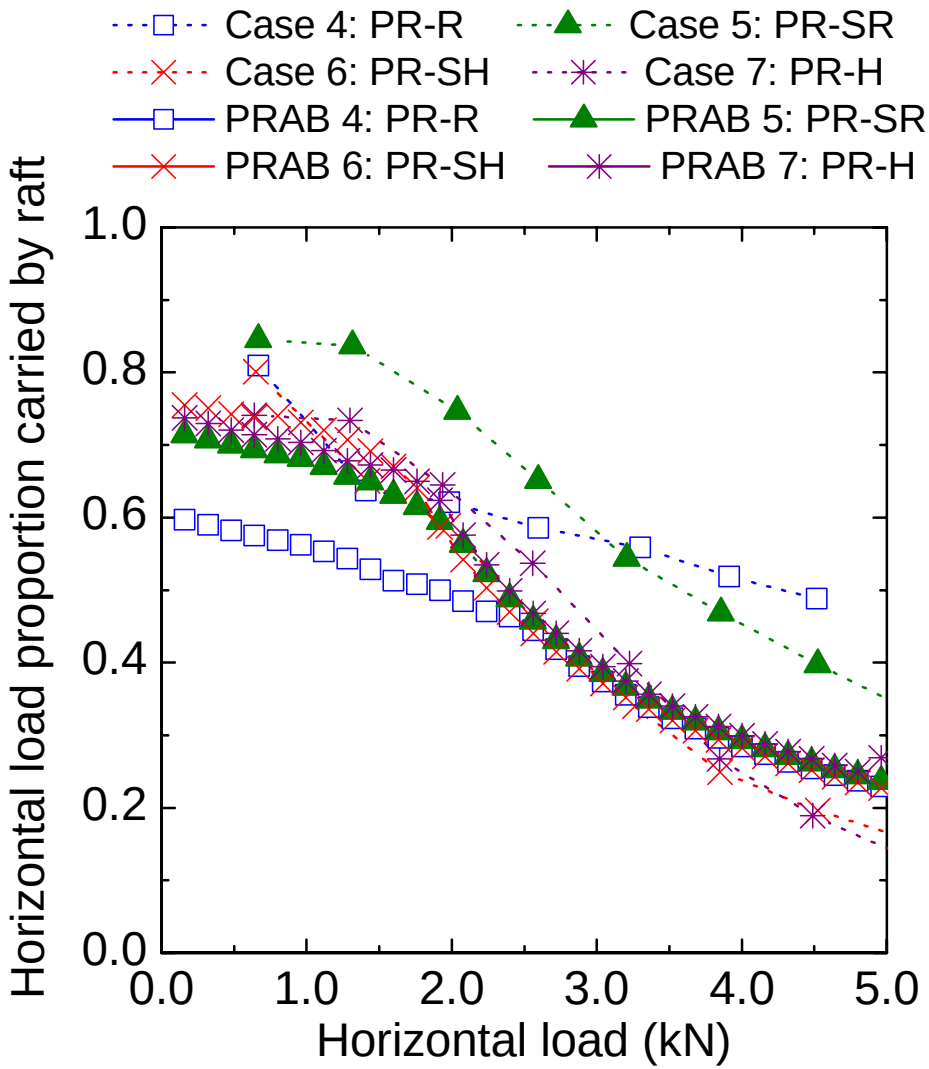

The piles in the piled raft with rigid pile head connection carry a high amount of the horizontal load in the initial stage from the analysis results.

From the analyses, the horizontal load carried by the raft for all cases are almost identical after the horizontal load reaches 2.5 kN.

Physical vs numerical

Distributions of pile bending moments

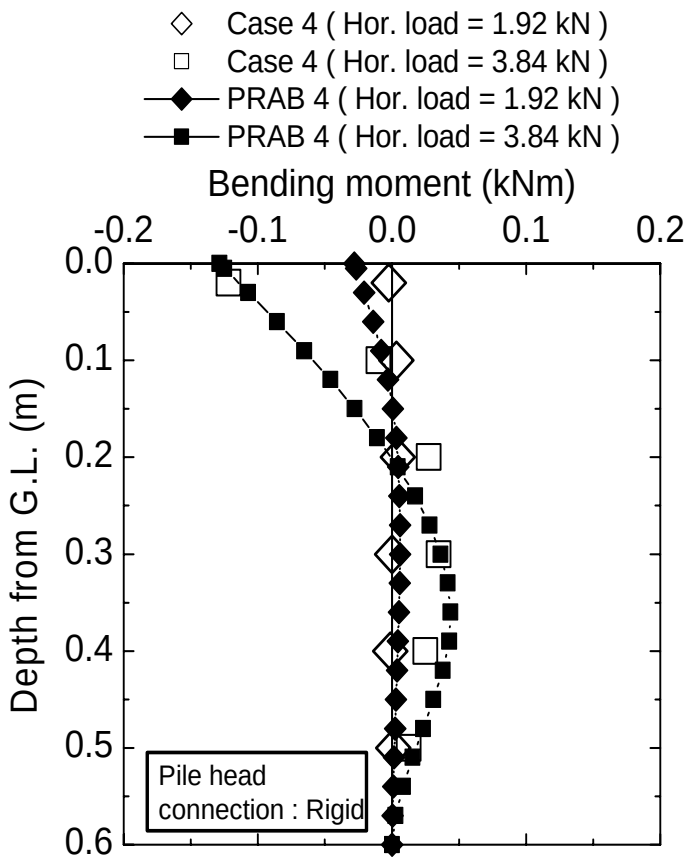

Rigid pile head connection

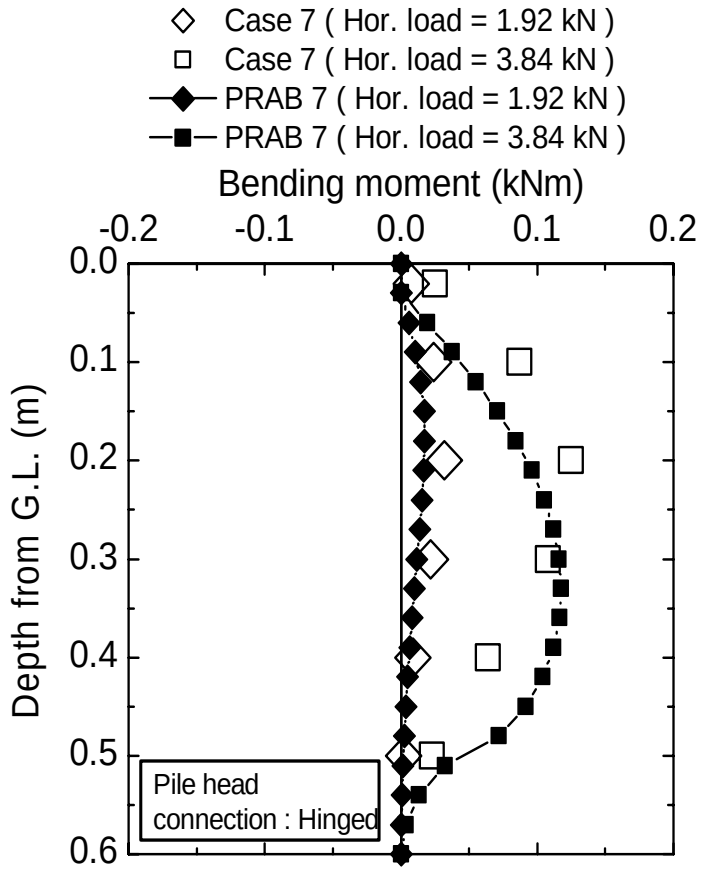

Hinged pile head connection

The analysis results match well with the measured values for both piled rafts with rigid and hinged pile head connection conditions.

Part IV: Application of PRAB

A Temporary Bridge (Kanazawa, Japan)

- A temporary road bridge having a span of 42.5 m and a width of 10 m was constructed over the existing Hokuriku railway line in 2002.
- Pile foundations were employed for abutments of the bridge
- The bridge was used temporarily until the year of 2005.
- The number of car traffics per day was about 2000, and about 200 trains passed under the bridge in a day.
- Much attention was paid to the design of pile foundation and load distribution of the piles during the construction of the bridge.

Role of STATNAMIC test and PRAB

- STATNAMIC test was conducted on one of the constructed piles in an abutment to confirm the load-settlement relation.
- The piles in the abutment were instrumented with strain gauges to monitor the axial load of each pile throughout the construction steps of the superstructure.
- PRAB was employed to predict the load distribution and the settlements of the piles during the construction of the bridge, using the profile of the soil properties obtained from the wave matching analysis of the STATNAMIC test results.

Site Description

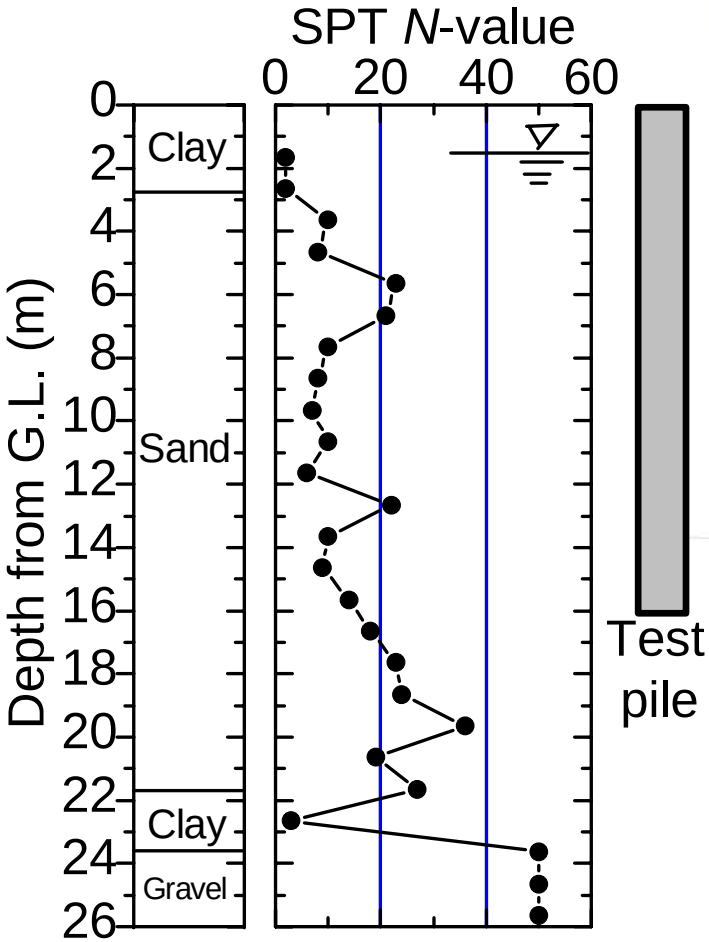

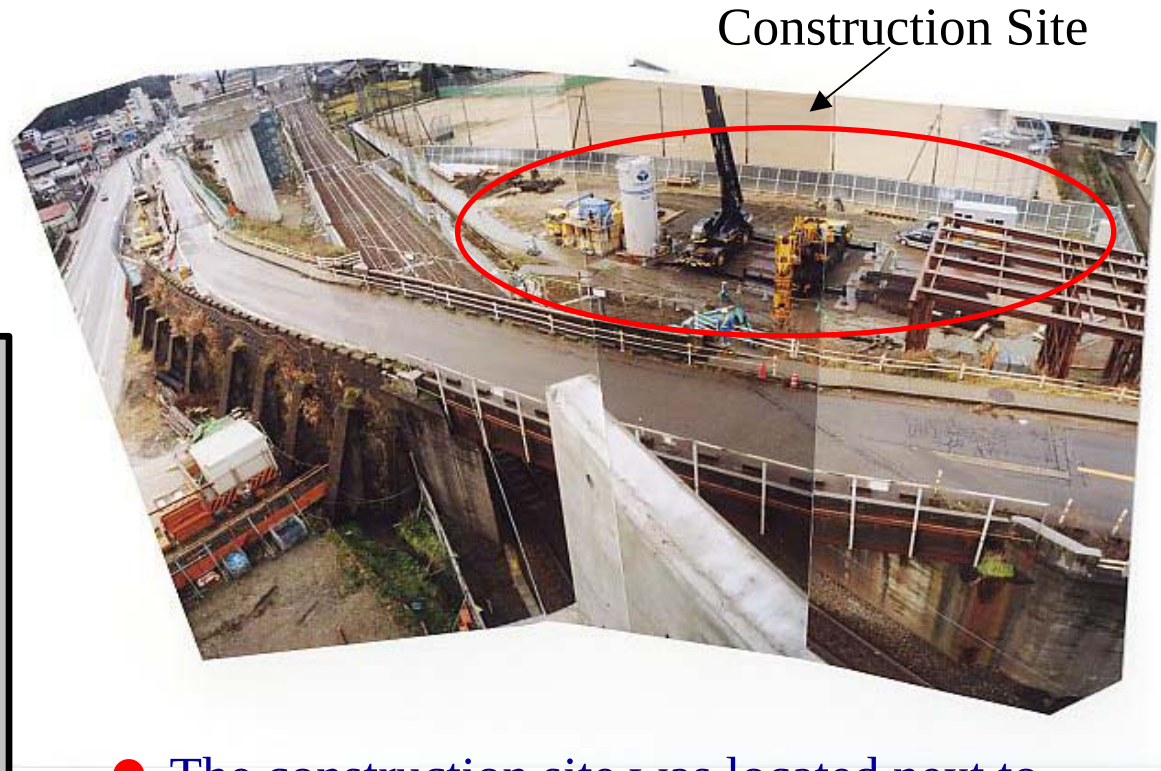

- The construction site was located next to the Hokuriku railway line.
- The top soft clay with a thickness of 2.76 m was underlain by a relatively uniform sand layer of 18.95 m in thickness. A soft clay layer of 1.89 m thickness was intercalated between the sand layer and a hard gravel layer existing below a depth of 23.6 m.

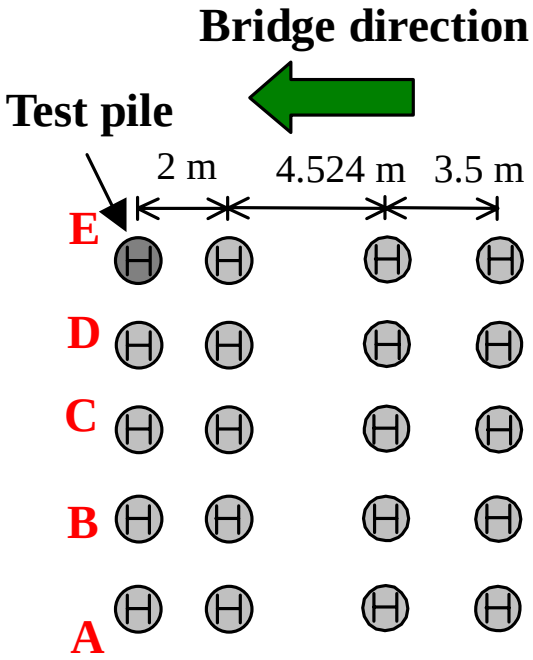

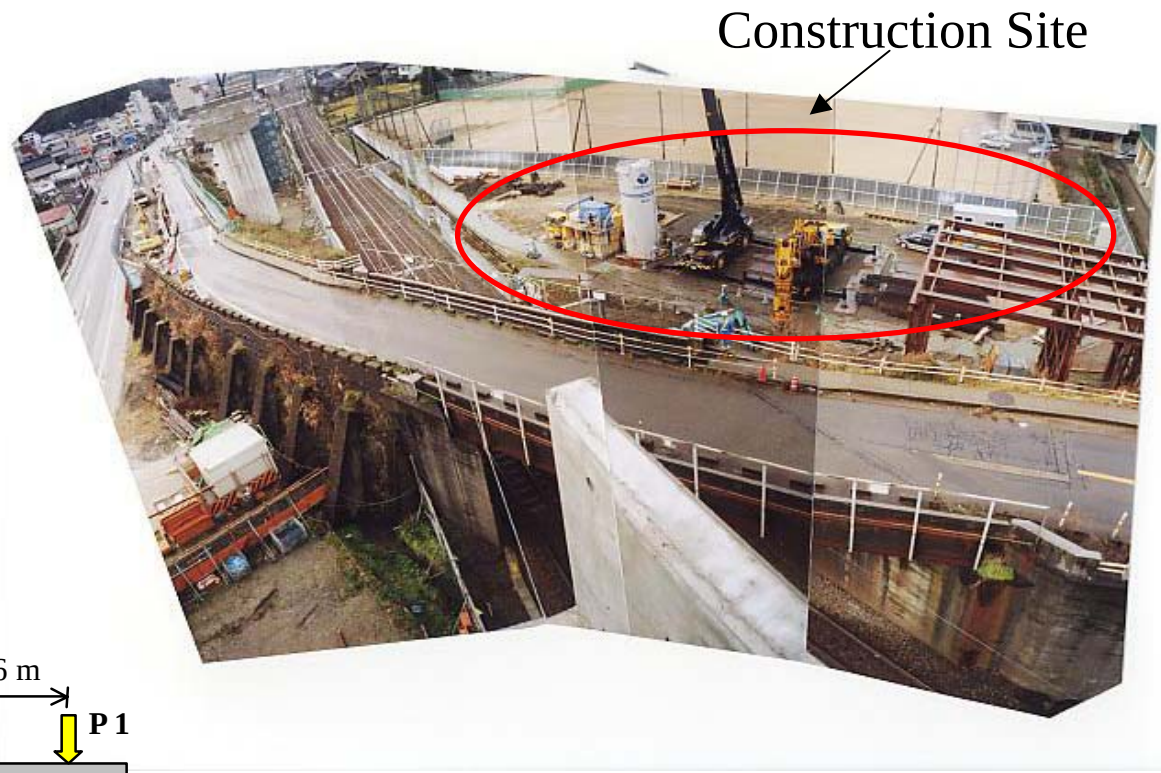

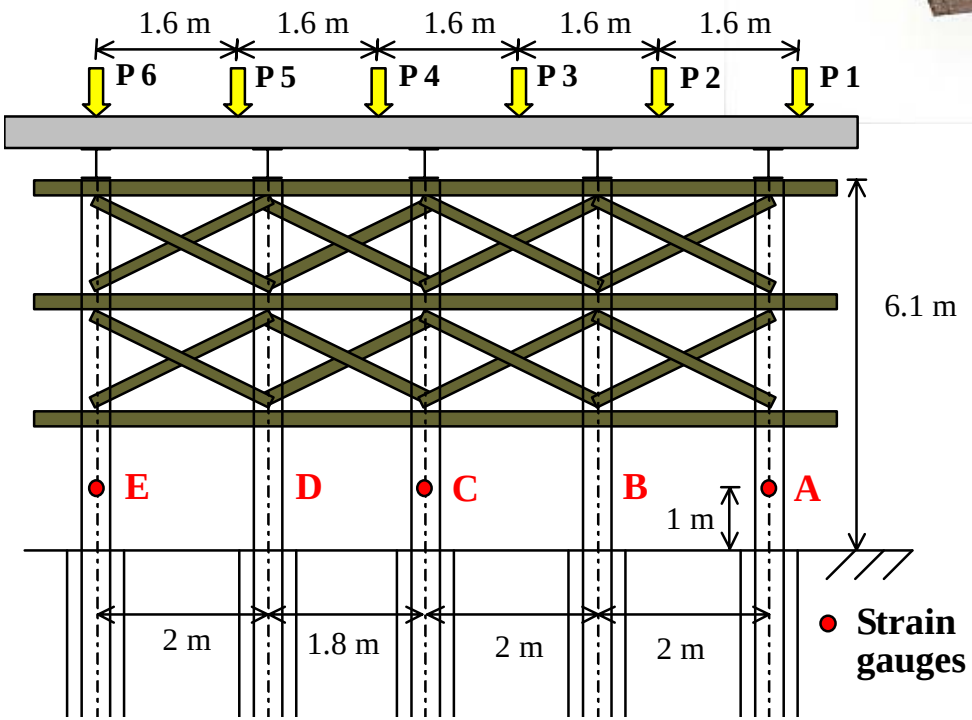

- A total of 20 piles were constructed for an abutment of the temporary bridge.
- The piles were bored concrete piles with H-shaped steel reinforcing bars.
- The H-shaped steel bars were extended to support the superstructure.
- Piles A, C and E were instrumented with strain gauges.

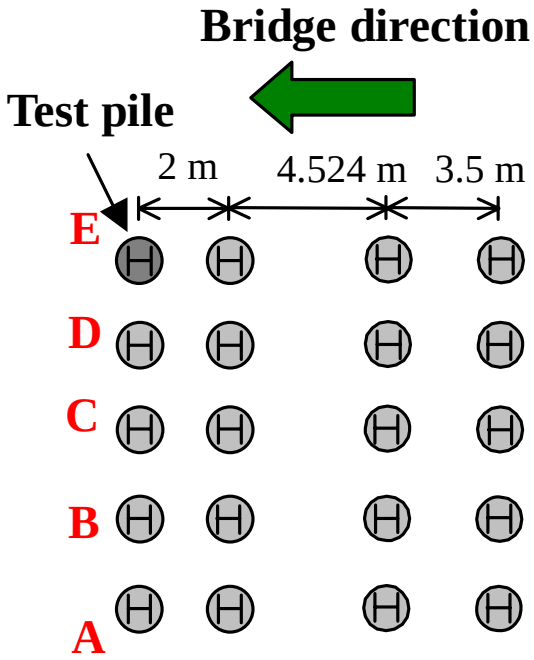

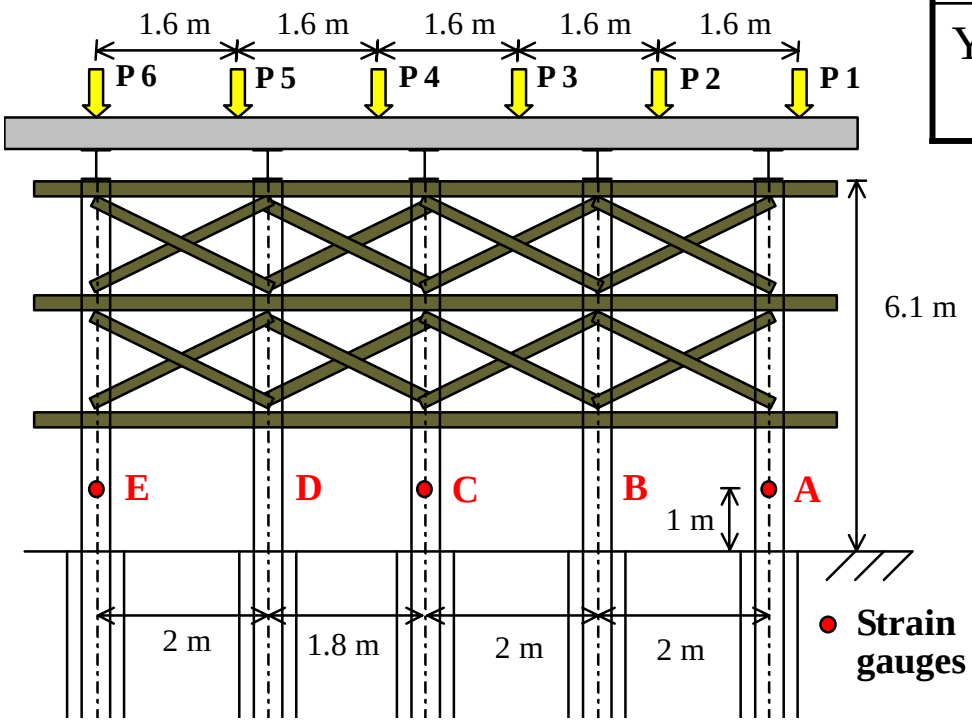

Property		Value
Length, m		16
Diameter, m		0.650
Cross-sectional area, m^2		0.332
Mass, ton		11.475
Density, ton/m^3	Concrete H-core	1.760 7.865
Wave velocity, m/s	Concrete H-core	4129 5043
Young's modulus	Concrete H-core	3×10^7 20×10^7

- A total of 20 piles were constructed for an abutment of the temporary bridge.
- The piles were bored concrete piles with H-shaped steel reinforcing bars.
- The H-shaped steel bars were extended to support the superstructure.
- Piles A, C and E were instrumented with strain gauges.

Statnamic test

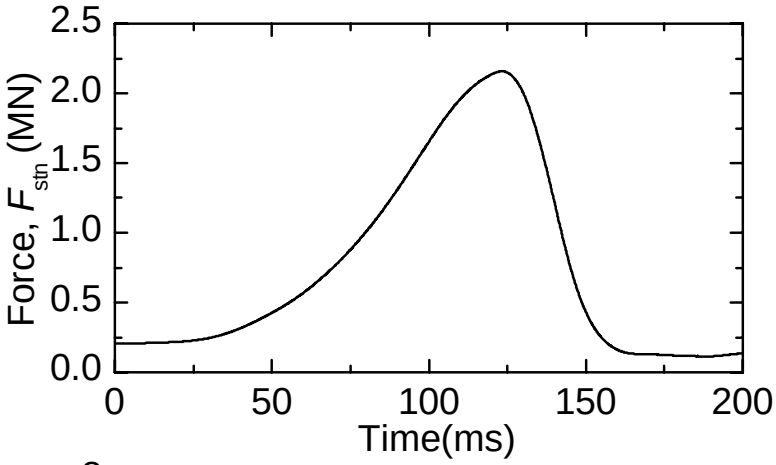

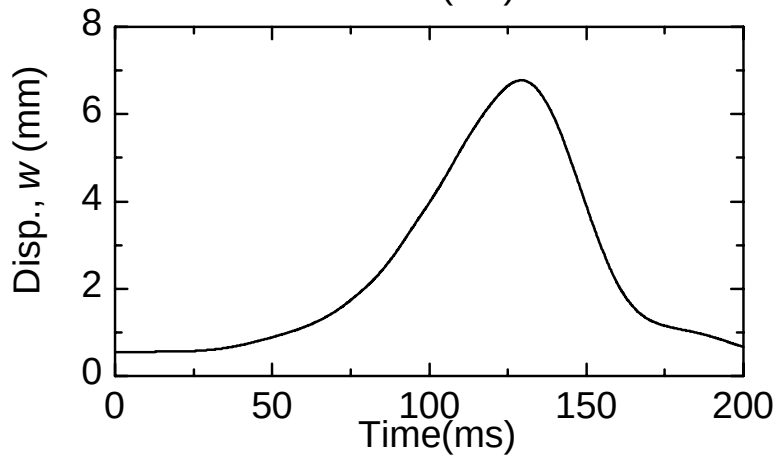

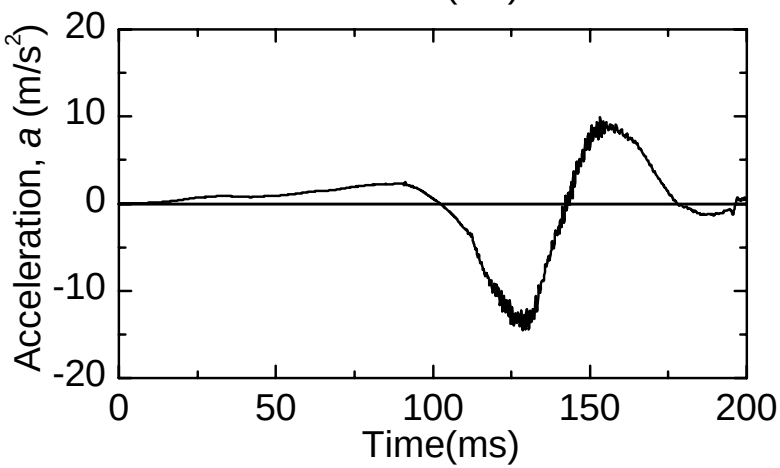

Measured signals

- Maximum applied load in the test was 2.2 MN.

Interpretations

Wave matching analysis

Wave matching analysis

KWAVE (Matsumoto & Takei, 1991)

- The one-dimensional stress–wave analysis was repeated using the measured F_{stn} as the force boundary condition at the pile head, until a good matching between the calculated and the measured pile head displacements was obtained.

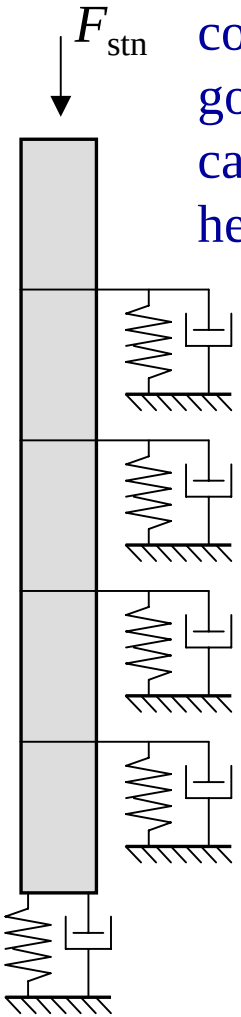

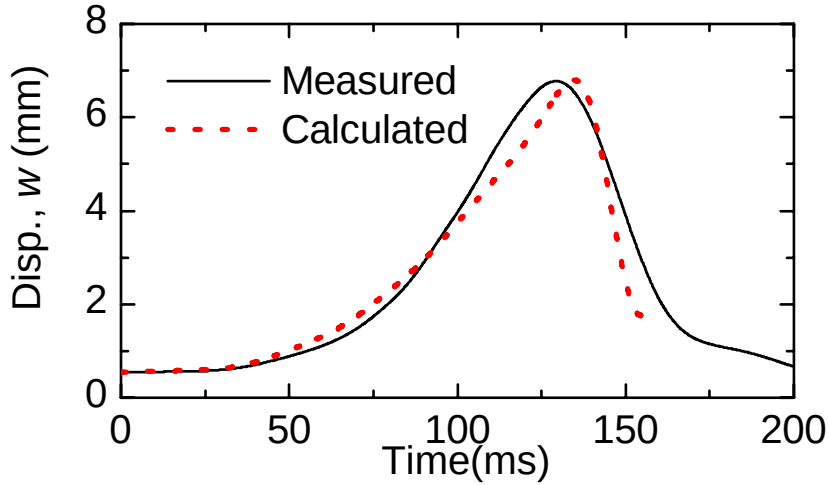

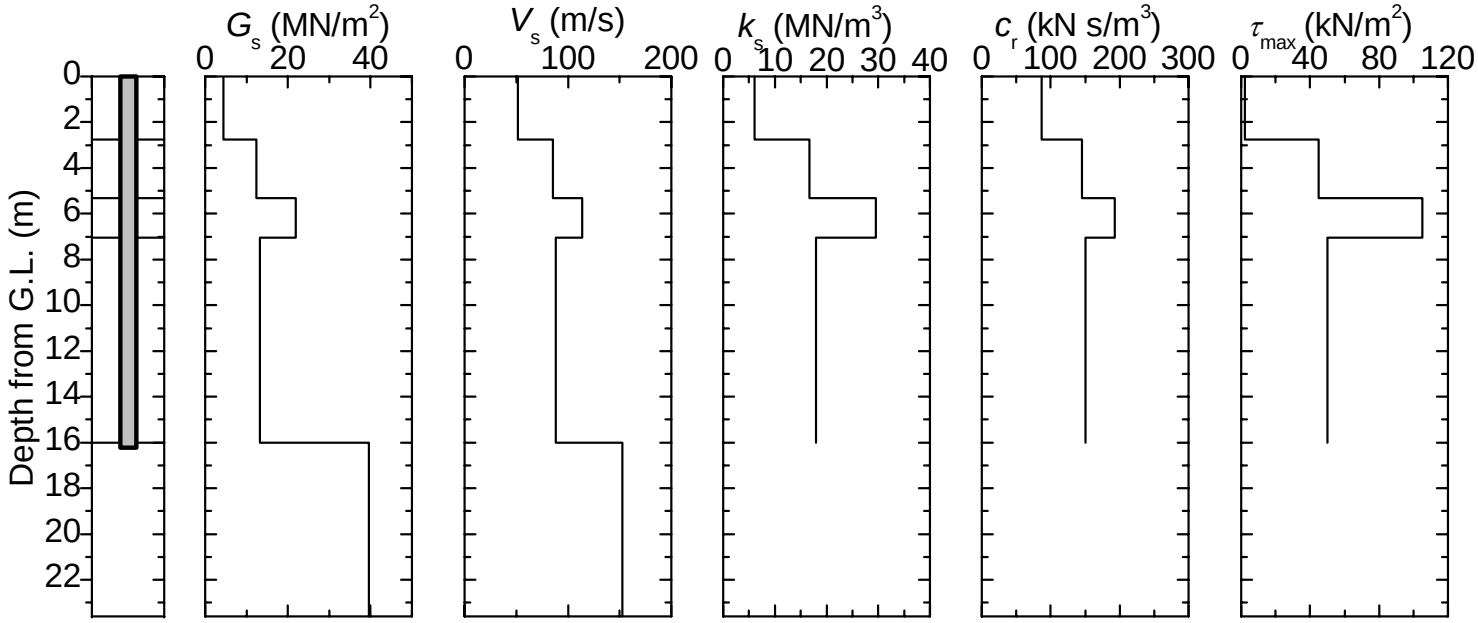

Load distribution and settlement of piles

Step	Load at the point (kN)					
	P1	P2	P3	P4	P5	P6
1 (mount of 1st bridge girder)	75.6	75.6	0	0	0	0
2 (mount of 2nd bridge girder)	75.6	75.6	75.6	75.6	0	0
3 (mount of 3rd bridge girder)	75.6	75.6	75.6	75.6	75.6	75.6
4 (after completion of pavement and other facilities)	158	168	176	190	208	266

Load distribution and settlement of piles

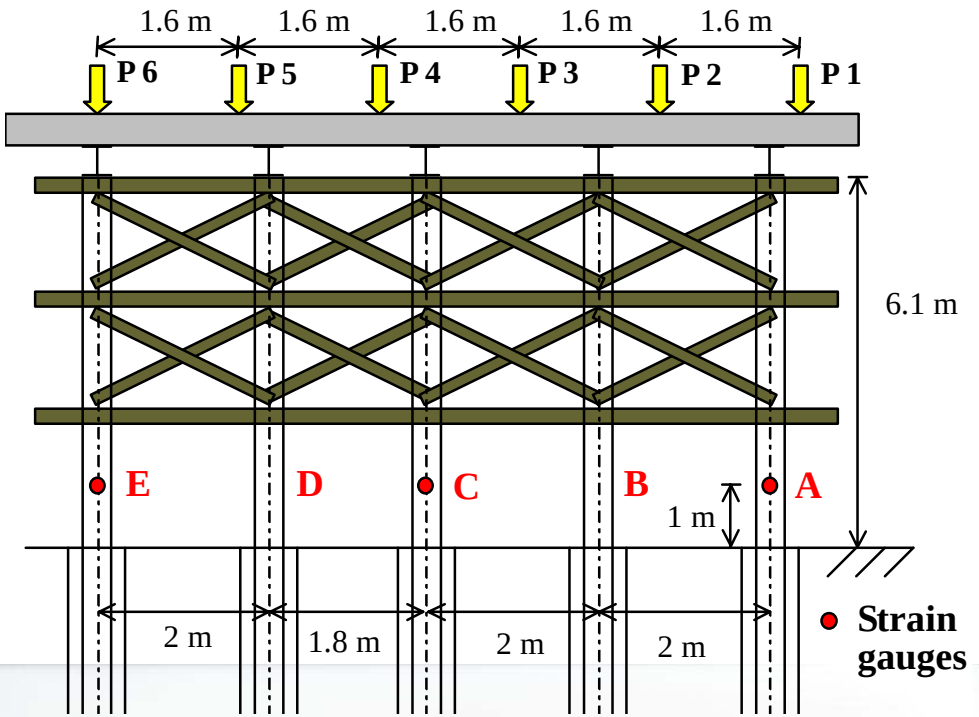

Step	Load at the point (kN)					
	P1	P2	P3	P4	P5	P6
1 (mount of 1st bridge girder)	75.6	75.6	0	0	0	0
2 (mount of 2nd bridge girder)	75.6	75.6	75.6	75.6	0	0
3 (mount of 3rd bridge girder)	75.6	75.6	75.6	75.6	75.6	75.6
4 (after completion of pavement and other facilities)	158	168	176	190	208	266

Analysis using PRAB

- A group of five piles with a cap(raft) was modelled in the analysis.
- The profiles of the soil shear modulus, the maximum shaft resistance, the base resistance obtained from the wave matching analysis were employed.

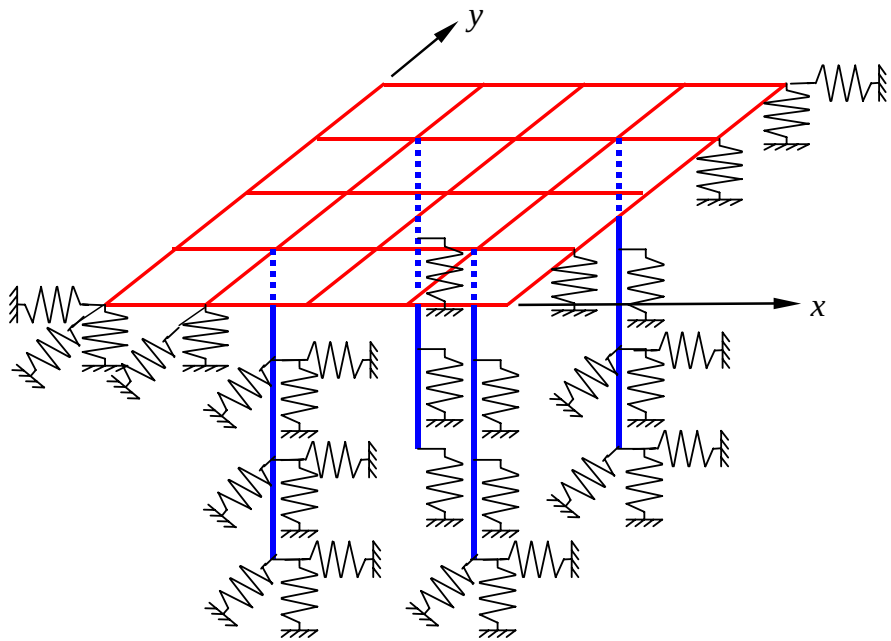

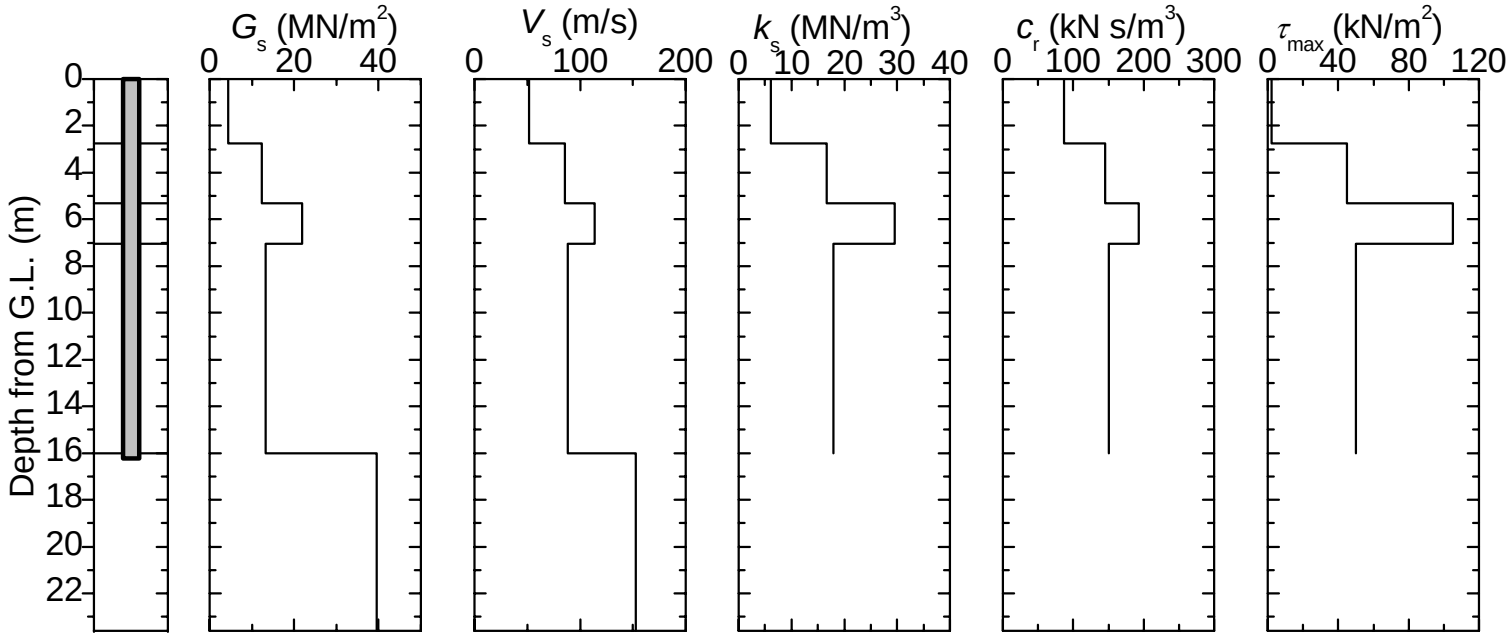

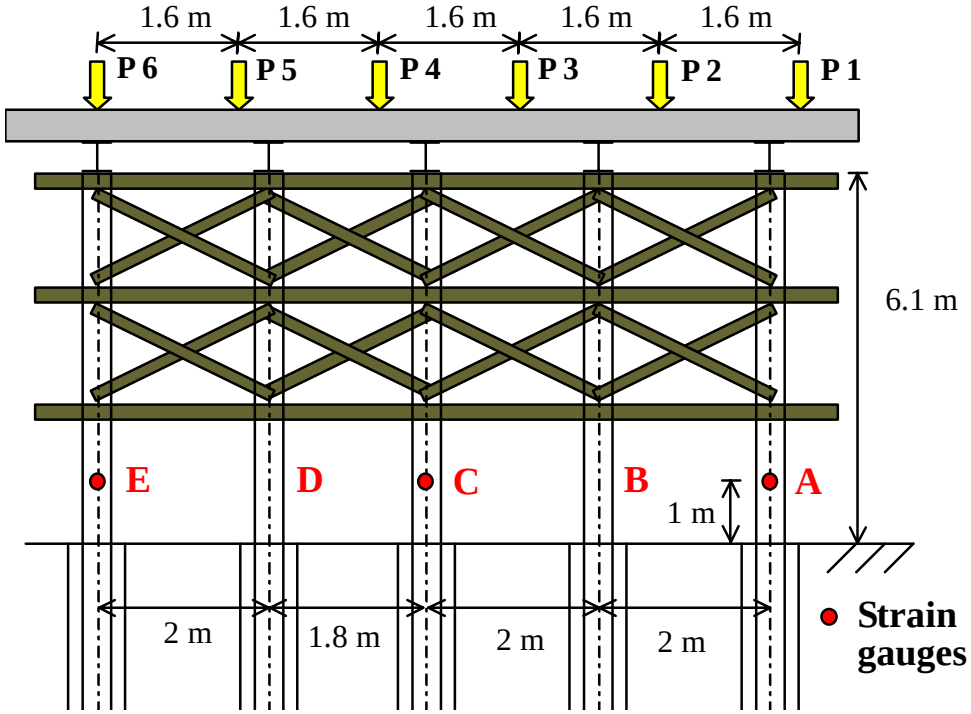

Step	Load at the point (kN)					
	P1	P2	P3	P4	P5	P6
1 (mount of 1st bridge girder)	75.6	75.6	0	0	0	0
2 (mount of 2nd bridge girder)	75.6	75.6	75.6	75.6	0	0
3 (mount of 3rd bridge girder)	75.6	75.6	75.6	75.6	75.6	75.6
4 (after completion of the bridge)	158	168	176	190	208	266

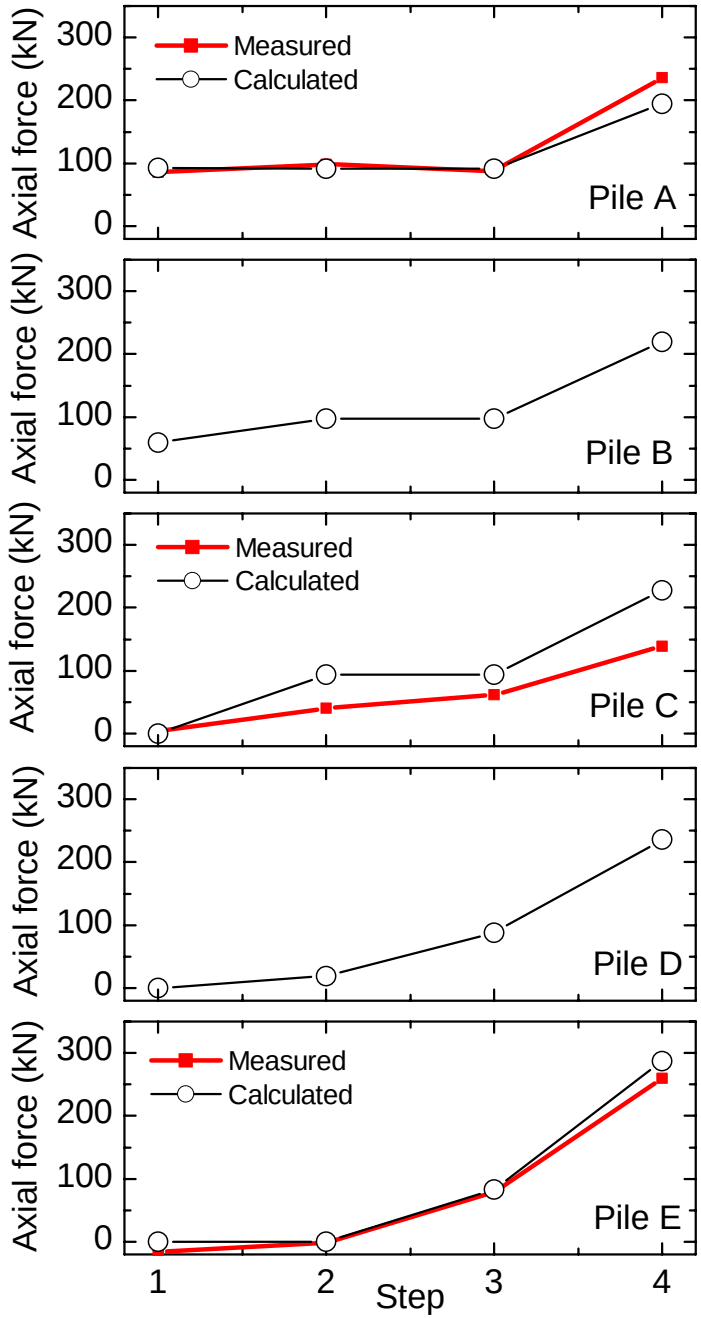

Axial force

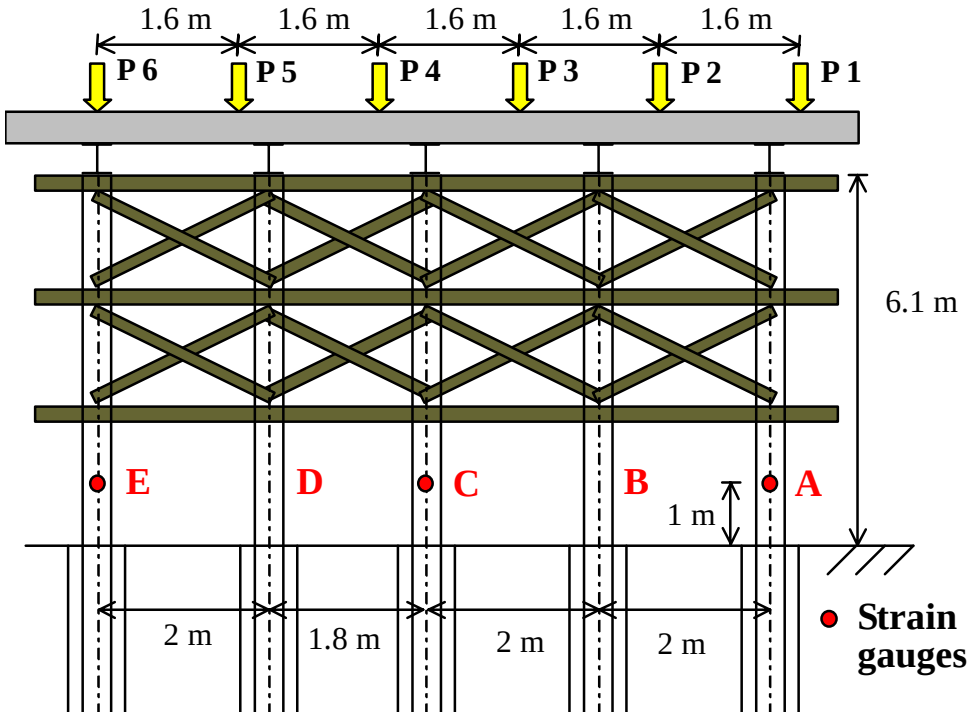

Step	Load at the point (kN)					
	P1	P2	P3	P4	P5	P6
1 (mount of 1st bridge girder)	75.6	75.6	0	0	0	0
2 (mount of 2nd bridge girder)	75.6	75.6	75.6	75.6	0	0
3 (mount of 3rd bridge girder)	75.6	75.6	75.6	75.6	75.6	75.6
4 (after completion of the bridge)	158	168	176	190	208	266

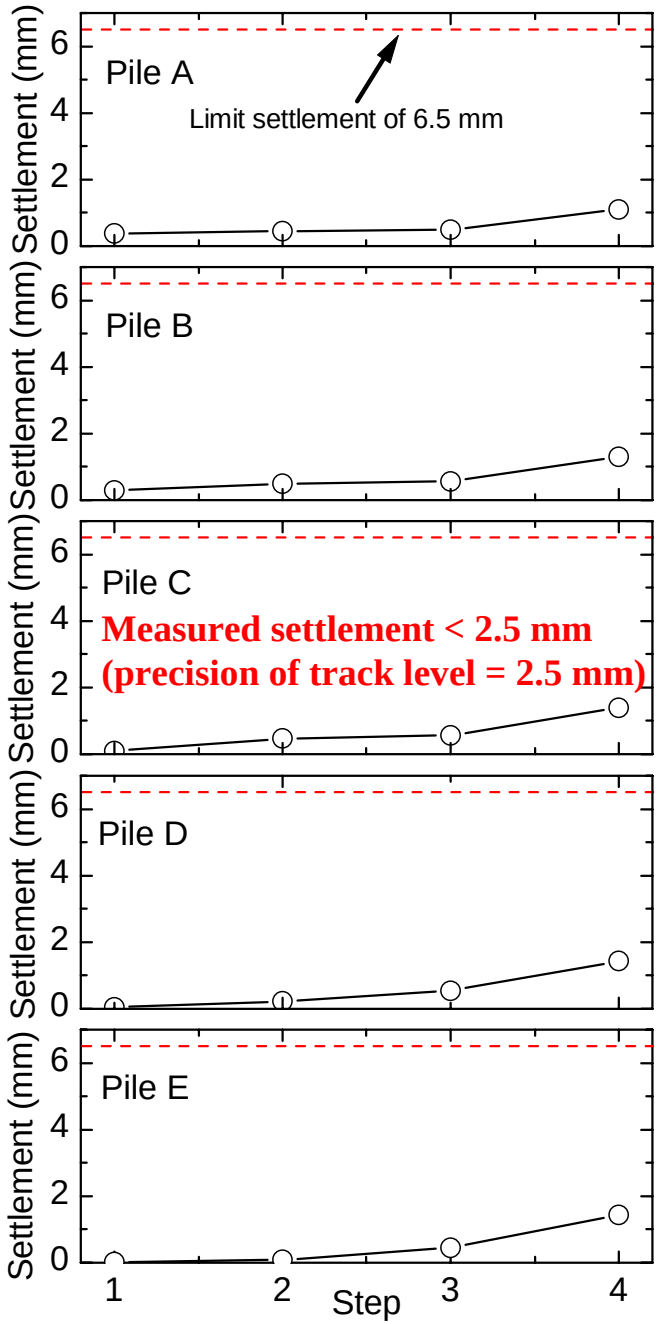

Settlement

"The load distribution and the settlements of the piles in the abutments calculated using PRAB match well with the field measurement values. Through the field measurements and the analyses, the safety of the pile foundation was confirmed. "

Step	Load at the point (kN)					
	P1	P2	P3	P4	P5	P6
1 (mount of 1st bridge girder)	75.6	75.6	0	0	0	0
2 (mount of 2nd bridge girder)	75.6	75.6	75.6	75.6	0	0
3 (mount of 3rd bridge girder)	75.6	75.6	75.6	75.6	75.6	75.6
4 (after completion of the bridge)	158	168	176	190	208	266

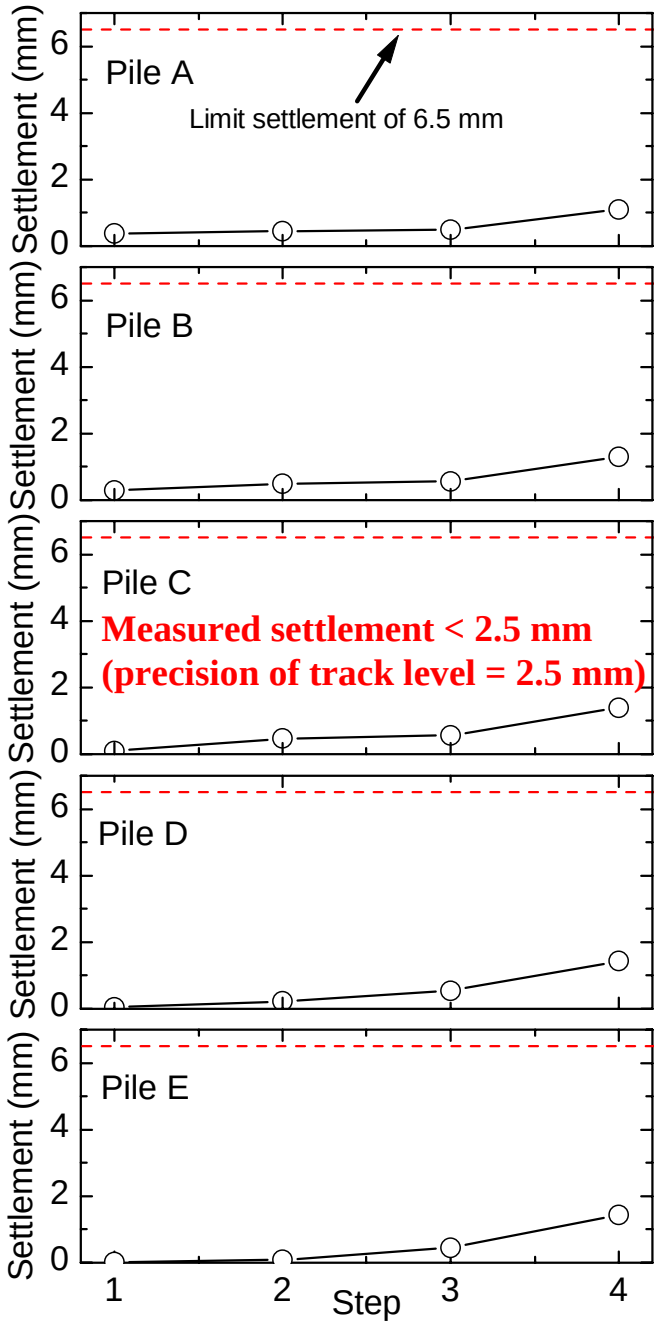

Settlement

Concluding remarks

1. As a simplified method of numerical analysis for estimation of the deformation and load distribution of piled raft foundations subjected to active loading and passive loading, PRAB has been developed.
2. The validity and applicability of PRAB were verified through comparison with several published solutions, three-dimensional FEM and model test results.
3. Through the field measurements and the analyses using PRAB, the safety of the pile foundation of a bridge was confirmed.
4. A combination of field measurements with an appropriate deformation analysis of a whole pile foundation structure may lead to a rational reduction of the safety factor.
5. PRAB can be used with a confidence as a design tool for piled raft foundations.